UNIVERSITÉ YORK UNIVERSITY

VISUAL AND AUDITORY SENSITIVITIES AND DISCRIMINATIONS

AFOSR F49620-94-1- 0083

Final Report 15 Dec. 1993 — 14 Dec. 1996

D. Regan

York University, 4700 Keele Street, North York, Ontario, Canada, M3J 1P3

VISUAL AND AUDITORY SENSITIVITIES AND DISCRIMINATIONS

AFOSR F49620-94-1- 0083

Final Report 15 Dec. 1993 — 14 Dec. 1996

D. Regan

York University, 4700 Keele Street, North York, Ontario, Canada, M3J 1P3

REPORT DOCUMENTATION PAGE

Form Approved
OMB No. 0704-0188

1. AGENCY USE ONLY (Leave blank)	2. REPORT DATE	3. REPORT TYPE AND DATES COVERED
	12/14/96	Final 15 Dec 93 - 14 Dec 96

4. TITLE AND SUBTITLE

Visual and Auditory Sensitivities and Discriminations

5. FUNDING NUMBERS

61102F
2313/BS

6. AUTHOR(S)

David Regan

7. PERFORMING ORGANIZATION NAME(S) AND ADDRESS(ES)

York University (Mrs Noli Swatman)
Rm. 5415 Ross Bldg.,
4700 Keele Street, North York,
Ontario, Canada, M3J 1P3

8. PERFORMING ORGANIZATION REPORT NUMBER

9. SPONSORING/MONITORING AGENCY NAME(S) AND ADDRESS(ES)

Air Force Office of Scientific Research, /NL
AFOSR/PKA 110 Duncan Ave., Suite B115,
Bolling AFB, DC 20332-8080,
U.S.A.
Dr John Tangney

10. SPONSORING/MONITORING AGENCY REPORT NUMBER

F49620-94-1-0083

11. SUPPLEMENTARY NOTES

12a. DISTRIBUTION/AVAILABILITY STATEMENT

Approved for public release

Distribution unlimited

12b. DISTRIBUTION CODE

13. ABSTRACT (Maximum 200 words)

(1) The ability to judge time to collision with an approaching object is high in central vision but considerably poorer in peripheral vision. (2)A pilot's time to collision with a simulated approaching helicopter depends on the relative contributions of ownship speed and target speed. (3) Binocular judgements of the direction of motion in depth are similar for motion in the vertical and horizontal meridians. (4) Spatial frequency, temporal frequency, orientation and contrast are processed independently and in parallel. (5) Orientation discrimination for cyclopean form and texture-defined form can be as acute as for luminance-defined form. (6) A letter test for measuring the ability to see and recognize texture-defined form has been made freely available. (7) A physiologically-plausible model of the recognition of texture-defined letters has been developed. (8) The ability to recognize texture-defined, motion-defined and luminance-defined letters can be independently lost in patients with multiple sclerosis. (9) Magnetic brain recording has been used to identify and locate an audio-visual convergence area in human brainand centres for color-defined, texture-defined and luminance-defined form. (10) Mathematical methods for obtaining the response of auditory hair cells to complex amplitude modulated tones and the harmonic distortion of a pure tone caused by the hair cell transducer function have been developed. Results fit empirical data closely.

14. SUBJECT TERMS	15. NUMBER OF PAGES
vision; visual flying skills; intersubject differences; visual navigation; perception of motion and self-motion; stereo; neuromagnetism; models of visual and auditory processing; multisensory convergence	160
	16. PRICE CODE

17. SECURITY CLASSIFICATION OF REPORT	18. SECURITY CLASSIFICATION OF THIS PAGE	19. SECURITY CLASSIFICATION OF ABSTRACT	20. LIMITATION OF ABSTRACT
unclassified	unclassified	unclassified	

Department of Psychology

FAX: (416) 736-5814

UNIVERSITÉ YORK UNIVERSITY

FACULTY OF ARTS

4700 KEELE STREET • NORTH YORK • ONTARIO • CANADA • M3J 1P3

1. RESEARCH OBJECTIVES

The research objectives for three years were listed in the grant proposal as follows.

1.1 Long Term Aims

1.1.1 We will further explore the role of the channeling hypothesis by: (a) identifying new visual channels; (b) elucidating rules for cue combination in rich visual environments; (c) advancing understanding of eye-limb coordination in skilled visual performance and the role of inter-individual variations of visual sensitivities in limiting skilled visual performance; (c) specifying visual parameters likely to be important in both training eye-limb coordination in flight simulators and in predicting flying performance in real aircraft.

1.1.2 We will use neuromagnetic recording techniques to: (d) identify the brain sites of different kinds of visual processing, auditory processing and multisensory integration, and relate these sites to the organization of visual, auditory and multisensory convergence areas in macaque monkey cortex; (e) relate objective data on visual and auditory processing in human brain to psychophysical models of human vision and hearing.

1.2 Specific Aims: Psychophysics in Normally-Sighted Individuals

1.2.1 *Camouflage and the Visual Processing of Objects Defined by Binocular Disparity, Relative Motion and Luminance Contrast*

Department of Psychology

FAX: (416) 736-5814

UNIVERSITÉ YORK UNIVERSITY

FACULTY OF ARTS

4700 KEELE STREET • NORTH YORK • ONTARIO • CANADA • M3J 1P3

We will determine spatial discrimination thresholds and the dynamics of these thresholds for spatial form defined by disparity alone over a wide range of crossed and uncrossed disparities. We will compare these discrimination thresholds with corresponding discrimination thresholds for spatial form defined by luminance contrast alone, for spatial form defined by motion contrast alone and for spatial form defined by texture contrast alone over the same range of disparities.

Drawing closer to the everyday visual world, we will measure spatial discrimination thresholds for form that is defined by two rather than one attribute (specifically disparity plus relative motion and disparity plus luminance contrast).

Finally, by means of cross-adaptation and cross-masking paradigms, we will investigate whether the detection and discrimination of spatial form defined by disparity alone, luminance contrast alone and relative motion alone are mediated by different neural mechanisms.

1.2.2 *Camouflage and the Visual Processing of Objects Defined by Texture Contrast*

Using our texture-defined letter stimulus we will compare intersubject differences in thresholds for detecting and for reading letters defined by texture contrast for a population of 20 normally-sighted individuals. We will carry out measurements for static texture and also for dynamic texture where a new texture pattern is created up to 70 times per sec.

Department of Psychology
FAX: (416) 736-5814

UNIVERSITÉ
YORK
UNIVERSITY

FACULTY OF ARTS
4700 KEELE STREET • NORTH YORK • ONTARIO • CANADA • M3J 1P3

1.2.3 *Cyclopean Processing of Motion-in-Depth, and Changing-Size*

We will generate targets that are visible in binocular view but invisible monocularly, and compare the sensitivities and dynamic characteristics of the processing of motion-in-depth generated by changing-disparity and changing-size for such cyclopean targets. By comparing these data with corresponding data for noncyclopean targets we will distinguish between the processing of motion-in-depth and changing-size that occurs before and after convergence of the signals from left and right eyes.

1.2.4 *Visual Judgement of Time to Collision*

First, we will extend our work on time-to-collision thresholds on foveally-viewed stimuli to map peripheral visual fields for time-to-collision thresholds.

Second, by using cyclopean stimuli we will dissociate the processing of time to collision information that occurs before and after binocular convergence.

Third, we will find how time-to-collision judgements are affected by imbalance between the rate of expansion of retinal image size and retinal image texture.

1.2.5 *Monocular and Binocular Cues to the Direction of Motion in Three Dimensions*

We will compare a subject's ability to judge the direction of motion in depth when (a) binocular and monocular cues are available with (b) only the

Department of Psychology
FAX: (416) 736-5814

UNIVERSITÉ
YORK
UNIVERSITY

FACULTY OF ARTS
4700 KEELE STREET • NORTH YORK • ONTARIO • CANADA • M3J 1P3

binocular cue is available and (c) only the monocular cue is available. We will also elucidate how the visual system combines these two cues. (The binocular cue is the ratio of retinal image velocities in left and right eyes, and the monocular cue is ($d\phi/d\theta$) as discussed on page 44 -46). We have previously described the processing of motion-in-depth using the binocular cue alone (Refs. 34, 49) and the monocular cue alone (Refs. 154, 220, 230,233).

1.3 Specific Aims: Psychophysics in Subjects With Known Visual Disorders

1.3.1 *Detection and Recognition of Letters Defined by Texture, Motion and Luminance*

Here we take a different approach to the same question as that addressed in 1.2.1 (paragraph 3) above, i.e. whether the detection and discrimination of three kinds of spatial form involve different neural mechanisms. Rather than testing normally-sighted individuals, we will compare the ability of selected neurological patients to detect and recognise texture-defined letters, motion-defined letters and luminance-defined letters.

1.3.2 *Binocular Processing of Texture-Defined Form, Motion-Defined Form and Luminance-Defined Form*

We will find whether binocular processing differs for three kinds of form by measuring monocular and binocular acuity for texture-defined letters, motion-defined letters and luminance-defined letters in normally-sighted subjects and in patients with unilateral focal cerebral lesions.

Department of Psychology
FAX: (416) 736-5814

UNIVERSITÉ
YORK
UNIVERSITY

FACULTY OF ARTS
4700 KEELE STREET • NORTH YORK • ONTARIO • CANADA • M3J 1P3

1.4 Specific Aims: Theoretical

1.4.1 *Multi-Rectifier Models of the Auditory Pathway*

We will extend our theoretical work on the response of the auditory hair cell to amplitude-modulated tones by developing a theoretical treatment of multi-rectifier models for inputs consisting of sums of amplitude-modulated tones.

1.4.2 *Multi-Rectifier Models of the Visual Pathway*

We will extend our theoretical work on multi-rectifier models of the visual pathway (Refs. 179, 183) to include dynamics.

1.4.3 *Multi-Channel Model of the Detection and Discrimination of Texture-Defined Form*

We will develop parallel-process models of the detection and spatial discrimination of texture-defined form and compare these models against psychophysical data that we will collect on a subject's ability to detect and discriminate texture-defined letters.

1.5 Specific Aims: Experimental Neuromagnetic Studies

1.5.1 *Visual and Auditory Projections*

We will identify evoked activity in different visual, and auditory projections in human cortex, elucidate the differences between the type of processing occurring in the different areas, and link these data with the known functional neuroanatomy of macaque monkey brain and with human psychophysics.

Department of Psychology
FAX: (416) 736-5814

UNIVERSITÉ
YORK
UNIVERSITY

FACULTY OF ARTS
4700 KEELE STREET • NORTH YORK • ONTARIO • CANADA • M3J 1P3

1.5.2 *Multi-Sensory Areas*

We will identify the cortical sites of interactions between responses to stimuli of different modalities, and compare these sites with the known multi-sensory cortical areas in nonhuman primates (Van Essen et al.,1990; Zeki, 1990).

1.6 **Specific Aims: Development of Operational Tests**

1.6.1 *Glare Susceptibility*

We will find whether our laboratory procedure for quantifying intersubject differences of susceptibility to glare predicts intersubject differences in flying safety in glare conditions.

1.6.2 *Collision Avoidance*

We will find whether our laboratory procedure for quantifying intersubject differences in the ability to judge time to collision predicts intersubject differences in flying safety in realistic visual environments.

2. STATEMENT OF WORK

The statement of work for three years was set out in the grant proposal as follows.

2.1 **Experiment 1. Psychophysics: Aspect ratio discrimination for cyclopean, luminance-defined and motion-defined rectangles.**

Using temporal two-alternative forced choice we will measure aspect ratio (shape) discrimination for a rectangular area within a region of random dots. The rectangular area will be perfectly camouflaged in monocular vision,

Department of Psychology
FAX: (416) 736-5814

UNIVERSITÉ
YORK
UNIVERSITY

FACULTY OF ARTS
4700 KEELE STREET • NORTH YORK • ONTARIO • CANADA • M3J 1P3

and rendered visible by binocular disparity alone. Aspect ratio discrimination will be defined as the just noticeable (75% correct) difference in the ratio *a/b*, where *a* and *b* are, respectively, the rectangle's horizontal and vertical side lengths. To ensure that aspect ratio judgements are based on a comparison of side lengths rather than the value of *a* or *b* alone, the area of the stimulus rectangle will be varied randomly between successive presentations.

Measurements will be carried out over a wide range of crossed and uncrossed disparities for static and for dynamic random noise. Ocular convergence will be monitored using nonious lines.

A luminance-defined rectangle with the same spatial sampling as the stereo rectangle will be created by switching off all dots outside the rectangle, and the above measurements repeated.

A motion-defined rectangle will be created by moving the dots inside and outside the rectangle at equal and opposite speeds, and the above measurements repeated.

2.2 **Experiment 2. Psychophysics: Orientation discrimination for cyclopean, luminance-defined and motion-defined bars.**

The procedures described above will then be repeated except that orientation discrimination for a bar will be measured.

2.3 **Experiment 3: Psychophysics: Vernier acuity for cyclopean, luminance-defined and motion-defined spatial form.**

Department of Psychology
FAX: (416) 736-5814

UNIVERSITÉ
YORK
UNIVERSITY

FACULTY OF ARTS
4700 KEELE STREET • NORTH YORK • ONTARIO • CANADA • M3J 1P3

The procedures described in 2.2.1 will be repeated except that vernier acuity for a bar will be measured.

2.4 **Experiment 4. Psychophysics: Aspect ratio discrimination, orientation discrimination and vernier acuity for spatial form defined by a combination of disparity and luminance contrast.**

The procedures described in 2.2.1 to 2.2.3 will be repeated with the stimuli defined by a combination of disparity and luminance contrast.

2.5 **Experiment 5. Psychophysics: Cross-adaptation of aspect ratio aftereffect between cyclopean, luminance-defined and motion-defined form.**

We previously discovered an aspect ratio adaptation aftereffect for luminance-defined form that transferred from rectangles to ellipses independently of size (Ref. 211). Here we will adapt to a luminance-defined rectangle and test for an aspect ratio aftereffect with luminance-defined, disparity-defined and motion-defined rectangles by constructing psychometric functions as in Ref. 211. Then we will repeat the procedure, but adapting to a disparity-defined rectangle and then again, but adapting to a motion-defined rectangle.

2.6 **Experiment 6. Psychophysics: Recognition and detection of texture-defined letters.**

Using temporal 2AFC, two texture patterns will be presented, one containing a texture-defined letter and the other no letter (See section 6.1.1). The subject's tasks will be (a) identify the letter and (b) state whether the letter

Department of Psychology
FAX: (416) 736-5814

UNIVERSITÉ
YORK
UNIVERSITY

FACULTY OF ARTS
4700 KEELE STREET • NORTH YORK • ONTARIO • CANADA • M3J 1P3

was presented in the first or second interval. Ten letters will be presented. This procedure will be repeated with one noise dot per texture line degrading visibility, then with two noise dots per letter line, and so on. Thresholds will be estimated from psychometric functions. Measurements will be made for 1 sec presentations with the same texture pattern throughout the 1-sec presentation, with ten new patterns per sec and with 70 new patterns per sec. Ten subjects will be used.

2.7 **Experiment 7. Psychophysics: Monocular and binocular cues to the perception of motion in depth; comparison of results for cyclopean and monocularly-visible targets.**

We will generate two dot patterns and view them dichoptically. A new dot pattern will be generated at 50 times per sec so as to create dynamic random noise and one pattern will be routed optically to the left eye and the other pattern to the right eye. It is necessary to use dynamic rather than static random noise because a moving target in static random noise breaks camouflage and would, therefore, be visible monocularly, while a moving target in dynamic random noise is not visible monocularly (Julesz, 1971).

A rectangular area within the dot pattern will be rendered visible by a relative displacement of the left and right eye's rectangles so as to create binocular disparity as described by Julesz (1971). First we will modulate the rectangle's size sinusoidally and using temporal 2AFC, separately measure the oscillation amplitude that gives just-detectable size oscillation and just

Department of Psychology
FAX: (416) 736-5814

UNIVERSITÉ
YORK
UNIVERSITY

FACULTY OF ARTS
4700 KEELE STREET • NORTH YORK • ONTARIO • CANADA • M3J 1P3

detectable motion-in-depth for a range of oscillation frequencies from 0.2 Hz upwards. Then we will oscillate disparity at fixed size and use 2AFC to measure the amplitude of disparity oscillation for just-detectable motion-in-depth. These experiments will be repeated at fixed values of mean disparity (crossed and uncrossed).

A pilot experiment using our new hardware dot generator indicates that motion-in-depth sensation generated by changing-disparity can be canceled by pitting changing-disparity against changing-size stimulation. This pilot result suggests that changing-size and changing-disparity signals converge at a single motion-in-depth stage. For sinusoidally oscillating disparity and changing-size we will use temporal 2AFC to measure the amplitude of size oscillation that cancels the sensation of motion-in-depth produced by a fixed amplitude of disparity oscillation for different oscillation frequencies. This experiment will be repeated for different fixed amplitudes of disparity oscillation. Then we will investigate dynamics in the time domain using transient (ramping) changes of disparity and changing-size. We will use temporal 2AFC to measure formally the ramping rates of change of size that cancels the sensation of motion-in-depth a fixed rate of change of disparity for different ramp durations. This experiment will be repeated for different fixed rates of change of disparity.

The above experimental protocols are the same as these used earlier for monocularly-visible targets (Ref. 85). By comparing our cyclopean data with

Department of Psychology
FAX: (416) 736-5814

UNIVERSITÉ
YORK
UNIVERSITY

FACULTY OF ARTS
4700 KEELE STREET • NORTH YORK • ONTARIO • CANADA • M3J 1P3

data for monocularly-visible dotted targets we will endeavour to distinguish between the processing underlying motion-in-depth perception that takes place after and before convergence of the signals from left and right eyes.

2.8 **Experiment 8. Psychophysics: Visual fields for time to contact judgements.**

This experiment follows on from Ref. 220. Consider a rigid object moving directly towards the eye at constant speed. The relation between the angular size of the object's retinal image (θ_t) and time (t) is given by

$$\tan \theta_t = \frac{\tan \theta_o}{1 - t / T_o} \quad \text{----------} \quad (1)$$

We will use our special purpose hardware to create a retinal image that exactly mimics an approaching object. Ten different values of time to collision will be where To is time to collision at time t = 0. As described previously (Ref. 220). presented, and subjects will be instructed to press one button if the simulated object would arrive sooner than the mean of the stimulus set and a second button if it would arrive later than the mean of the set (a procedure first described by McKee, 1981). As described below (Section 7.5, page 69 - 78) we will generate a 8 x 8 stimulus matrix and analyse it in two ways so as to demonstrate that subjects base their judgements on variations in $\theta/(d\theta/dt)$ rather than variations in $(d\theta/dt)$.

We construct a visual field perimeter with nonious line control of vergence and use it to measure discrimination threshold for time to contact at

Department of Psychology
FAX: (416) 736-5814

UNIVERSITÉ
YORK
UNIVERSITY

FACULTY OF ARTS
4700 KEELE STREET • NORTH YORK • ONTARIO • CANADA • M3J 1P3

the fovea and the following retinal locations: 2°, 4°, 8°, 16° left and right, up and down and the two obliques. Similar measurements will be made for 5 subjects for mean times to collision of 1 sec, 2 sec and 4 sec.

2.9 Experiment 9. **Psychophysics: Judgement of time to contact for textured targets; effect of mismatching rate of expansion of texture and object size.**

As in 2.8 we will generate a retinal image whose rate of change of size exactly mimics the retinal image of a rigid approaching object. This time, however, the retinal image will be textured. We will design an instrument based on an earlier design (Ref. 125) that will create texture whose density can be varied by indefinitely small amounts. We will measure discrimination threshold for time to collision with rate of expansion of texture and rate of expansion of size matched exactly as in real-world conditions, and then with a range of mismatch conditions. Specifically, we will use the following values of the ratio (rate of expansion of texture)/(rate of expansion of size) in the retinal image of the simulated object: 0.8; 0.9; 1.0; 1.2; 1.4.

2.10 **Experiment 10. Psychophysics: Comparison of time to collision judgements for cyclopean and monocularly-visible targets.**

As in 2.8 we will generate a retinal image whose rate of change of size exactly mimics the retinal image of a rigid approaching object. However, in 2.10 we will use our stereo dynamic random noise stimulator to ensure that the simulated object is perfectly camouflaged monocularly, and only visible in binocular view. This will ensure that all processing of time to collision

Department of Psychology
FAX: (416) 736-5814

UNIVERSITÉ
YORK
UNIVERSITY

FACULTY OF ARTS
4700 KEELE STREET • NORTH YORK • ONTARIO • CANADA • M3J 1P3

takes place in cyclopean vision, i.e, after the signals from the left and right eyes have converged. Discrimination threshold for time to contact will be measured using our 8 x 8 matrix method as in 6.2.8. Then we will switch off all dots outside the camouflaged stimulus so as to allow it to be seen monocularly, and repeat the experiment. By comparing the cyclopean and non-cyclopean thresholds we will attempt to separate the processing of time to collision that occurs before and after convergence of the signals from left and right eyes.

2.11 **Experiment 11. Psychophysics: Discrimination of the direction of motion in depth in different meridia using monocular and binocular cues.**

We will generate two bright squares using our special-purpose hardware (Ref. 220), and route one to the left eye and one to the right eye. Stereo motion in depth will be created by translating the squares on the Tektronix 608 monitors, and the direction of motion in depth will be simulated straightforwardly by adjusting the relative velocity of these translations as described previously (Refs. 34, 49). Simulating the monocular direction of motion in depth is more difficult, as we discuss next.

We have shown that an object moving along a straight line in depth creates a retinal image whose angular location (ϕt) on the retina varies with time (t) as follows

$$\tan \phi_t = \frac{n \tan \theta_o}{(T_o / t)-1} \quad \text{----------(2)}$$

Department of Psychology
FAX: (416) 736-5814

UNIVERSITÉ
YORK
UNIVERSITY

FACULTY OF ARTS
4700 KEELE STREET • NORTH YORK • ONTARIO • CANADA • M3J 1P3

where n is the number of object linear radii by which the centre of the object misses the eye's first nodal point, and θ_t is the object's angular radius at time t=0. At the same time the size of the retinal image grows progressively larger, as given by equation (1) above, i.e.

$$\tan \theta_t = \frac{\tan \theta_O}{1-(t / T_O)}$$

where θ_t is the objects' angular radius at the eye at time t=0 (Ref. 230).

We have also shown that the direction of motion in depth is given by

$$n = \left(\frac{d\phi}{dt}\right) / \left(\frac{d\theta}{dt}\right)$$

By means of arbitrary waveform generators (Wavetek Model 75) we will control the size and locations of the squares on the monitors so as to exactly mimic the retinal images of an approaching object.

Motion-in-depth along different trajectories will be mimicked by moving the rectangle across the CRT screen at different speeds and at the same time changing the rectangle's size. The resulting stimulus will be quantified in terms of the relative velocity of the rectangle's opposite edges. The rectangle's motion will be controlled by a PC (2AFC, method of constant stimuli). We will measure the just discriminable change of trajectory for a

Department of Psychology
FAX: (416) 736-5814

UNIVERSITÉ
YORK
UNIVERSITY

FACULTY OF ARTS
4700 KEELE STREET • NORTH YORK • ONTARIO • CANADA • M3J 1P3

wide range of trajectories in the horizontal, vertical and the two 45 deg oblique planes for a population of 20 control subjects in the following conditions. (a) binocular and monocular cues both available and matched exactly as in the real world for the particular viewing distance and target size; (b) only the binocular cue available; (c) only the monocular cue available.

2.12 **Experiment 12. Psychophysics: Detection and recognition of texture-defined letters, motion-defined letters and contrast-defined letters in control subjects and in patients with multiple sclerosis.**

We will obtain norms for detection and recognition of texture-defined letters, motion-defined letters and luminance-defined letters. We will use two-response temporal 2AFC along the lines of our previous work with motion-defined letters. Then we will test 20 patients with multiple sclerosis. All patients will have acuity of 6/12 or better and normal visual fields.

2.13 **Experiment 13. Psychophysics: Detection and recognition of texture-defined letters, motion-defined letters and luminance-defined letters in patients with neurosurgical removal of brain tissue.**

This study will be similar to 2.13 except that the patient group will be 20 patients with neurosurgical removal of cerebral tissue unilaterally. All patients will have acuity of 6/12 or better and normal visual fields.

2.14 **Experiment 14. Psychophysics: Comparison of monocular and binocular thresholds for recognising texture-defined letters in patients with documented brain lesions.**

Department of Psychology

FAX: (416) 736-5814

UNIVERSITÉ
YORK
UNIVERSITY

FACULTY OF ARTS

4700 KEELE STREET • NORTH YORK • ONTARIO • CANADA • M3J 1P3

A group of 20 control subjects will carry out the following protocol: (1) Measurement of noise threshold for detecting and recognising texture-defined letters in binocular vision; (2) measurement of speed threshold for detecting and recognising motion-defined letters; (3) measurement of contrast threshold for detecting and recognising luminance-defined letters. All the measurements will then be repeated for left monocular vision and right monocular vision. A group of 20 patients with documented (CAT scan or MRI) unilateral focal cerebral lesions will then carry out the same protocol. The value of (binocular threshold)/(best monocular threshold) will then be calculated for each threshold separately and each separate mean and SD calculated. Then we will find whether the ratios differ significantly for any of the thresholds. All these calculations will then be repeated for the patient group.

2.15 **Experiment 15. Neuromagnetism: Comparison of brain responses to color-defined and luminance-defined gratings.**

We will compare electric (VEP) and magnetic (MEG) responses to chromatic contrast and to luminance contrast. Equiluminant red and green gratings will be generated and superimposed in either 180 deg or 0 deg spatial phase, thus giving a red-green chromatic grating or a yellow luminance grating. The dominant wavelengths of the red and green lights will be selected to fall along one of the cardinal directions of color space. Grating contrast will be abruptly increased and decreased with one sec periodicity.

Department of Psychology
FAX: (416) 736-5814

UNIVERSITÉ YORK UNIVERSITY
FACULTY OF ARTS
4700 KEELE STREET • NORTH YORK • ONTARIO • CANADA • M3J 1P3

First, response amplitude will be plotted versus red/green ratio on either side of equiluminance to check that the response is a true chromatic response. Responses produced by a 4 x 4 deg chromatic grating presented to the lower left visual macular quadrant will be recorded from about 56 coil locations and maps constructed. If any component is a close approximation to a single dipole distribution, the location of the single equivalent dipole will be calculated. This procedure will then be repeated for the remaining three quadrants. Then the entire procedure will be repeated for the luminance grating. Waveforms and source locations will be compared and discussed in terms of the visual areas in macaque. Then the entire procedure will be repeated for a yellow-blue grating. Three color-normal subjects will be tested.

Preliminary experiments show that, at some locations on the head, the MEG response to red-green chromatic grating is larger than the MEG response to the luminance grating and has a different waveform.

2.16 **Experiment 16. Neuromagnetism: Objective measurement of orientation and spatial frequency tuning of human brain cells sensitive to color-defined and luminance-defined gratings.**

We will generate a red-green chromatic grating of spatial frequency S1c/deg that is counterphase-modulated at F_1 Hz, and superimpose this on a second red-green chromatic grating of the same orientation and spatial frequency that is counterphase-modulated at F_2 Hz. The stimulus field will be 4 deg in diameter and placed in one of the macular quadrants. The intent is to

Department of Psychology
FAX: (416) 736-5814

UNIVERSITÉ
YORK
UNIVERSITY

FACULTY OF ARTS
4700 KEELE STREET • NORTH YORK • ONTARIO • CANADA • M3J 1P3

stimulate a relatively homogeneous retinal area and to minimize complications due to cortical folding. The red and green wavelengths will be chosen to fall along one of the cardinal axes in color space. While subjects view the grating we will subject the MEG to high-resolution zoom-FFT. By varying the relative spatial phase of the two gratings we will search for cross-modulation response components that are independent of relative spatial phase, and thus depend on the spatial frequency spectrum of the stimulus, but not on any particular luminance distribution on the retina. (We developed this approach in a previous study on luminance gratings and found that $2F_1 + 2F_2$ was such a component, at least for luminance gratings). Such a component must be generated by neurons that "see" both chromatic gratings. To study the spatial frequency bandwidth of neurons sensitive to a vertical S_1 c/deg red-green grating, we will plot the amplitude of the designated response component versus the spatial frequency of the second grating. To study the orientation tuning bandwidth of neurons sensitive to a vertical S_1 c/deg grating, the orientation of the second grating will be varied while holding its spatial frequency a little different from S_1 c/deg. To study the temporal tuning bandwidth of neurons sensitive to a vertical S_1 c/deg grating the temporal frequency of the second grating will be varied while holding its orientation vertical and its spatial frequency a little different from S_1 c/deg. We will then measure the spatial frequency, orientation and temporal frequency tuning bandwidths for a vertical yellow luminance

Department of Psychology
FAX: (416) 736-5814

UNIVERSITÉ
YORK
UNIVERSITY

FACULTY OF ARTS
4700 KEELE STREET • NORTH YORK • ONTARIO • CANADA • M3J 1P3

grating of frequency S_1 c/deg using the above procedure. We will compare these bandwidths at 1.5 c/deg, 4 c/deg and 8 c/deg. The basis of this approach is described in Refs. 167 & 178 and on pp. 420 - 427 of my 1989 book. Results will be discussed in terms of the corresponding bandwidths of neurons in monkey visual cortices.

2.17 **Experiment 17. Neuromagnetism: Objective measurement of the responses of human brain cells to binocular depth and stereomotion.**

For MEG experiments it is difficult to use a cyclopean depth stimulus generated by conventional passive optics as in 6.2.1—6.2.5 above, because the MEG dewar requires a prone position of the subject and variable head orientations. It is not possible to use active goggles to route the signals to left and right eyes because of interference. We will solve the problem of cyclopean stimulation as follows. The subject, located inside the magnetically-shielded room will wear passive circularly-polarized goggles, and the computer-generated stimulus will be viewed through a liquid crystal cell outside the room whose sense of circular polarization will be switched synchronously with the frame rate. By using dynamic rather than static random dots we will ensure that transitions between depth planes are not visible monocularly. We will generate a random dot pattern containing cyclopean gratings or checks and will alternate this stimulus with a zero-depth dot pattern. We will measure average transient responses for MEG and EEG for crossed and uncrossed disparities from each of four quadrants of the visual field. A range

Department of Psychology
FAX: (416) 736-5814

UNIVERSITÉ
YORK
UNIVERSITY

FACULTY OF ARTS
4700 KEELE STREET • NORTH YORK • ONTARIO • CANADA • M3J 1P3

of check sizes and spatial frequencies will be explored. Ocular vergence will be monitored using nonious lines. We will map the MEG response and, if any components fit a single-dipole field, we will estimate the location of the equivalent dipole.

As a control, we will carry out a similar experiment for vertical disparities. Also, we will induce periodic vergence changes and map the time-averaged MEG response. Three stereo-normal subjects will be tested. Results will be discussed in terms of single-unit responses to stereo stimulation in macaque.

In further experiments we will find which areas of human cortex are selectively sensitive to the direction of stereomotion-in-depth and compare their properties with the properties of stereomotion channels(Refs. 34, 49) and motion-in-depth neurons (Refs. 67, 108, 109). We will use areas of motion-in-depth "blindness" in control subjects to check that neuromagnetic responses to changing disparity are associated with motion-in-depth perception.

2.18 **Experiment 18. Neuromagnetism: Objective localization of an audio-visual convergence area in human brain cortex.**

An amplitude-modulated (AM) tone of modulation frequency F_1 Hz will be fed to a subject's ear while the subject views a light flickering at F_2 Hz. The MEG will be subjected to high-resolution zoom-FFT and a search made for terms of frequency ($nF_1 \pm MF_2$). These terms must originate in neurons that receive both auditory and visual input. We will then map these terms. If

Department of Psychology
FAX: (416) 736-5814

UNIVERSITÉ
YORK
UNIVERSITY

FACULTY OF ARTS
4700 KEELE STREET • NORTH YORK • ONTARIO • CANADA • M3J 1P3

any map approximates a single dipole field we will compute the equivalent dipole location, thus locating an audio-visual convergence area. Results will be discussed in terms of known audio-visual convergence areas in macaque.

Pilot experiments have already revealed an ($nF_1 \pm mF_2$) term, but it was weak, and we need to vary F_1 and also F_2 to find optimum values.

2.19 **Experiment 19. Operational tests: Evaluation of our laboratory test for glare sensitivity in predicting intersubject differences in pilot performance in high-glare, low-contrast conditions using ground-based flight simulators and the flying simulator.**

We will administer our laboratory glare susceptibility test (Refs. 195 & 208) to a group of 20 pilots. These pilots will then use a flight simulator to test their ability to see, while landing, objects of different contrasts without glare and in two kinds of high-glare environments, one with a point glare source (simulating the sun) and one with diffuse glare (as in low level flight over snow). We will use CAE commercial airline heavy jet simulators, the University of Toronto simulator and the NRC of Canada flying simulator. We will correlate intersubject differences in the laboratory and tests with intersubject differences in the flying tests.

2.20 **Experiment 20. Operational tests: Collision avoidance in aviation; pilot performance studied using ground-based flight simulators and the flying simulator.**

Department of Psychology
FAX: (416) 736-5814

UNIVERSITÉ YORK UNIVERSITY
FACULTY OF ARTS
4700 KEELE STREET • NORTH YORK • ONTARIO • CANADA • M3J 1P3

We will administer our laboratory tests for time to collision and for sensitivity to rate of expansion, i.e. looming (Ref. 220) and our motion-defined letter test (Ref. 190) to a group of 20 pilots. These pilots will then use a flight simulator to test their ability to avoid air to air collision and to avoid collision with terrain features at low altitude. We will use the CAE commercial airline heavy jet simulators, the University of Toronto simulator and the NRC of Canada flying simulator. We will compare intersubject differences in the laboratory and flying tests.

3 STATUS OF THE RESEARCH EFFORT

During the period 1993 to December 1996, 37 papers in refereed journals, 3 book chapters,and 2 chapters in Conference Proceedings have been published. A total of 12 abstracts were presented at the 1994, 1995 and 1996 ARVO meetings. Science Citation Index counts are as follows: 194 (1991), 251 (1992), 239 (1993), 255 (1994), 329 (1995).

Note: This report is organised as follows. A ground-based simulator study is reported in Section 3.1 and a paper on disorientation in aviation is summarized in Section 3.2. Experimental work on discriminating the direction and speed of motion in depth using binocular cues only is reported in Section 3.3. Section 3.4 reports a comparison of foveal and peripheral discriminations of time to collision with an approaching object.

In a series of previous reports I described work on the visual processing of spatial form defined by luminance contrast and the visual processing of

Department of Psychology
FAX: (416) 736-5814

UNIVERSITÉ
YORK
UNIVERSITY

FACULTY OF ARTS
4700 KEELE STREET • NORTH YORK • ONTARIO • CANADA • M3J 1P3

spatial form defined by motion contrast. This work is now extended to the visual processing of spatial form defined by binocular disparity, i.e. cyclopean form (Sections 3.7 - 3.8) and the visual processing of spatial form defined by texture contrast (Sections 3.9 - 3.13). Research on visual channeling and the independence of visual processing is reported in Sections 3.14 & 3.16. Magnetic and electrical recording from the human brain is reported in Sections 3.17 - 3.19. Theoretical and experimental research on the auditory processing of complex sounds is reported in Sections 3.20 - 3.21.

3.1 Ground-based flight simulator study.

The experiment is completed. A paper entitled "Collision avoidance: a helicopter simulator study" by R. Kruk & D. Regan has been published in Aviation, Space & Environmental Medicine (1996) 67, 111-114 (Ref. 254).

The broad issue here is collision avoidance, and in particular "when will it hit me?". This experiment addresses a pilot's ability to use the retinal image correlate of time to collision expressed by Hoyle's equation

$$T \approx \theta/(d\theta/dt) \text{ ---------- } (1)$$

where T is the time to collision with a rigid nonrotating object of angular diameter θ approaching at constant speed along the line of sight (Hoyle, 1957).

It will be useful to distinguish the following four kinds of collision between a helicopter and an external object (e.g. a terrain feature or a second aircraft). (1) Ownship stationary, an object approaching at constant speed on a collision course. (2) Ownship moving at constant speed towards a stationary

Department of Psychology
FAX: (416) 736-5814

UNIVERSITÉ
YORK
UNIVERSITY

FACULTY OF ARTS
4700 KEELE STREET • NORTH YORK • ONTARIO • CANADA • M3J 1P3

object. (3) Ownship and an object moving towards each other, both at constant speed. (4) Ownship and an object moving on the same course in the same direction, both at constant speed but ownship moving faster than the object.

The experiment was carried out using the Simulator Training Research Advanced Testbed for Aviation (STRATA) at the Army Research Institute (ARI) at Fort Rucker, Alabama. The STRATA is a research simulator based upon the AH-64 Apache Helicopter.

The display system used was a CAE fibre-optic-helmet-mounted-display system (FOHMD) providing a low resolution field (5 arcmin/pixel) 66° vertical by 82.5° horizontal to each eye, overlapped 38° to provide a total instantaneous field of view (FOV) of 66° x 127°. A high resolution field (1.5 arcmin/pixel) 19° vertical by 25° horizontal is centered in the overlap region. In the present study 3 FOV were used: FOV1 was 66° x 127° with centered 19° x 25° high resolution insert. FOV2 was 19° x 25° high resolution insert only. FOV3 was 3° x 3° in the centre of the high resolution insert. While the system is capable of stereoscopic image presentation, in the present study the image was bi-ocular (i.e. exactly the same image presented to each eye in the overlap area). Average scene luminance with the daytime database used for the study was 30 Ft.L.

The image was a real time (60 Hz update) of a valley near MESA, Arizona in daytime. It was generated by an Evans and Sutherland ESIG 1000

Department of Psychology
FAX: (416) 736-5814

UNIVERSITÉ
YORK
UNIVERSITY

FACULTY OF ARTS
4700 KEELE STREET • NORTH YORK • ONTARIO • CANADA • M3J 1P3

Image Generator. The targets were a grey CH-53 heavy helicopter and a green OH-58 light helicopter.

The altitude of own aircraft and the target was always 15 ft above ground. The pilot initiated each trial by pressing a button on the cyclic (control column). From time 0 to +10 seconds ownship either remained in a hover, accelerated to 30 knots (50 ft/sec, 30.5 m/sec) or accelerated to 60 knots (100 ft/sec, 60.1 m/sec). Ownship speed was constant from time +10 to +15 sec at 0, 30 or 60 knots. At +15 seconds the target appeared at a range of 300, 400, 600, 800 or 1200 feet (91.4, 122, 183, 244 or 366 m) and it could be in the hover, moving towards ownship at 30 knots or 60 knots, or flying backwards at 30 knots. Closing speed could be 30, 60, or 90 knots. Maximum time between target appearance and collision was 8 seconds, and minimum was 5.5 seconds. At either 2, 2.5 or 3 seconds before collision (randomly selected) the target disappeared. Pilots were instructed to extrapolate the closure rate of the target and press the trigger on the cyclic at the time when collision would have occurred. Two seconds after the trigger pull was recorded the system reinitialized the ownship to the hover and a 2000 Hz tone would sound to indicate that another trial could commence at pilot command. Six qualified U. S. Army Helicopter pilots, with experience ranging from 470 to 1650 hours (mean 765) participated in the study.

Department of Psychology

FAX: (416) 736-5814

UNIVERSITÉ
YORK
UNIVERSITY

FACULTY OF ARTS

4700 KEELE STREET • NORTH YORK • ONTARIO • CANADA • M3J 1P3

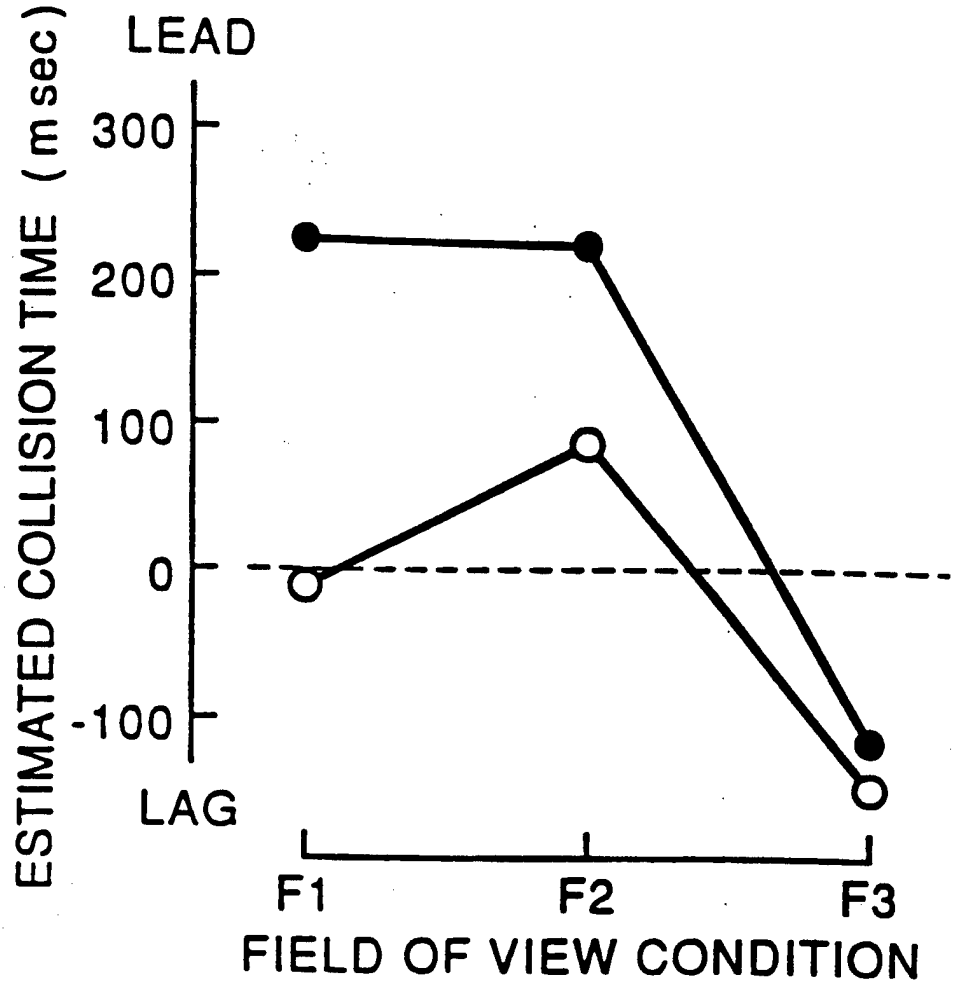

Figure 1 Estimated time to collision in msec (ordinate) versus field of view (FOV). FOV1, FOV2 and FOV3 were, respectively, 66 (vertical) x 127°, 19 x 25° and 3 x 3°. Filled symbols: ownship speed 60 knots, target stationary, closing speed 60 knots. Open symbols: ownship stationary, target speed 60 knots, closing speed 60 knots. (60 knots is 61 m/sec).

Department of Psychology
FAX: (416) 736-5814

UNIVERSITÉ
YORK
UNIVERSITY

FACULTY OF ARTS
4700 KEELE STREET • NORTH YORK • ONTARIO • CANADA • M3J 1P3

The difference in time (milliseconds) and range (feet) between pilot's trigger press and (system calculated) actual collision were collected for each trial. These data were subjected to a repeated measures, within subjects analysis of variance (ANOVA).

Fig. 1 compares findings in the conditions that closing speed was produced either entirely by ownship motion or entirely by target motion. Data were collapsed for both targets and for all six pilots. Estimated times of collision are plotted as ordinate. Zero on the ordinate is the time at which collision with the target aircraft would have occurred. The three conditions plotted along the abscissa are the large, intermediate and small fields of view (FOV1, FOV2 and FOV3 respectively). All pilots reported that, in the large and intermediate field of view conditions, ownship motion resulted in a strong sensation of self-motion. In the smallest field of view condition, however, even the highest ownship speed produced little or no sensation of self-motion.

Filled symbols in Fig. 1 plots estimated collision times for a stationary target and ownship forward speed of 60 knots (30.5 m/sec). In the large and intermediate field of view conditions, pilots estimated that collision with the stationary target would occur roughly 200 msec before the actual time of collision. Findings were different in the case of ownship stationary and the target approaching at 60 knots (open symbols). In that case, estimate of collision time showed considerably less lead in the large and intermediate

Department of Psychology

FAX: (416) 736-5814

UNIVERSITÉ
YORK
UNIVERSITY

FACULTY OF ARTS

4700 KEELE STREET • NORTH YORK • ONTARIO • CANADA • M3J 1P3

field of view conditions. When the smallest field of view was used, estimates were the same whether the 60 knot closing speed was produced entirely by ownship motion or entirely by target motion. Both lagged by roughly 150 msec. A possible reason for the lag is that the small field of view was so small that the angular size of the larger target exceeded the field of view during part of its approach so that the retinal image information expressed in equation (1) would have been degraded.

Our main finding is that a pilot's estimate of time to collision depends on the relative contributions of closing speed to ownship speed and of target speed. For example, estimates of time to collision lead more when a 60 knot (61 m/sec) closing speed is produced entirely by ownship motion than when it is produced by target motion when our 66° x 127° and 19° x 25° fields of view are used. This is surprising: one would not necessarily expect any difference in time to contact estimation in the ownship-only motion and target-only motion conditions because the closing speeds are identical and an accurate retinal image correlate of time to contact is available in both conditions (see equation 1). We assume that too-short estimates are caused by the vection-induced impression of self-motion that is present in the ownship-only motion but not in the target-only motion condition. This suggestion is consistent with the finding that estimates in the two conditions were similar when the smallest field of view was used; vection was weak or absent for the smallest field of view.

Department of Psychology
FAX: (416) 736-5814

UNIVERSITÉ YORK UNIVERSITY
FACULTY OF ARTS
4700 KEELE STREET • NORTH YORK • ONTARIO • CANADA • M3J 1P3

3.2 *A review entitled "Spatial orientation in aviation: Visual contributions" by D. Regan has been published in the Journal of Vestibular Research (Ref. 248).*

3.3 Binocular judgements of the direction of an approaching object

One paper entitled "Binocular correlates of the direction of motion in depth" by D. Regan has been published in Vision Research, 1993, 33, 2359-2360. A second paper entitled "Discrimination of the direction and speed of motion in depth from binocular information alone" by C. Portfors-Yeomans and D. Regan is in press in the Journal of Experimental Psychology: Human Perception and Performance, and the findings reported to ARVO 1995.

The broad issue here is collision avoidance and in particular "will it hit me or miss me?". This experiment addresses a subject's ability to judge the direction of motion in depth of a monocularly-visible approaching object using binocular cues only.

The background is as follows. We showed theoretically that (Ref. 231), for motion within the plane that contains the eyes, the direction (β in Fig. 2) of an object's motion in depth given by

$$\beta \approx \tan^{-1}\left[\frac{I\{(d\phi/dt)_R + (d\phi/dt)_L\}}{2D(d\delta/dt)}\right] \approx \tan^{-1}\left[\frac{I(d\phi/dt)}{D(d\delta/dt)}\right] \text{ ---------- (2)}$$

and

$$\beta \approx \tan^{-1}\left(\frac{I\{[(d\phi/dt)_R / (d\phi/dt)_L] + 1\}}{2D\{[(d\phi/dt)_R / (d\phi/dt)_L] - 1\}}\right) \text{ ---------- (3)}$$

Department of Psychology
FAX: (416) 736-5814

UNIVERSITÉ
YORK
UNIVERSITY

FACULTY OF ARTS
4700 KEELE STREET • NORTH YORK • ONTARIO • CANADA • M3J 1P3

Equations (2) and (3) indicate that, for an object in the straight-ahead position, there are two mathematically-equivalent binocular cues to the direction of motion in depth, namely the ratio $(d\phi/dt)/(d\delta/dt)$, and the ratio $(d\phi/dt)_R/(d\phi/dt)_L$, where $d\delta/dt$ is the rate of change of binocular disparity, and $d\phi/dt$ is the angular velocity of the object's binocularly-fused retinal image, $(d\phi/dt)_R$ is the angular speed of the object's retinal image in the right eye, and $(d\phi/dt)_L$ in the left eye. For motion within the plane perpendicular to the plane that contains the eyes only the $(d\phi/dt)/(d\delta/dt)$ cue is available.

Previous research had been restricted to motion in depth within the horizontal meridian where the two cues are confounded. Nothing was known about binocular discrimination of the detection of motion in depth for motion within the vertical meridian, and little was known about the relative importance of these two cues for motion within the horizontal meridian.

Any given trial consisted of two presentations. The first was always a reference stimulus. The second was one of 64 test stimuli. Each of the 64 test stimuli comprised a different combination of 8 values of $[(d\phi/dt)/(d\delta/dt)]$ and 8 values of speed. Speed and direction [i.e. $(d\phi/dt)/(d\delta/dt)$] were orthogonal in stimulus space, i.e. there was zero correlation between the two variables. The speed and the value of $[(d\phi/dt)/(d\delta/dt)]$ for the reference stimulus were equal to the means for the 64 test stimuli. Subjects were instructed signal (1)

Department of Psychology
FAX: (416) 736-5814

UNIVERSITÉ
YORK
UNIVERSITY

FACULTY OF ARTS
4700 KEELE STREET • NORTH YORK • ONTARIO • CANADA • M3J 1P3

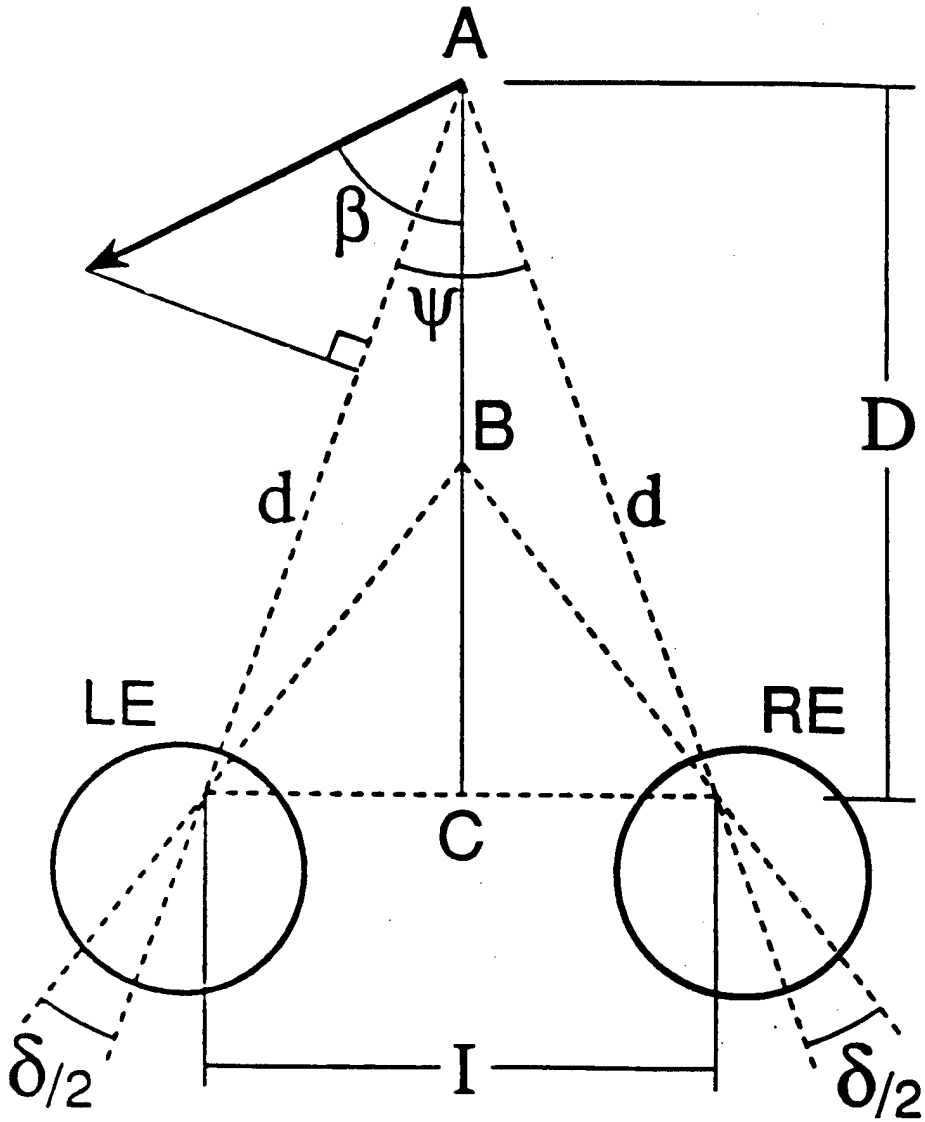

Figure 2 Geometry of binocularly-viewed motion in depth. LE, RE: left eye, right eye. N_L, N_R: first nodal points of left and right eyes respectively. The heavy arrowed line represents the velocity of an object at point A moving in a straight line at constant speed V. Point B is midway between the eyes, and AC=D.

Department of Psychology

FAX: (416) 736-5814

UNIVERSITÉ
YORK
UNIVERSITY

FACULTY OF ARTS

4700 KEELE STREET • NORTH YORK • ONTARIO • CANADA • M3J 1P3

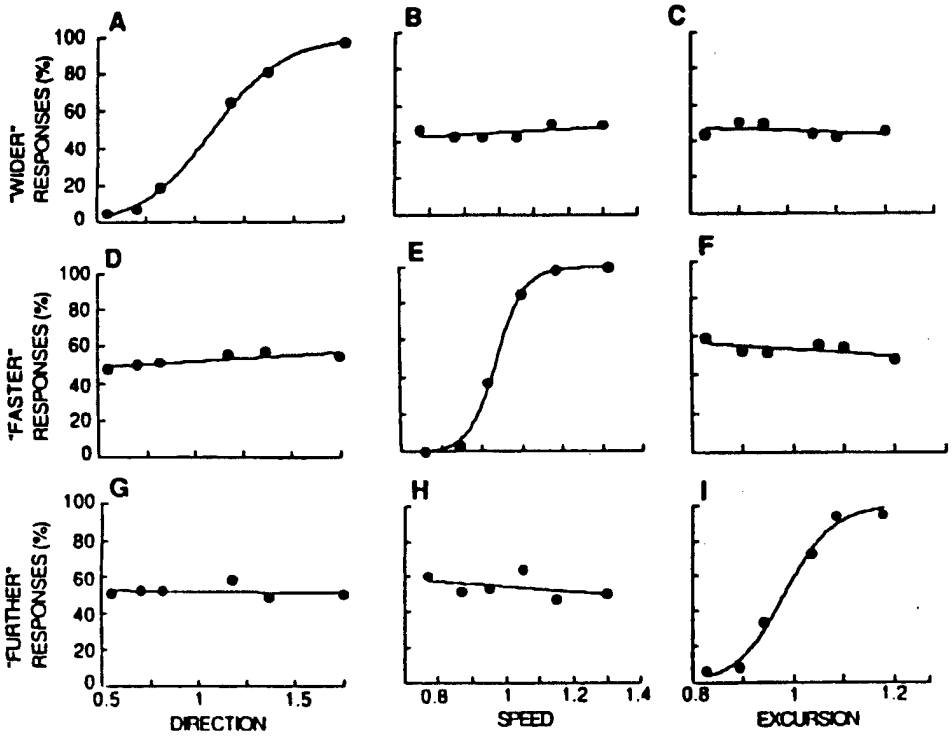

Figure 3 A-C: The percentage of "wider of the head than the reference trajectory" responses is plotted versus the task-relevant variable $(d\phi/dt)/(d\delta/dt)$ in A, versus the task-irrelevant variable $d\delta/dt$ in B, and versus the task-irrelevant variable $\Delta\delta$ in C. D-F: The percentage of "faster than the reference" responses is plotted versus the task-irrelevant variable $(d\phi/dt)/(d\delta/dt)$ in D, versus the task-relevant $d\delta/dt$ variable in E, and versus the task-irrelevant variable $\Delta\delta$ in F. G-I: The percentage of "excursion farther than the reference" responses is plotted versus the task-irrelevant variable $(d\phi/dt)/(d\delta/dt)$ in G, versus the task-irrelevant variable $d\delta/dt$ in H and versus the task-relevant variable $\Delta\delta$ in I. All three variables are expressed as fractional departures from the reference value. The reference values of $(d\phi/dt)/(d\delta/dt)$, $d\delta/dt$ and $\Delta\delta$ were, respectively, 0.6 deg, 0.4 deg/s and 11 min arc (1.0 on the abscissae).

Department of Psychology

FAX: (416) 736-5814

UNIVERSITÉ
YORK
UNIVERSITY

FACULTY OF ARTS

4700 KEELE STREET • NORTH YORK • ONTARIO • CANADA • M3J 1P3

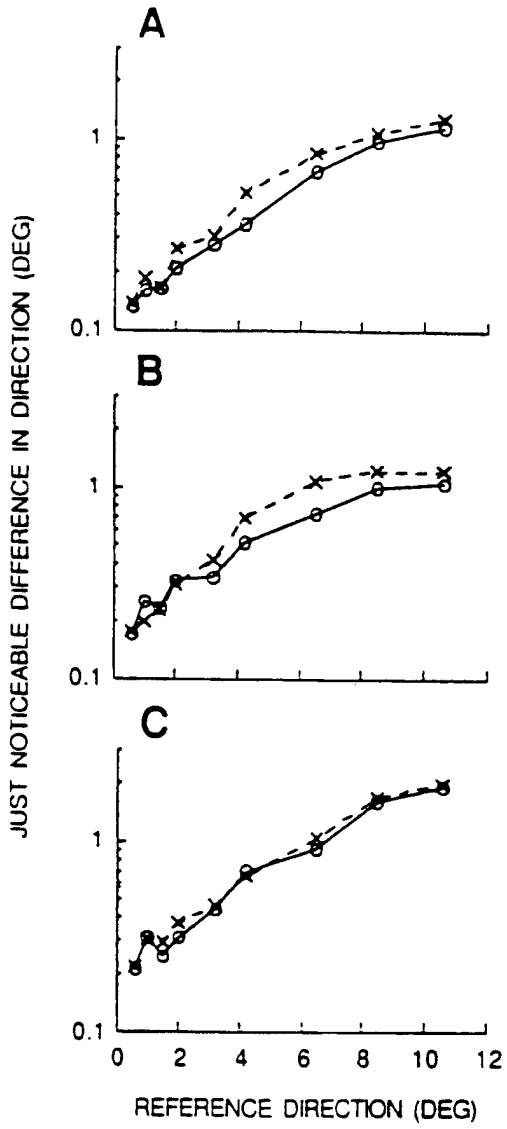

Figure 4 Discrimination threshold for simulated direction (β) are plotted as ordinate versus simulated reference direction (β_{REF}). Task-relevant thresholds for horizontal and vertical meridians are shown, respectively, as m and X. A: Observer 1. B: Observer 2. C: Observer 3.

Department of Psychology
FAX: (416) 736-5814

UNIVERSITÉ
YORK
UNIVERSITY

FACULTY OF ARTS
4700 KEELE STREET • NORTH YORK • ONTARIO • CANADA • M3J 1P3

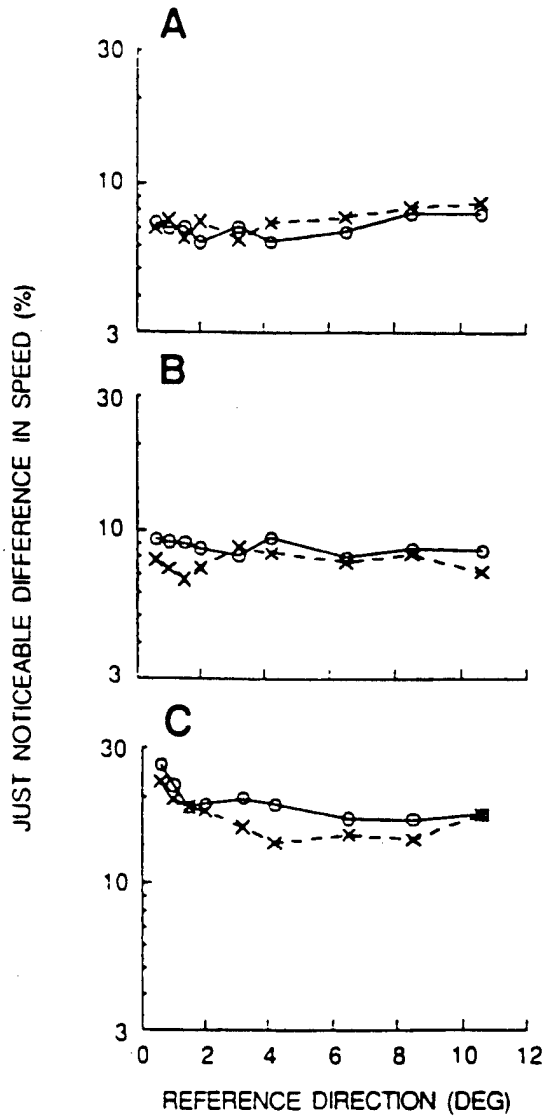

Figure 5 Discrimination thresholds for simulated speed (S) are expressed as a percentage of the reference speed (S_{REF}), and plotted as ordinate versus simulated reference direction(β_{REF}). Task-relevant thresholds for horizontal and vertical meridians are shown, respectively, as m and X. A: Observer 1. B: Observer 2. C: Observer 3.

Department of Psychology
FAX: (416) 736-5814

UNIVERSITÉ
YORK
UNIVERSITY

FACULTY OF ARTS
4700 KEELE STREET • NORTH YORK • ONTARIO • CANADA • M3J 1P3

whether the test stimulus would pass wider of the head than the reference and (2) whether the test stimulus was faster than the reference.

Data were collected for 36 different reference trajectories, 18 for motion within the plane countering the eyes and 18 for motion perpendicular to that plane.

In a control experiment we required observers to make the following three discrimination after each trial. (a) the direction of motion; (b) the speed of motion; (c) the disparity displacement (excursion). We used a set of 216 test stimuli comprising 6 values of direction [i.e. $(d\phi/dt)/(d\delta/dt)$], 6 values of speed $(d\delta/dt)$ and 6 values of disparity excursion $(\Delta\delta)$. These three variables were orthogonal within a set of 216 stimuli. The three sets of responses were each analysed along three stimulus directions giving the 9 psychometric functions shown in Fig. 3A-I. When the task was to discriminate direction the psychometric function was steep when plotted with respect to direction (Fig. 3A) but flat when plotted with respect to the other two variables. We conclude that observers ignored speed and excursion when discriminating direction. Fig. 3D-F and G-I support corresponding conclusions for speed and excursion discriminations.

We used stepwise multiple regression to show that when discriminating the direction of motion in depth, observers based their discriminations on the ratio $(d\phi/dt)/(d\delta/dt)$ and totally ignored trial-to-trial variations in the frontal plane component of speed $(d\phi/dt)$ and in $(d\delta/dt)$ and

Department of Psychology
FAX: (416) 736-5814

UNIVERSITÉ YORK UNIVERSITY
FACULTY OF ARTS
4700 KEELE STREET • NORTH YORK • ONTARIO • CANADA • M3J 1P3

in displacement $\Delta\delta$ and in displacement $\Delta\phi$ and in the speed of the left or right eye's retinal image alone. We used stepwise multiple regression to show that, when discriminating speed, observers based their discriminations on $d\delta/dt$ and totally ignored trial-to-trial variations in $d\phi/dt$, $\Delta\delta$, $\Delta\phi$ and in the speed of either eye's retinal image alone. Direction discrimination thresholds and speed discrimination thresholds were the same for motion within horizontal and vertical meridians. Fig. 4A - C and Fig. 5A - C respectively show how direction discrimination thresholds and speed discrimination thresholds varied with reference direction (β in Fig. 2) for three observers.

3.4 Time to collision judgements in foveal and peripheral vision

This experiment is completed. A paper entitled "Visual processing of looming and time to contact throughout the visual field" by D. Regan & A. Vincent has been reported to ARVO 1994 and published in Vision Research (1995) 35, 1845-1857 (Ref. 235).

The broad issue is collision avoidance in real aircraft. This experiment addresses the question of a subject's ability to judge time to collision when the subject does not gaze directly at the approaching object, but rather views the object in peripheral vision. No previous information was available on this question because all previous studies were restricted to foveal vision.

First, we addressed the point that the rate of expansion of an object's retinal image does not indicate time to collision. For example, deg/sec rate of retinal image expansion for an object 20ft wide is twice the rate of expansion

Department of Psychology
FAX: (416) 736-5814

UNIVERSITÉ
YORK
UNIVERSITY

FACULTY OF ARTS
4700 KEELE STREET • NORTH YORK • ONTARIO • CANADA • M3J 1P3

for an object 10ft wide, even though they are at the same distance and approaching at the same speed with the same time to collision. To judge time to collision (T) for an object of unknown size on the basis of equation (1) above [i.e. $T \approx \theta/(d\theta/dt)$], a subject must respond to the ratio $\theta/(d\theta/dt)$ independently of variations in retinal image size (θ) and rate of expansion ($d\theta/dt$). We showed that this can be done using the following procedure.

An approaching object was simulated by generating a square on a monitor using electronics of our own design that have been described elsewhere (Ref. 220). The size of the square varied according to the equation

$$\tan \theta_t = \frac{\tan \theta_0}{1-t/T_0} \quad \text{----------} \quad (4)$$

where $2\theta_t$ was the square's angular subtense at time t, and $2\theta_0$ & T_0 were, respectively, the square's angular subtense and time to collision at time t=0. Equation (4) is depicted graphically in Fig. 6.

Experiment 1

Psychophysical methods

The rationale of the psychophysical method can be understood by reference to Fig. 6. The three curves are for times to contact of T_0, $2T_0$ and $3T_0$ respectively, and the starting diameter (i.e., $2\theta_0$) is arbitrarily set at 2 deg.

Suppose that we presented a subject with several values of time to contact as illustrated in Fig. 6, four of which were shorter than 2.0 sec and four of which were longer than 2.0 sec, and measured the just-noticeable difference from 2.0 sec. We would be unable to conclude that the discrimination

Department of Psychology

FAX: (416) 736-5814

UNIVERSITÉ
YORK
UNIVERSITY

FACULTY OF ARTS

4700 KEELE STREET • NORTH YORK • ONTARIO • CANADA • M3J 1P3

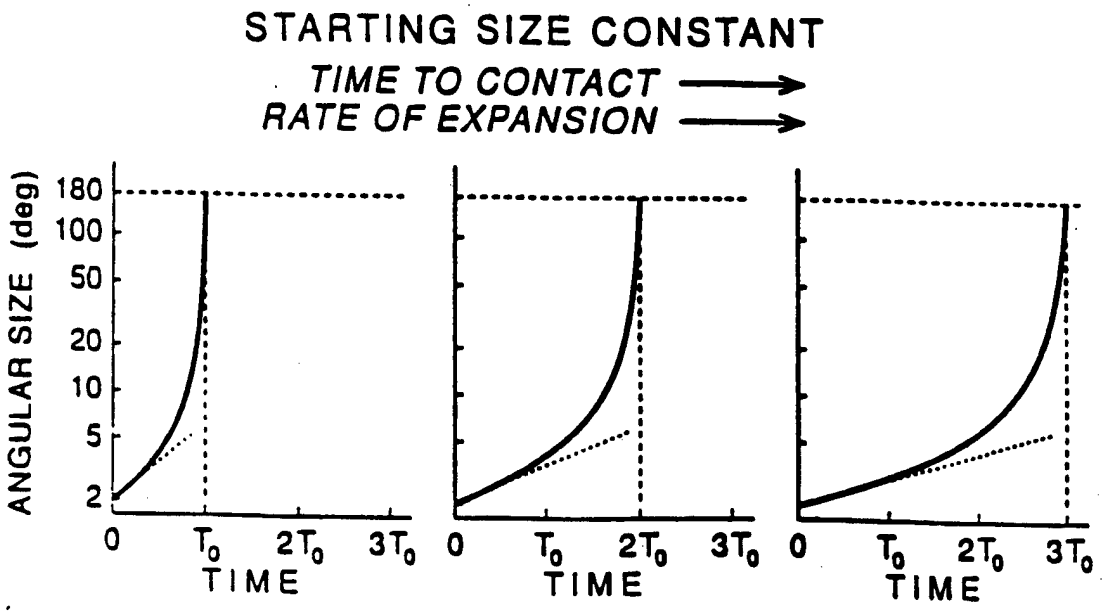

Figure 6 The angular size of the retinal image of a rigid spherical object that is moving at constant speed along the line of sight (ordinate) is plotted versus time (abscissa). Curves are shown for three times to contact: T_0, $2T_0$ and $3T_0$. The dotted lines illustrate that the initial rate of expansion of the retinal image is inversely proportional to the time to contact. Starting size is arbitrarily taken to be 2 deg.

Department of Psychology

FAX: (416) 736-5814

UNIVERSITÉ
YORK
UNIVERSITY

FACULTY OF ARTS

4700 KEELE STREET • NORTH YORK • ONTARIO • CANADA • M3J 1P3

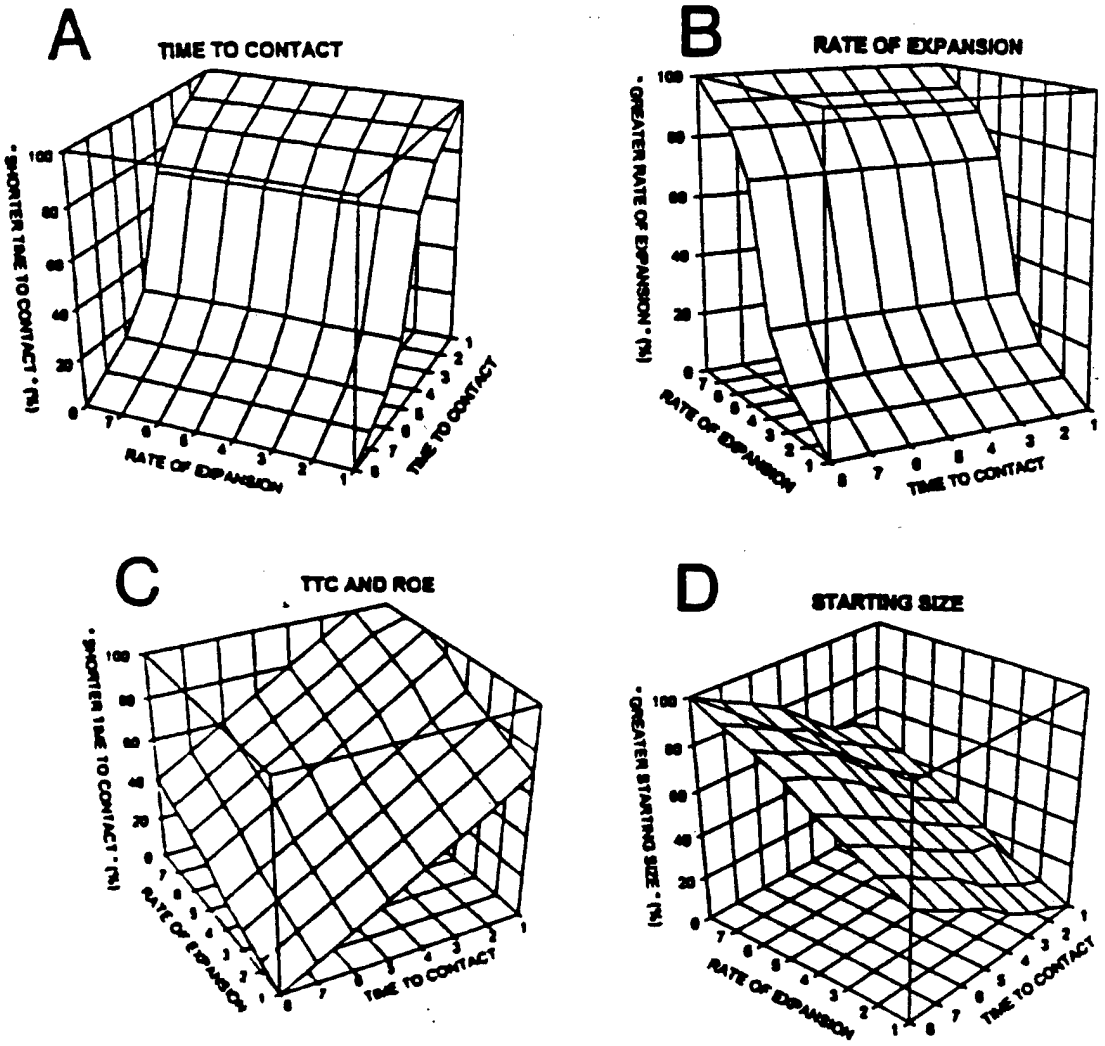

Figure 7 A-D: Predicted response patterns for (A) discriminations of time to contact (TTC), (B) discriminations of rate of expansion (ROE), (C) discriminations of TTC assuming that variations of TTC produce illusory variations in perceived ROE so that variations in ROE and TTC are completely confounded and (D) discriminations of starting size (SS).

Department of Psychology

FAX: (416) 736-5814

UNIVERSITÉ
YORK
UNIVERSITY

FACULTY OF ARTS

4700 KEELE STREET • NORTH YORK • ONTARIO • CANADA • M3J 1P3

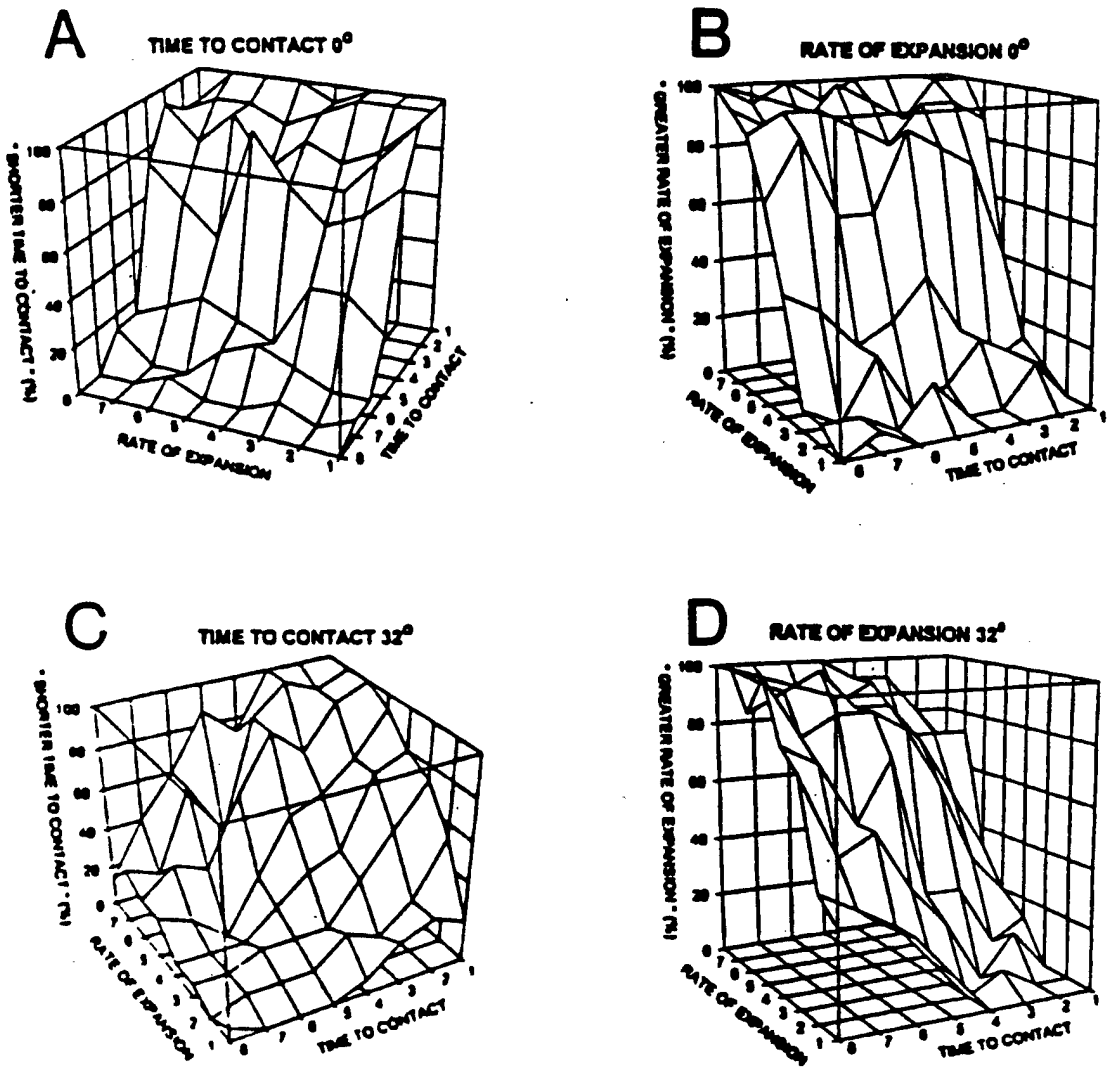

Figure 8 A, C: Empirical response patterns for discriminating time to contact (TTC) at 0 deg and 32 deg eccentricity respectively. B, D: Empirical response patterns for discriminating rate of expansion (ROE) at 0 deg and 32 deg eccentricity respectively.

Department of Psychology

FAX: (416) 736-5814

UNIVERSITÉ
YORK
UNIVERSITY

FACULTY OF ARTS

4700 KEELE STREET • NORTH YORK • ONTARIO • CANADA • M3J 1P3

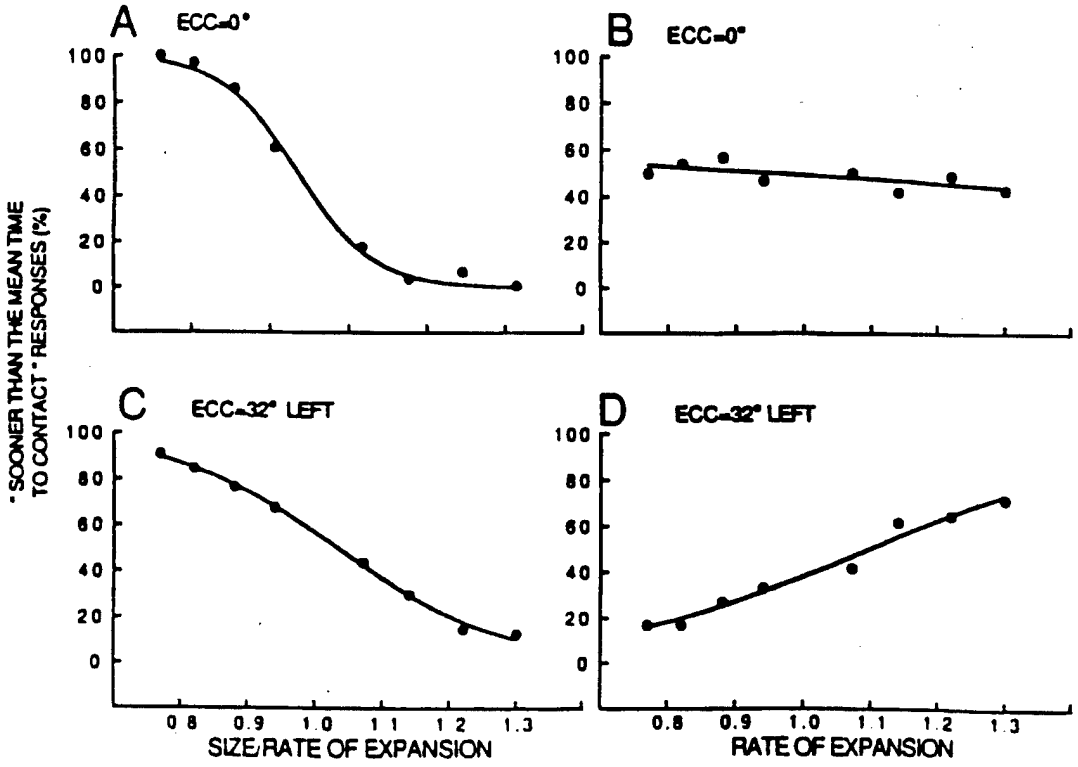

Figure 9 Two psychometric functions for the same task. The percentage of 1.0 on the abscissa corresponds to a 2.0 sec time to contact . In B & D, 1.0 on the abscissa corresponds to an initial rate of expansion of 0.17 deg/sec.

Department of Psychology

FAX: (416) 736-5814

UNIVERSITÉ YORK UNIVERSITY

FACULTY OF ARTS

4700 KEELE STREET • NORTH YORK • ONTARIO • CANADA • M3J 1P3

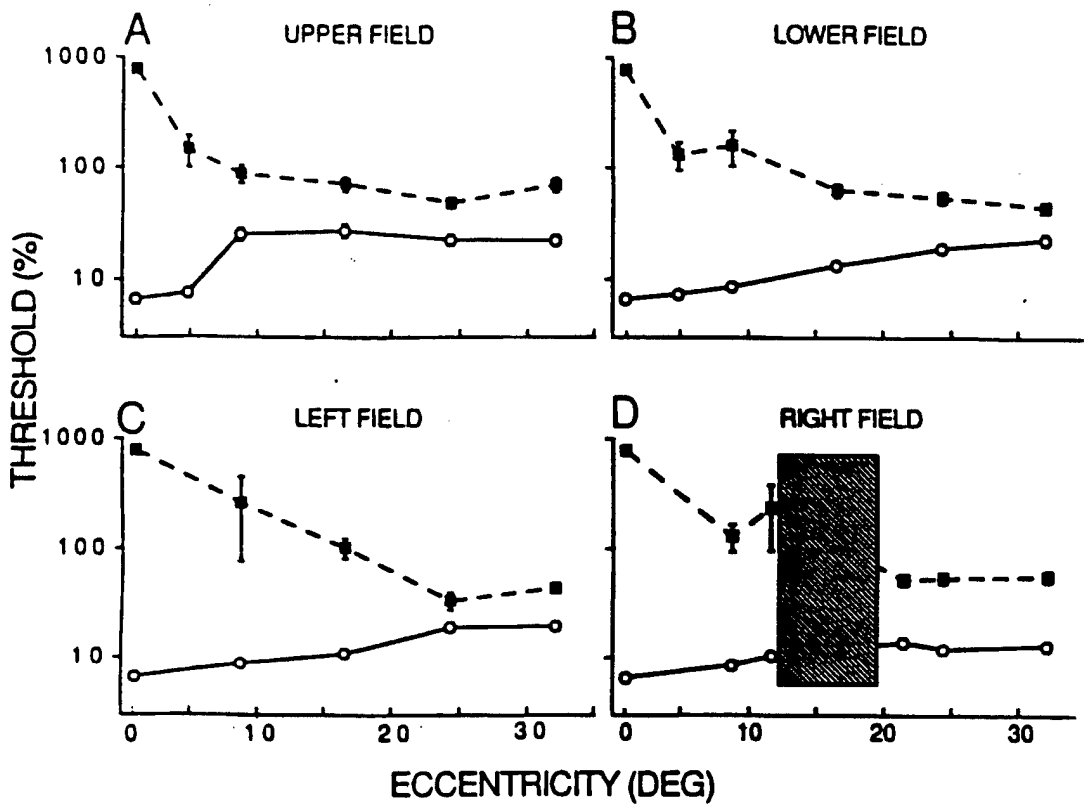

Figure 10 Discrimination threshold (ordinate) versus visual field eccentricity for vertical and horizontal meridia. The observer's task was to judge whether the time to contact of any given stimulus was sooner or later than the mean of the set of 64 stimuli. Open circles indicate thresholds calculated with respect to $\theta_0/(d\theta/dt)_0$. Filled squares indicate thresholds calculated with respect to $(d\theta/dt)_0$. The hatched area in D marks the blind spot. A: Upper field. B: Lower field. C: Left field. D: Right field.

Department of Psychology
FAX: (416) 736-5814

UNIVERSITÉ
YORK
UNIVERSITY

FACULTY OF ARTS
4700 KEELE STREET • NORTH YORK • ONTARIO • CANADA • M3J 1P3

threshold measured was for time to contact, because the stimulus illustrated in Fig. 6 completely confounds time to contact with rate of expansion. The dotted lines in Fig. 6 show that the initial rate of expansion, for example, decreased according to the progression 3; 2; 1 while time to contact increased according to the progression 1; 2; 3. The basic idea is as follows. We use a segment of the graphs in Fig. 6A-C between t = 0 and, at most, two-thirds of the time to contact. Suppose now that the ordinates in these three segments are multiplied by 1.0, 2.0 and 3.0 respectively. The initial rate of expansion (i. e., the slope of the dotted line) will now be the same for the three times to contact, and the rates of expansion will be approximately equal at corresponding values along the three segments for the three times to contact. Now suppose we construct a second and a third horizontal row by multiplying the ordinate in the three new graph segments by factors of 2 and 3 respectively. We now have a 3 x 3 array of stimuli in which time to contact varies horizontally, rate of expansion varies vertically, and starting size varies both horizontally and vertically.

In the present study we used an 8 x 8 rather than a 3 x 3 array of stimuli. In addition, rather than a 1; 2; 3 progression, time to contact varied horizontally according to the following progression: $n^{-1.0}$; $n^{-0.75}$; $n^{-0.5}$; $n^{-0.25}$; $n^{0.25}$; $n^{0.5}$; $n^{0.75}$; $n^{1.0}$. (The value of n set the difficulty of the task. We set n = 1.3). Initial rate of expansion varied vertically according to the same

Department of Psychology
FAX: (416) 736-5814

UNIVERSITÉ
YORK
UNIVERSITY

FACULTY OF ARTS
4700 KEELE STREET • NORTH YORK • ONTARIO • CANADA • M3J 1P3

progression. Our purpose in structuring the array in this way was to create a diagonal symmetry for starting size (see Fig. 7D).

The subject was provided with two buttons in the first two parts of Experiment 1. In part 1, the subject was instructed to press button 1 or 2 depending on whether time to contact was sooner or later than the mean of the set of 64 stimuli. In part 2, the subject was instructed to press button 1 or 2 depending on whether the rate of expansion was faster or slower than the mean for the set of 64 stimuli. Auditory feedback was provided. The subject's responses were stored in an 8 x 8 response array, which corresponded to the 8 x 8 stimulus array. In part 1, the response array was for time to contact judgements, and in part 2 for rate of expansion judgements. Each of the 64 cells in each of the two arrays had 16 repeats (i.e. 2,048 responses in all). Data were collected at eccentricities of 0 deg and 32 deg in the left visual field.

Response prediction and data analysis

Fig. 7A-D illustrate four patterns of response predicted from the structure of the stimulus array. In Fig. 7A we assume that the subject bases responses entirely on trial-to-trial variations of time to contact and ignores trial-to-trial variations in rate of expansion and starting size. In Fig. 7B we assume that the subject bases responses entirely on trial-to-trial variations in rate of expansion, and ignores trial-to-trial variations in time to contact and starting size. In Fig. 7C we assume that the subject confounds trial-to-trial variations of time to contact with trial-to-trial variations in rate of expansion,

Department of Psychology

FAX: (416) 736-5814

UNIVERSITÉ YORK UNIVERSITY

FACULTY OF ARTS

4700 KEELE STREET • NORTH YORK • ONTARIO • CANADA • M3J 1P3

but ignores trial-to-trial variations in starting size. Trial-to-trial variations in time to contact and trial-to-trial variations in rate of expansion were combined by linear summation with a relative weighting of 2·1:1 (see below for the reason for choosing this weighting). In Fig. 7D we assume that the subject bases responses entirely on trial-to-trial variations in starting size, and ignores trial-to-trial variations in time to contact and rate of expansion. The major difference between the predictions shown in Fig. 7C and D is that the 100% response prediction is for the largest rate of expansion and shortest time to contact in Fig. 7C but for the largest rate of expansion and longest time to contact in Fig. 7C. This difference is a consequence of assuming that an increase in rate of expansion produces an illusory *decrease* in time to contact.

Data obtained in Experiment 1 were analyzed quantitatively as follows. "Sooner than the mean time to contact" responses in each of the vertical columns of the time to contact 8 x 8 response array were summed and plotted versus the initial time to contact $\theta_0/(d\theta/dt)_0$ to give a psychometric function. Then the same response array was re-analysed by summing each of the horizontal rows, and plotted versus the initial rate of expansion $(d\theta/dt)_0$ to give a second psychometric function. Discrimination threshold with respect to time to contact was defined as $(1/2)\{[\theta_0/(d\theta/dt)_0]_{75} - [\theta_0/(d\theta/dt)_0]_{25}\}$, where $[\theta_0/(d\theta/dt)_0]_{75}$ and $[\theta_0/(d\theta/dt)_0]_{25}$ were, respectively, the values of $\theta_0/(d\theta/dt)_0$ for 75% and 25% "sooner than the mean time to contact" responses. Discrimination threshold with respect to rate of expansion was defined

Department of Psychology
FAX: (416) 736-5814

UNIVERSITÉ
YORK
UNIVERSITY

FACULTY OF ARTS
4700 KEELE STREET • NORTH YORK • ONTARIO • CANADA • M3J 1P3

analogously. Discrimination thresholds were estimated from the psychometric functions by Probit analysis.

Results

Comparison of predicted response patterns with foveal and peripheral data

In Fig. 8A the subject was instructed to judge whether the time to contact of any given stimulus was sooner or later than the mean time to contact of the set of 64 stimuli (part 1 of Experiment 1). Stimulus eccentricity was 0 deg. The pattern of responses was close to the Fig. 7A prediction and quite different from any of the Fig. 7B-D predictions. We conclude that, in foveal vision, the subject based responses on trial-to-trial variations of time to contact and ignored trial-to-trial variations in rate of expansion and starting size.

In Fig. 8B the stimulus set was exactly the same as in Fig. 8A. Only the subject's instructions were different. In Fig. 8B the subject was instructed to judge whether the rate of expansion of any given stimulus was greater or smaller than the mean rate of expansion of the set of 64 stimuli (part 2 of Experiment 1). Stimulus eccentricity was 0 deg. The pattern of responses was close to the Fig. 7B prediction, and quite different from any of the Fig. 7A, C or D predictions. We conclude that, in foveal vision, the subject based responses on trial-to-trial variations in rate of expansion, and ignored trial-to-trial variations in time to contact and starting size.

Department of Psychology
FAX: (416) 736-5814

UNIVERSITÉ
YORK
UNIVERSITY

FACULTY OF ARTS
4700 KEELE STREET • NORTH YORK • ONTARIO • CANADA • M3J 1P3

Compared with 0 deg eccentricity, at 32 deg eccentricity the subject was less able to base his judgements entirely on trial-to-trial; variations in time to contact (compare Fig. 8C with Fig. 7A). The similarity between the Fig. 8C response pattern and the Fig. 7C prediction is consistent with the hypothesis that an x% variation in rate of expansion produced an illusory variation in time to contact of roughly $(x/2)^{\%}$, and the subject ignored trial-to-trial variations in starting size. Additional confirmation of this point is provided by the considerable difference between the Fig. 8C response pattern and the Fig. 7D prediction.

Comparison of discrimination thresholds in the fovea and periphery

The two psychometric functions in Fig. 9A & B were obtained from the Fig. 8A response matrix. When the percent of "sooner" responses was plotted vs the ratio $\theta_0/(d\theta/dt)_0$, a much steeper psychometric function resulted than when the same responses were plotted vs $(d\theta/dt)_0$. [(Discrimination threshold was 6.7 % (SE = 0.4) in Fig. 9A. In Fig. 9B threshold was so high that it was not possible to be more precise than to say that it was greater than 100%]. Fig. 9C & D, were obtained from the 9C response matrix, and show that at an eccentricity of 32 deg the difference between the two psychometric functions was considerably less than in foveal vision. Although the subject's responses were still predominantly determined by the ratio $\theta_0/(d\theta/dt)_0$, discrimination threshold in Fig. 9C was only 2·1 times lower than in Fig. 9D (21% compared with 44%).

Department of Psychology
FAX: (416) 736-5814

UNIVERSITÉ
YORK
UNIVERSITY

FACULTY OF ARTS
4700 KEELE STREET • NORTH YORK • ONTARIO • CANADA • M3J 1P3

Experiment 2

Psychophysical methods

In Experiment 2, data were collected for judgements of time to contact and rate of expansion at 20 locations in the visual field between 0 deg and 32 deg eccentricity along the horizontal and vertical meridia.

Results

Effect of eccentricity on the ability to discriminate time to contact.

The data shown in Fig. 10 were obtained by instructing subject 1 to judge whether the time to contact for any given stimulus was sooner than or later than the mean for the set of 64 stimuli. The thresholds plotted in Fig. 10 were estimated from psychometric functions of the kind shown in Fig. 9. Open circles (continuous lines) were obtained by plotting the subject's response vs the task-relevant variable, and filled squares (dashed lines) were obtained by plotting the subject's responses vs the initial rate of expansion (a task-irrelevant variable).

Conclusions

Our main conclusion concerns the ability to discriminate between different times to contact with an approaching object independently of the size and rate of expansion of the object's retinal image. This ability is high within the central visual field (within about 4 to 8 deg eccentricity depending on the subject and meridian). Our results suggest that, outside this central

Department of Psychology
FAX: (416) 736-5814

UNIVERSITÉ
YORK
UNIVERSITY

FACULTY OF ARTS
4700 KEELE STREET • NORTH YORK • ONTARIO • CANADA • M3J 1P3

visual field judgements of an object's time to contact would no longer be independent of the object's size.

The qualitative agreement between the Fig. 8C data and the Fig. 7C prediction is consistent with the hypothesis that, in peripheral vision, trial-to-trial variations in rate of expansion produced an illusory percept of trial-to-trial variations in time to contact. We conclude that illusory percepts are an important reason why, for time to contact discrimination, the separation between the task-relevant and task-irrelevant thresholds in Fig. 10 decreases with increasing eccentricity.

Relevance for Aviation

The relevance for collision avoidance in aviation is as follows. It is natural that to judge time to collision a pilot should look directly at an oncoming object on a collision course. We report that that is the correct thing to do. However, it is impossible to look directly at two things at once. It is not intuitively obvious that judgements of time to contact are unreliable in peripheral vision. Our results imply that pilots should be made aware of this deficiency in the human visual system so that, when confronted by a collision hazard with two or more oncoming objects the pilot can adopt some deliberate strategy such as, for example, glancing rapidly from one to the other.

3.5 Time to collision judgements: effects of mismatching rates of expansion of size and texture elements.

Department of Psychology
FAX: (416) 736-5814

UNIVERSITÉ
YORK
UNIVERSITY

FACULTY OF ARTS
4700 KEELE STREET • NORTH YORK • ONTARIO • CANADA • M3J 1P3

A paper is in press in Perception and Psychophysics (Ref. 258)

The broad issue is flight simulator training for collision avoidance. This experiment addresses the question of whether a subject's ability to judge the time to collision with a simulated oncoming object is degraded by a mismatch between the rates of expansion of the object and its surface texture. The relevance of the study is that many flight simulators generate object texture, but in not all cases are the texture and object dynamics matched.

The background is our previous (1983) laboratory study in which we investigated the perception of motion-in-depth produced by an expanding image texture. We found that if image size and texture were not matched accurately, the motion in depth aftereffect could be weakened or even abolished (Ref. 125).

Apparatus and methods

We designed and built hardware electronics that generates a square covered with sharp-edged rectangular texture elements on a monitor (Fig. 11). The expansion of the square and the expansion of the texture element can be controlled independently so as to vary the ratio R, where R = TE/SE (TE and SE are, respectively, the % expansion per sec of texture elements and the square). The ratio R can be varied from 0.0 (texture size constant, square expands) through 1.0 (texture size and square size perfectly locked) to 2.0 (texture expands twice as fast as the square).

Department of Psychology

FAX: (416) 736-5814

UNIVERSITÉ
YORK
UNIVERSITY

FACULTY OF ARTS

4700 KEELE STREET • NORTH YORK • ONTARIO • CANADA • M3J 1P3

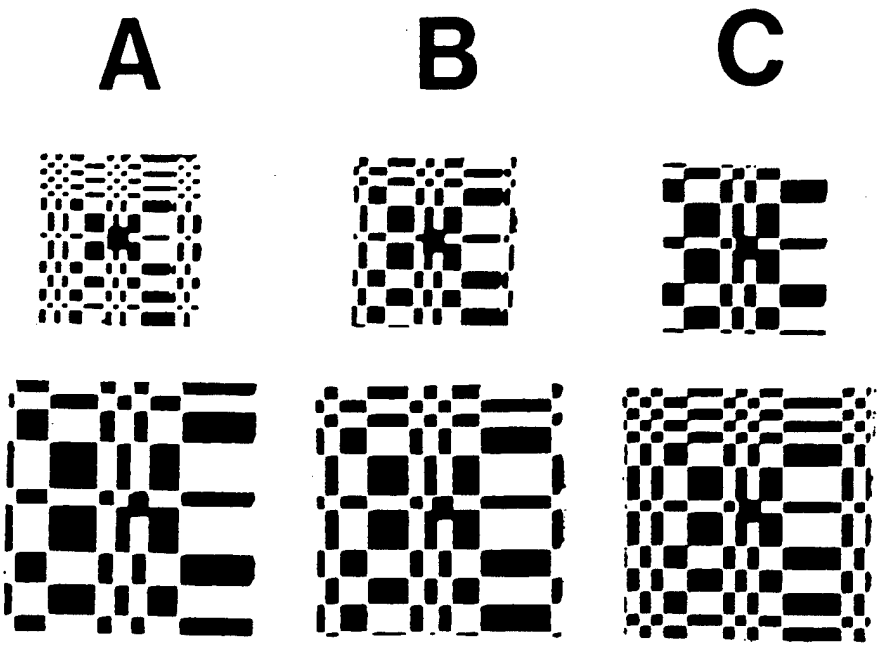

Figure 11 Photographs of three of the stimulus displays. The conditions shown are R = 2.0, R = 1.0 and R = 0.0 in A, B & C respectively where R = (relative rate of expansion of the texture elements within the square)/(relative rate of expansion of the square).

Department of Psychology
FAX: (416) 736-5814

UNIVERSITÉ
YORK
UNIVERSITY

FACULTY OF ARTS
4700 KEELE STREET • NORTH YORK • ONTARIO • CANADA • M3J 1P3

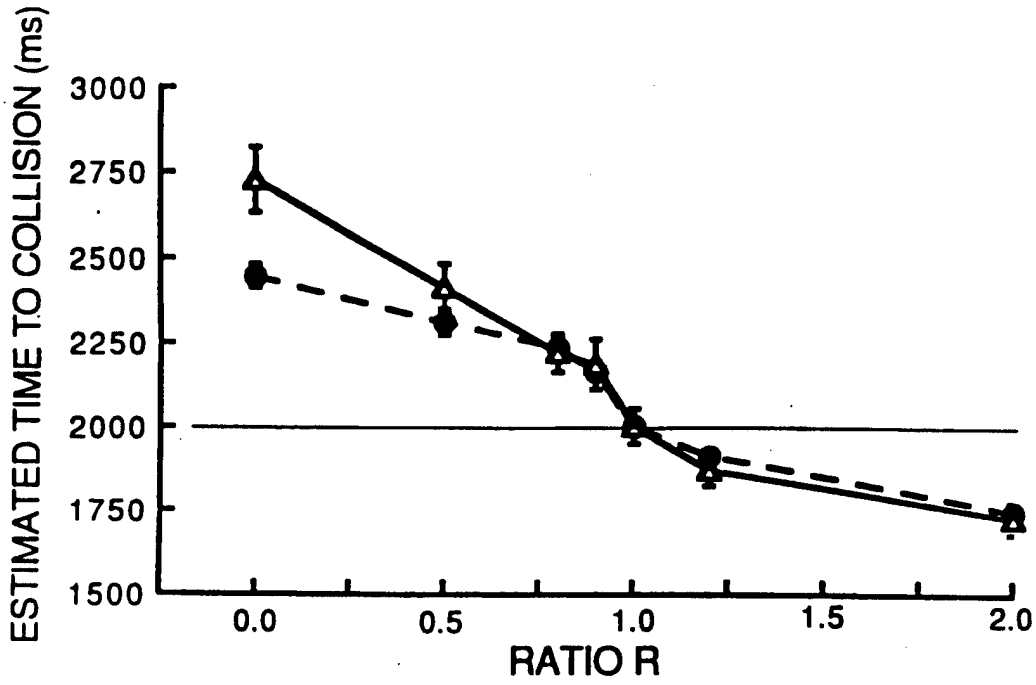

Figure 12 Estimated time to collision in msec is plotted as ordinate versus the ratio R where R = (relative rate of expansion of the texture elements within the square)/(relative rate of expansion of the square). Filled circles and open triangles are for two observers. The vertical bars indicate ±1 standard error.

Department of Psychology
FAX: (416) 736-5814

UNIVERSITÉ
YORK
UNIVERSITY

FACULTY OF ARTS
4700 KEELE STREET • NORTH YORK • ONTARIO • CANADA • M3J 1P3

The psychophysical procedure is the same as just described in Section 3.4 above. Subjects were presented with 64 stimuli, each of which comprised a different combination of time to collision, square starting size and square rate of expansion. The ratio TE/SE was fixed. Subjects were instructed to judge whether time to contact was sooner or later than the mean of the set of 64 stimuli. Data were analysed as in Section 3.4 above so as to reveal the degree to which subjects unconfounded trial-to-trial variations in time to contact and trial-to-trial variations in starting size and in rate of expansion. The experiment was then repeated for several values of the ratio TE/SE.

Results

Our main finding, illustrated in Fig. 11, is that the ability to ignore trial-to-trial variations in rate of expansion when discriminating time to contact is excellent when texture size and square size are locked (TE/SE = 1.0), but is poor when texture expands more slowly than the square. In addition, discrimination threshold rises as the ratio TE/SE is reduced.

3.6 Cyclopean processing of changing-disparity and changing-size.

Results have been reported to ARVO 1995 and a report "Cyclopean motion perception produced by oscillations of size, disparity and location" by R. Gray and D. Regan published in Vision Research (1996) 35,655-666.

The broad issue is the perception of motion-in-depth produced by either binocular or monocular cues (specifically, changing-disparity and changing-size). This experiment is designed to distinguish between

Department of Psychology
FAX: (416) 736-5814

UNIVERSITÉ
YORK
UNIVERSITY
FACULTY OF ARTS
4700 KEELE STREET • NORTH YORK • ONTARIO • CANADA • M3J 1P3

processing that occurs before and after the signals from left and right eyes unite.

Apparatus and methods

A stereopair of random dots was generated on a pair of monitors by our own hardware electronics, and presented to the subject dichoptically. In binocular view the dot pattern contained a square standing out in depth. In our present experiment a different pair of random dot patterns was generated 50 times per sec so that in binocular view the square and the background were filled with twinkling dots (the so-called dynamic random noise display). We used dynamic random noise so that, even when it moved, the square could not be seen when one eye was closed. The square just described was cyclopean. A monocularly-visible square was created by using a static random dot pattern in the surround while leaving the square filled with dynamic random noise just as in the cyclopean case. The subject's ocular convergence was controlled by fixating on nonious lines in the plane of the background.

The method of constant stimuli was used in Expt 1. The square's disparity was oscillated by a wavetrain of 5 sinewave cycles windowed by a Gaussian. Each trial comprised a reference presentation (oscillation amplitude zero) and a test presentation with oscillation amplitude set to one of 5 values. The task was to decide which presentation contained the depth oscillation. Oscillation thresholds were measured over a frequency range of 0.25 to 8 Hz for the cyclopean square.

Department of Psychology

FAX: (416) 736-5814

UNIVERSITÉ
YORK
UNIVERSITY

FACULTY OF ARTS

4700 KEELE STREET • NORTH YORK • ONTARIO • CANADA • M3J 1P3

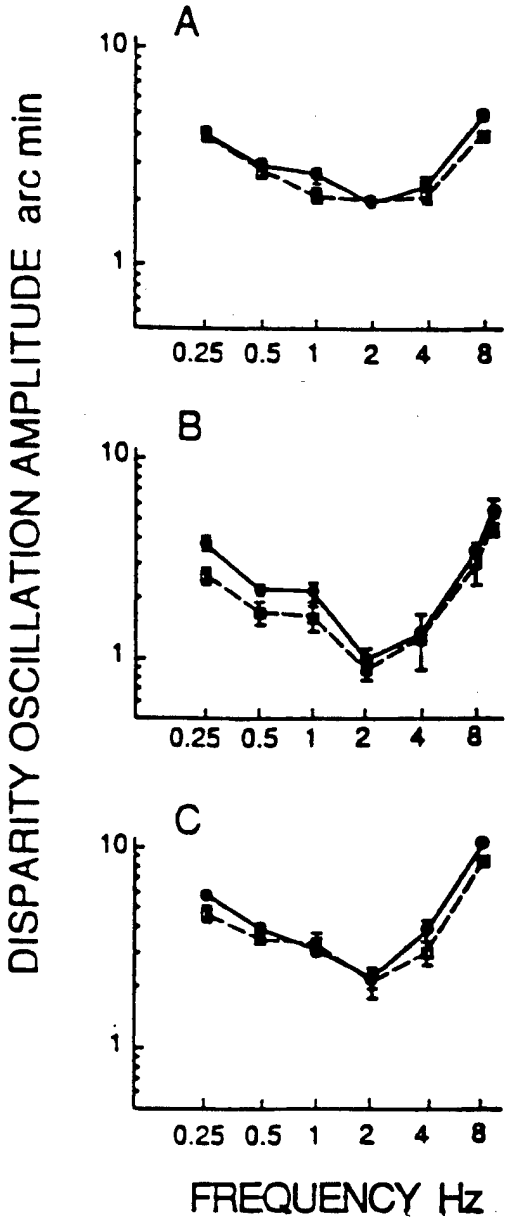

Figure 13 A: Peak-to-peak amplitude of disparity oscillation at threshold for motion in depth perception (ordinate) is plotted versus oscillation frequency. Filled and open symbols are for cyclopean and monocularly-visible targets respectively. B, C: Corresponding data for two other observers.

Department of Psychology

FAX: (416) 736-5814

UNIVERSITÉ
YORK
UNIVERSITY

FACULTY OF ARTS

4700 KEELE STREET • NORTH YORK • ONTARIO • CANADA • M3J 1P3

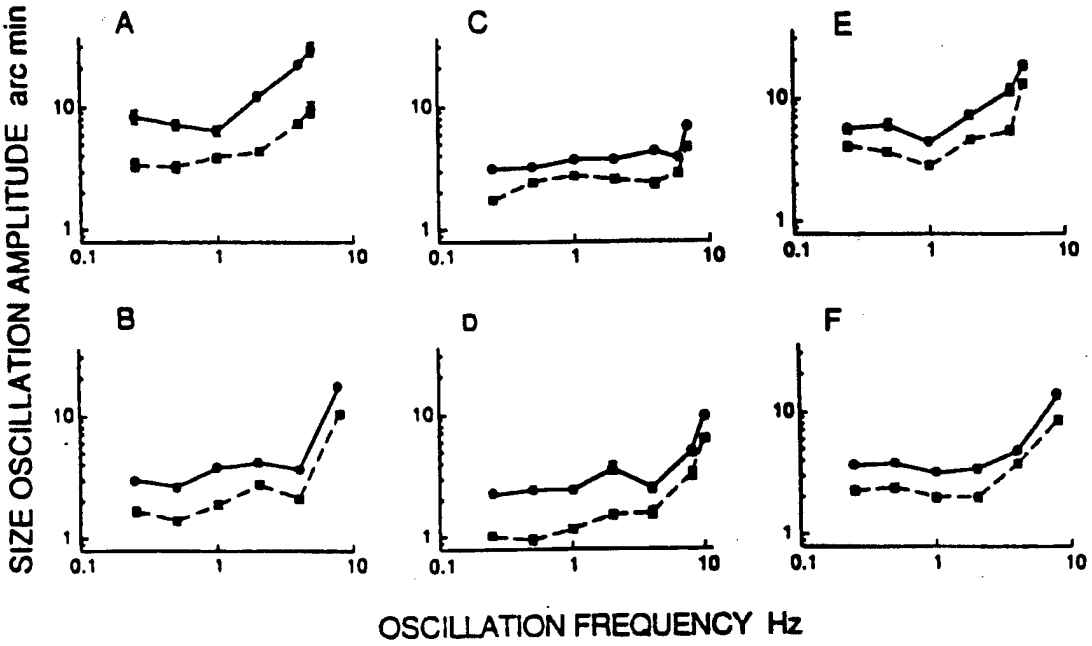

Figure 14 A: Peak-to-peak amplitude of size oscillations at threshold for motion in depth perception (ordinate) is plotted versus oscillation frequency. Filled and open symbols are for cyclopean and monocularly-visible targets respectively. C, E: Corresponding data for two other observers. B, D, F: As for A, C & E except that observers set for threshold of size oscillation perception.

Department of Psychology
FAX: (416) 736-5814

UNIVERSITÉ YORK UNIVERSITY
FACULTY OF ARTS
4700 KEELE STREET • NORTH YORK • ONTARIO • CANADA • M3J 1P3

In Fig. 13, filled circles (continuous lines) plot motion-in-depth thresholds for the cyclopean square. Open squares (dashed lines) plot corresponding data for the monocularly-visible square. The similarity of cyclopean and noncyclopean data lead us to conclude that the shape of the curve is determined by completely before signals from the two eyes have united, i.e. attenuation at cyclopean level is negligible.

In Expt 2 the size of the square rather than its disparity was oscillated. The size oscillation produced the impression that the square was moving in depth, but the illusory depth movement was much stronger for the noncyclopean square than for the cyclopean square. Filled and open circles in Fig. 14A, C & E plot depth oscillation thresholds for the cyclopean and monocularly-visible squares respectively. In contrast with the corresponding data for motion-in-depth sensation produced by disparity oscillations (Fig. 13), the cyclopean and noncyclopean thresholds are quite different, indicating that a cyclopean changing-size stimulus is much less effective than a monocularly-visible changing size stimulus.

This finding was confirmed in Expt 3 where we pitted size oscillations versus simultaneous oscillations of disparity. Subjects were instructed to adjust the disparity oscillation amplitude so as to cancel the sensation of depth oscillations produced by a fixed amplitude of size oscillation.

3.7 Shape discrimination for cyclopean form

Department of Psychology
FAX: (416) 736-5814

UNIVERSITÉ
YORK
UNIVERSITY

FACULTY OF ARTS
4700 KEELE STREET • NORTH YORK • ONTARIO • CANADA • M3J 1P3

A report has been published. D. Regan & S. J. Hamstra "Shape discrimination for rectangles defined by disparity alone, disparity plus luminance and by disparity plus motion. Vision Research, 34, 2277-2291 (1994).

The broad issue is the role of binocular vision in seeing and recognizing objects. The work is relevant to (a) the design of stereo displays viewed by the operators of remotely-controlled vehicles and (b) collision avoidance in nap-of-the-Earth flight. The experiment addresses a subject's ability to discriminate a change in the shape (aspect ratio) of a rectangle that is visible in binocular vision but invisible in monocular vision, i.e. a cyclopean rectangle.

Methods

A pseudo-random pattern of bright dots was generated by shift registers in laboratory-designed and built hardware electronics (Ref.130) and displayed on electrostatically-controlled monitors. As illustrated in Fig. 15A, the two monitors (M1 & M2) were viewed dichoptically. At the viewing distance of 120 cm, the dot pattern was a 4 x 4 deg square. Each dot subtended about 2.0 min arc. There were approximately 770 dots on each monitor so that dot density was approximately 48 per deg^2. By means of pellicles P1 and P2, nonious lines were optically superimposed on the dot displays. The nonious lines were created by back-illuminating by means of light-emitting diodes two slits S1 and S2.

Department of Psychology
FAX: (416) 736-5814

UNIVERSITÉ
YORK
UNIVERSITY

FACULTY OF ARTS
4700 KEELE STREET • NORTH YORK • ONTARIO • CANADA • M3J 1P3

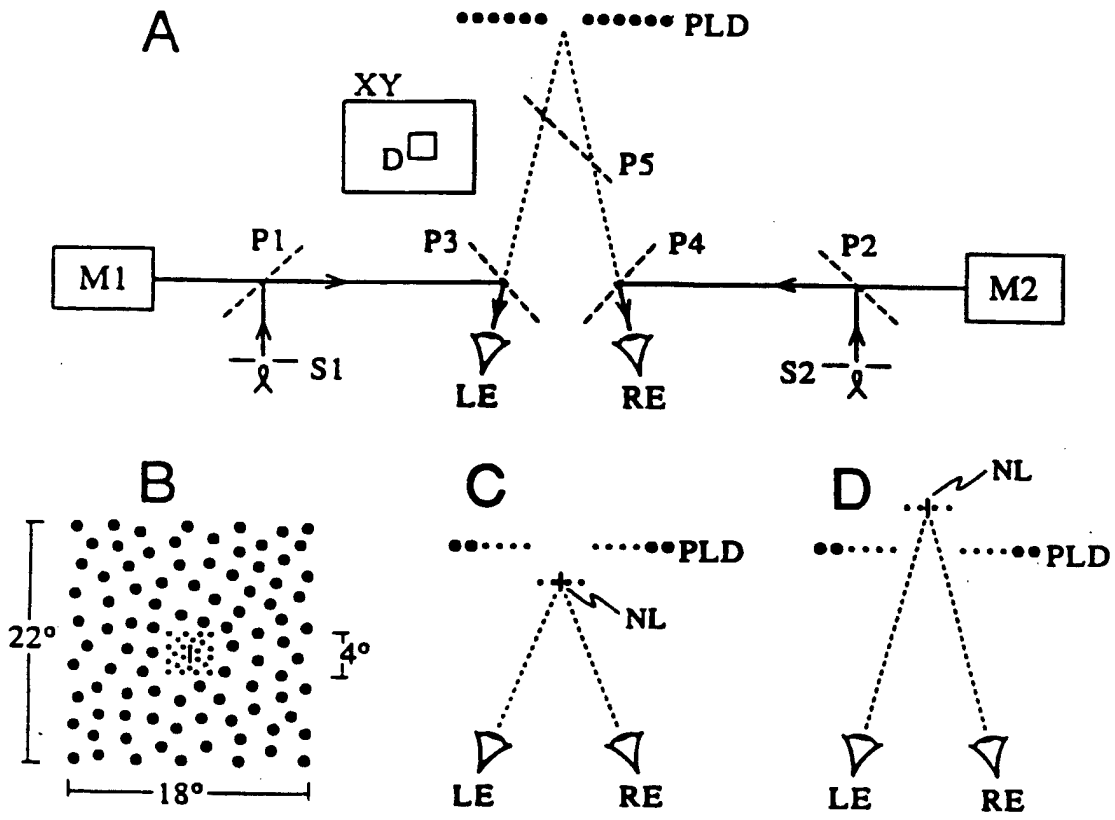

Figure 15 A: Optical arrangement. M1 and M2 are monitors. P_1-P_5 are pellicles. S_1 and S_2 are illuminated slits. PLD is an illuminated plane of large dots. XY: XY plotter with the pen replaced by an illuminated bar (D). B: Stimulus field from observer's viewpoint showing the square central dichoptically-viewed surround pattern of fine dots generated by the monitors surrounded by the binocularly-viewed surround plane of large dots. Nonious lines are shown at the centre of the pattern of fine dots. C: View from above the subject. For clarity, the pattern of fine dots is enlarged. The PLD plane has crossed disparity and the nonious lines (NL) have been adjusted to place them in the plane of the stimulus rectangle. D: As for C, but the PLD plane has uncrossed disparity.

Department of Psychology

FAX: (416) 736-5814

UNIVERSITÉ
YORK
UNIVERSITY

FACULTY OF ARTS

4700 KEELE STREET • NORTH YORK • ONTARIO • CANADA • M3J 1P3

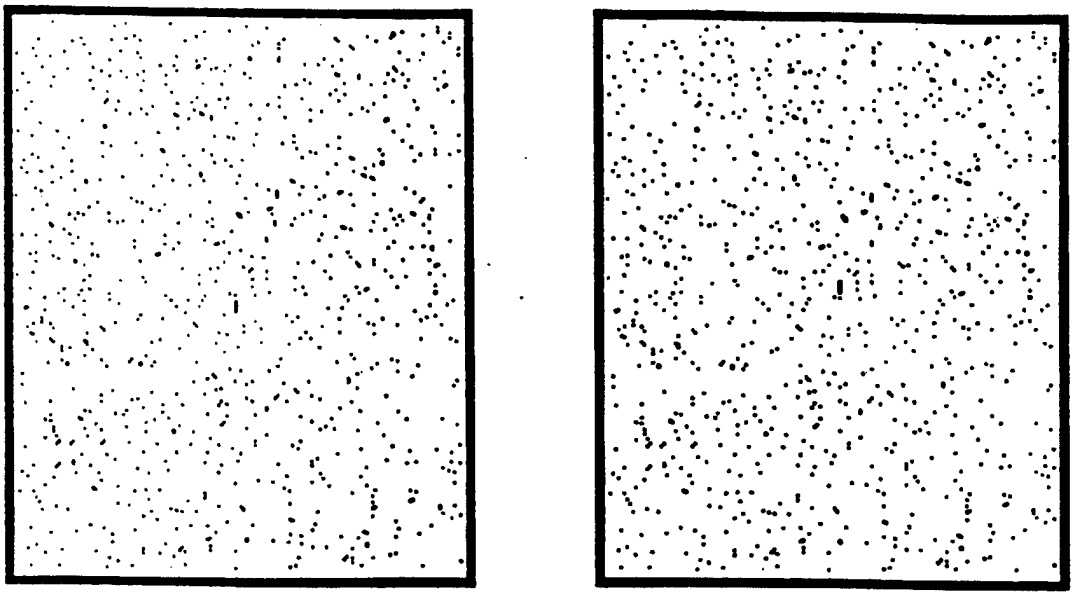

Figure 16 Stereograms to illustrate a disparity-defined rectangle with nonious lines. View the stereogram from arm's length. Hold a pencil in front of the page at such a distance that with the left eye closed the point is at the centre of the left dot pattern, and with the right eye closed the point is at the centre of the right dot pattern. Now open both eyes and look at the pencil point. After a few moments you will see three rather than two dot patterns. The central pattern is binocularly-fused and the camouflaged rectangle will emerge. The pencil can now be removed.

Department of Psychology
FAX: (416) 736-5814

UNIVERSITÉ
YORK
UNIVERSITY

FACULTY OF ARTS
4700 KEELE STREET • NORTH YORK • ONTARIO • CANADA • M3J 1P3

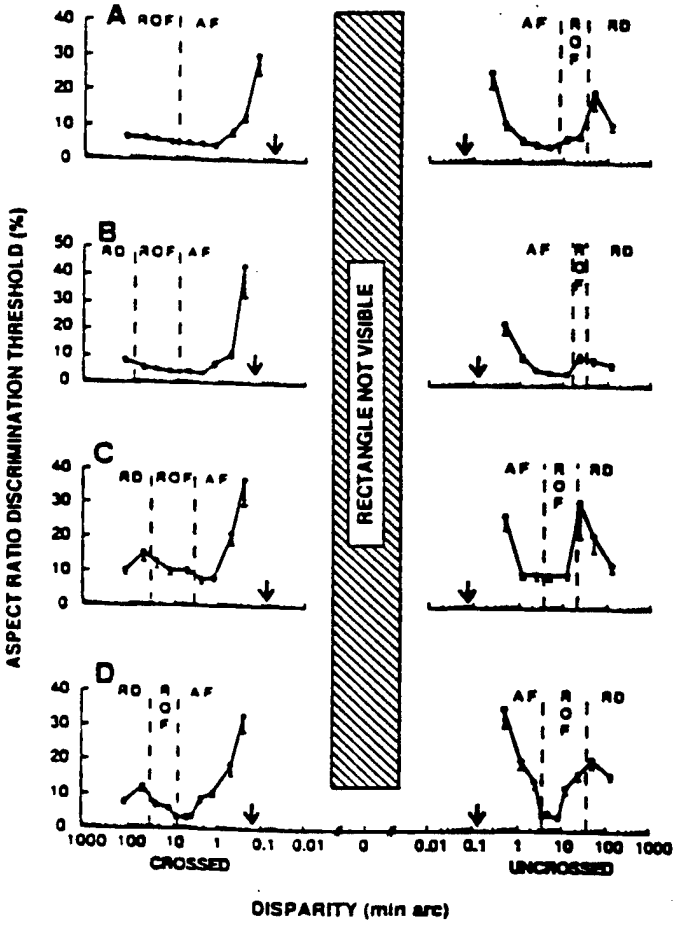

Figure 17 Aspect ratio discrimination threshold for a disparity-defined rectangle is plotted as ordinate versus the disparity of the surround. The y axis is linear and the x axis is logarithmic. Vertical bars through the data points indicate 1 standard error. For disparities below about 0.1 min arc the visibility of the rectangle was so low that the discrimination task could not be carried out. A, observer 1. B, observer 2. C, observer 3. D, observer 4. Vertical arrows indicate disparity thresholds for detecting the rectangle. Vertical dashed lines demarcate disparity ranges where all dots were fused (AF), where only the rectangle was fused (ROF) and where the rectangle was diplopic (RD).

Department of Psychology

FAX: (416) 736-5814

UNIVERSITÉ
YORK
UNIVERSITY

FACULTY OF ARTS

4700 KEELE STREET • NORTH YORK • ONTARIO • CANADA • M3J 1P3

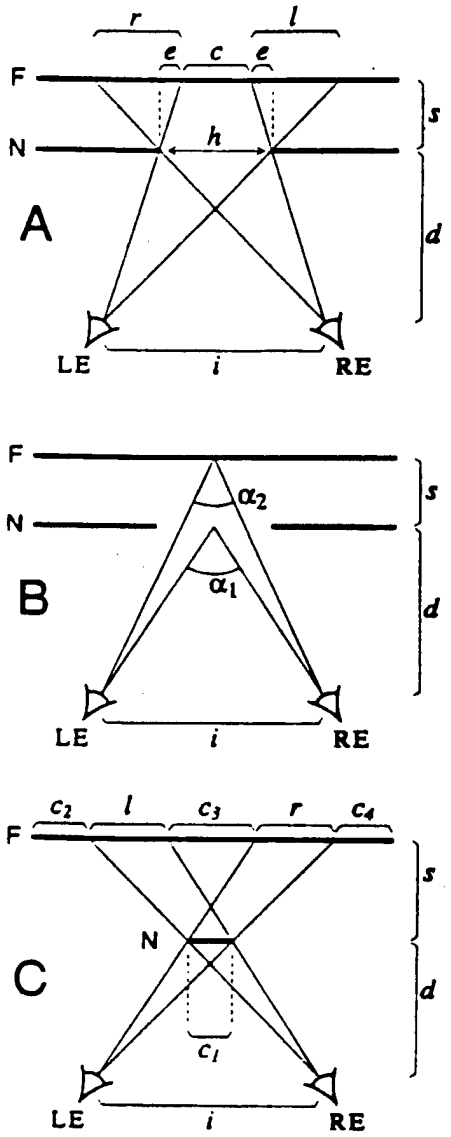

Figure 18 A: An observer's left (LE) and right (RE) eyes view a far plane (F) through a hole of width *h* in a near plane (N). The dashed lines pass through the edges of the hole, and are at right angles to the two planes. B: The observer's left and right eyes subtend a_1 radians at the near plane and a_2 radians at the far plane. C: An observer's left and right eyes view a restricted region of a near plane (N) that occludes part of a far plane (F).

Department of Psychology

FAX: (416) 736-5814

UNIVERSITÉ
YORK
UNIVERSITY

FACULTY OF ARTS

4700 KEELE STREET • NORTH YORK • ONTARIO • CANADA • M3J 1P3

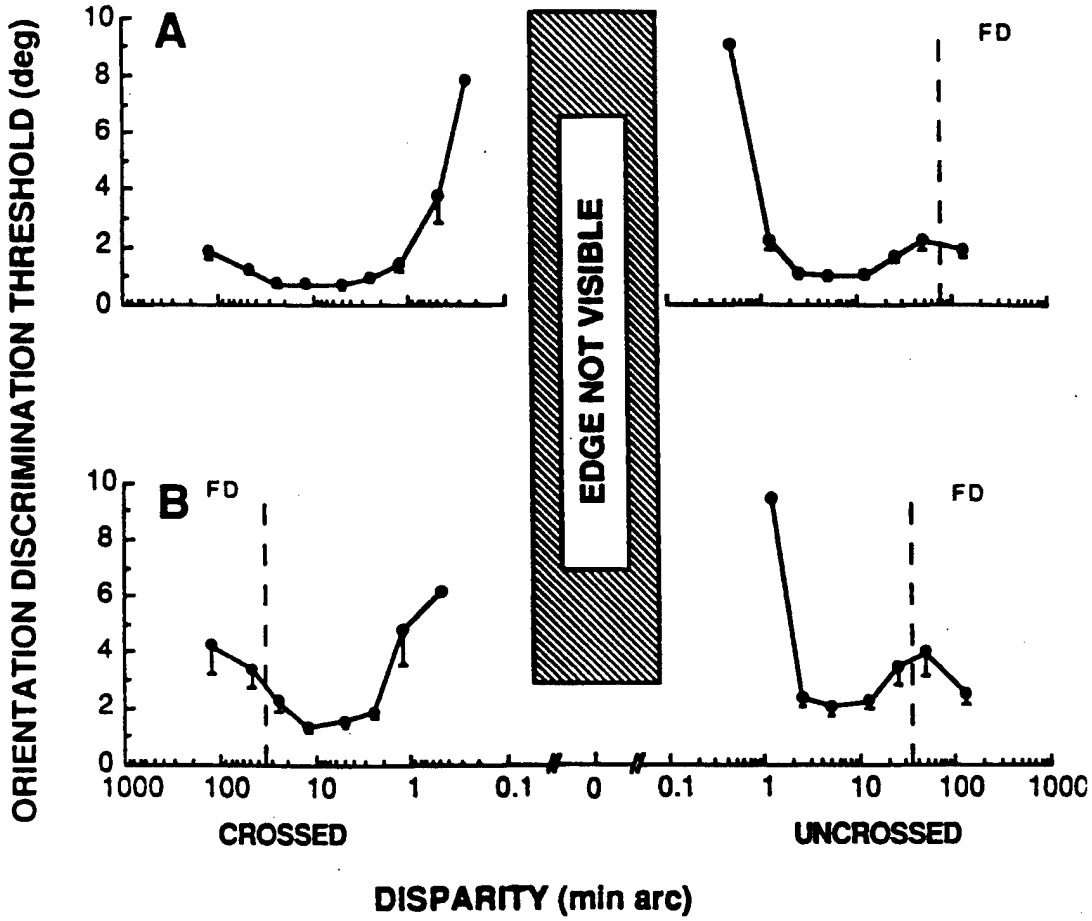

Figure 19 A & B: Solid circles plot orientation discrimination threshold (ordinate) vs disparity for a constant-width bar. The vertical arrows indicate threshold for bar detection.

Department of Psychology

FAX: (416) 736-5814

UNIVERSITÉ
YORK
UNIVERSITY

FACULTY OF ARTS

4700 KEELE STREET • NORTH YORK • ONTARIO • CANADA • M3J 1P3

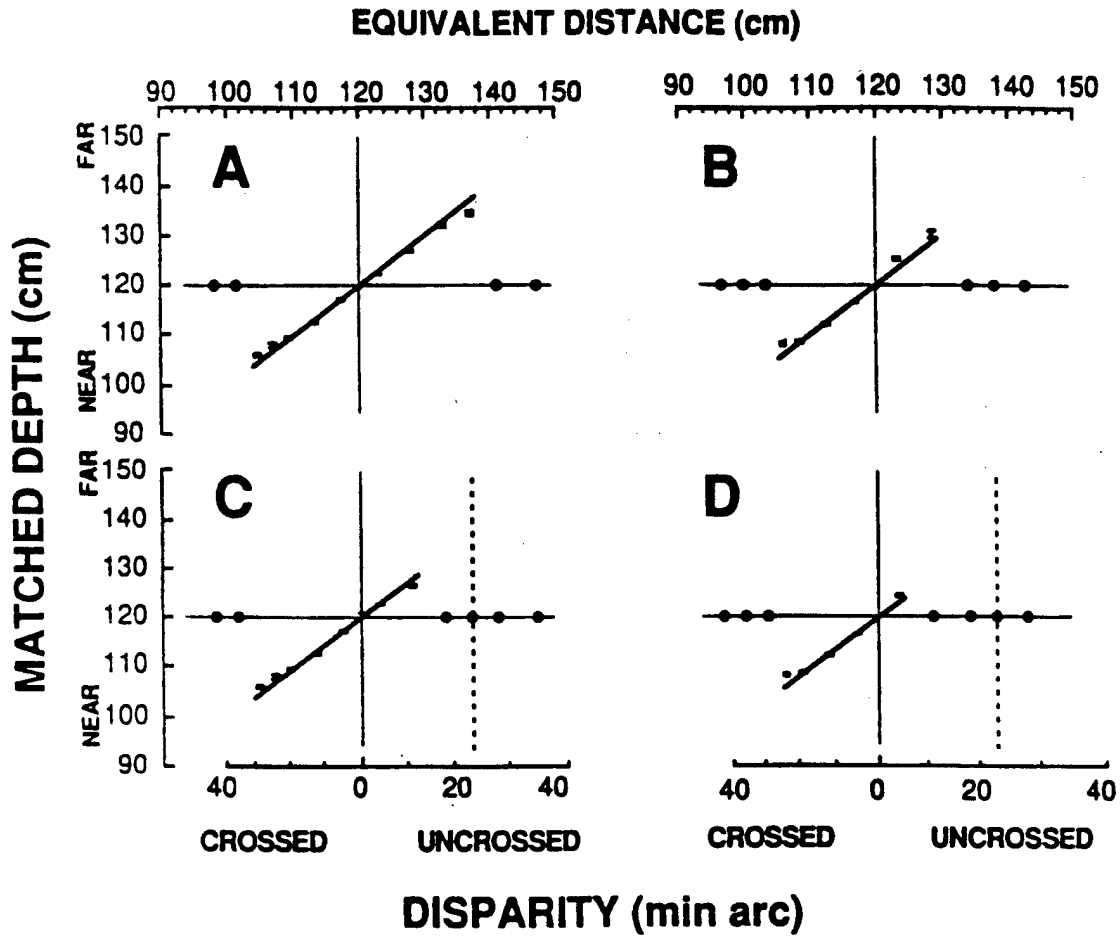

Figure 20 Matched depth (ordinate) vs disparity of a cyclopean bar for observer 1 (A, C) and 2 (B, D). The fine continuous lines indicate zero disparity at the viewing distance of 120 cm. The vertical dashed lines indicate the critical disparity. A and B are for a constant-width bar, and C and D for a variable-width bar.

Department of Psychology
FAX: (416) 736-5814

UNIVERSITÉ
YORK
UNIVERSITY

FACULTY OF ARTS
4700 KEELE STREET • NORTH YORK • ONTARIO • CANADA • M3J 1P3

The dichoptically-viewed 4.0 x 4.0 deg pattern of small dots was superimposed on a 4.0 x 4.0 deg square black area located at the centre of a binocularly-viewed uniformly-illuminated plane (PLD) of randomly scattered large circular black dots. Fig. 15B shows what the subject saw; the dichoptically-viewed stereogram of small dots with superimposed nonious lines, all surrounded by the plane of large dots. Fig. 15C & D are views from above, showing enlarged views of the rectangle with the nonious lines adjusted to be in the same plane as the rectangle. The small dots surrounding the rectangle were always in the same plane as the plane of large dots (PLD).

The cyclopean rectangle is illustrated in Fig. 16.

Each trial consisted of a single 1.5 sec presentation of the rectangle. All dots on both monitors were switched off except during a trial. The surrounding plane of large dots was illuminated throughout. The subject was instructed to press one of two buttons to signify whether the rectangle was more elongated in the horizontal or in the vertical direction. Ten different aspect ratios were presented in random order, and in any given run each aspect ratio was repeated 6 times. A run lasted about 5 mins. Auditory feedback was provided.

Results

First we describe the subjective appearance of the stimulus. When the disparity of the DD rectangle was zero, the rectangle was perfectly camouflaged even when viewed dichoptically, so that the aspect ratio

Department of Psychology
FAX: (416) 736-5814

UNIVERSITÉ
YORK
UNIVERSITY

FACULTY OF ARTS
4700 KEELE STREET • NORTH YORK • ONTARIO • CANADA • M3J 1P3

discrimination task was impossible. For crossed disparities substantially above detection threshold (arrowed in Fig. 17A) the rectangle was seen quite clearly, standing out in front of the surround dots, all dots in the rectangle and surround being fused (AF in Fig. 17A "crossed"). At higher disparities, fusion was lost for the surround dots, though the rectangle itself remained fused (ROF in Fig. 17A "crossed"). For uncrossed disparities substantially above detection threshold, the rectangle was seen quite clearly through what appeared to be a hole in the surround dots, all dots in the rectangle and surround being fused (AF in Fig. 17A "uncrossed"). Fusion was lost for the surround dots at higher disparities, though the rectangle itself remained fused (ROF in Fig. 17A "uncrossed"). At still higher disparities the rectangle became diplopic (RD in Fig. 17A "uncrossed").

Although the best values for crossed and uncrossed disparities were similar (4.0 ± 0.5% for crossed and 4.3 ± 0.5%, for uncrossed), results for crossed and uncrossed disparities differed in that discrimination threshold remained low over a comparatively broad range of crossed disparities (e.g. for subject 1, threshold changed from 4.0 ± 0.5 min arc to 6.3 ± 0.8 min arc as disparity increased from 1.0 to 126 min arc) while, for uncrossed disparities, threshold rose steeply on either side of the minimum.

Conclusions

We report psychophysical evidence that the human visual pathway contains a mechanism sensitive to the ratio between the height and width of

Department of Psychology
FAX: (416) 736-5814

UNIVERSITÉ
YORK
UNIVERSITY

FACULTY OF ARTS
4700 KEELE STREET • NORTH YORK • ONTARIO • CANADA • M3J 1P3

a disparity-defined rectangle. On the grounds that we jittered the rectangle's area randomly we conclude that this ratio-tuned mechanism operates rather independently of the rectangle's linear dimensions.

Further conclusions are as follows. First, the effect of disparity on aspect ratio was different for crossed and uncrossed disparities (Fig. 17). Second, the lowest aspect ratio discrimination threshold was approximately the same for crossed and uncrossed disparities. For both crossed and uncrossed disparities, aspect ratio discrimination threshold was at its lowest value at or just before the maximum disparity at which both rectangle and surround dots were still fused, and beyond this point discrimination threshold increased.

3.8 Orientation discrimination for cyclopean form

Results were reported to ARVO in 1994 and a paper has been published. S. J. Hamstra & D. Regan (1994). "Orientation discrimination in cyclopean vision" Vision Research, 35, 365-374.

The broad issue is the same as in Section 3.7. This experiment addresses a subject's ability to discriminate the orientation of a bar that is visible in binocular vision, but invisible in monocular vision, i.e. a cyclopean bar.

Methods

The equipment is diagrammed in Fig. 15. The procedure was as just described in Section 3.7 except that the rectangle was replaced by a 2.3 x 0.4 deg

Department of Psychology
FAX: (416) 736-5814

UNIVERSITÉ
YORK
UNIVERSITY

FACULTY OF ARTS
4700 KEELE STREET • NORTH YORK • ONTARIO • CANADA • M3J 1P3

vertical bar and the subject's task was to discriminate whether the bar was clockwise or anticlockwise of vertical.

For bars whose relative disparity placed them further than the surround dots, two kinds of bar were generated. This can be understood as follows. For such a bar binocular fusion is not possible beyond a critical disparity δ_{CRIT} given by

$$\delta_{CRIT} = \frac{57h}{d} \quad \text{---------- (5)}$$

where h is the width of the aperture, and d is the distance from the eyes to the nearer plane. A derivation of this result follows.

Consider the situation depicted in Fig. 18A that an observer uses both left (LE) and right (RE) eyes to view an indefinitely extended far plane (F) through a hole of width h in an indefinitely extended near plane (N). In Fig. 18A the region of the far plane visible to the observer has an uncrossed disparity of δ radians with respect to an extended surrounding area of the near plane, where

$$\delta = a_1 - a_2 \quad \text{---------- (6)}$$

(angles a_1 and a_2 are illustrated in Fig. 18B) so that

$$\delta \approx \frac{si}{d\,(d+s)} \quad \text{---------- (7)}$$

In Fig. 18A, the part of the far plane marked l is seen by the left eye only, and the part marked r is seen by the right eye only. The width of the part of the far plane that is seen by both left and right eyes is c, where

$$c = h - 2e \quad \text{---------- (8)}$$

Department of Psychology

FAX: (416) 736-5814

UNIVERSITÉ YORK UNIVERSITY

FACULTY OF ARTS

4700 KEELE STREET • NORTH YORK • ONTARIO • CANADA • M3J 1P3

Since

$$e \approx \frac{s\,(i - h)}{2d} \quad \text{---------- (9)}$$

it follows from equations (8) and (9) that

$$c \approx h - \frac{s\,(i - h)}{d} \quad \text{---------- (10)}$$

Hence

$$\frac{c}{d + s} \approx \frac{h}{d} - \frac{si}{d\,(d + s)} \quad \text{---------- (11)}$$

From equations (7) and (11)

$$\frac{c}{d + s} \approx \frac{h}{d} - \delta \quad \text{---------- (12)}$$

In words: equation (12) indicates that the angle subtended by the part of the far plane that is seen by both eyes is approximately equal to the angle subtended by the hole minus the relative disparity of the far plane. Thus, only for zero disparity is there no part of the far plane that is seen by one eye only.

Equation (12) indicates that there is a critical disparity (δ_{CRIT}) beyond which there is no part of the far plane that is seen by both eyes, and that

$$\delta_{CRIT} \approx \frac{h}{d} \quad \text{---------- (13)}$$

In degrees,

$$\delta_{CRIT} \approx \frac{57h}{d} \quad \text{---------- (14)}$$

Department of Psychology
FAX: (416) 736-5814

UNIVERSITÉ
YORK
UNIVERSITY

FACULTY OF ARTS
4700 KEELE STREET • NORTH YORK • ONTARIO • CANADA • M3J 1P3

The narrower the hole in the near plane, the smaller the uncrossed disparity beyond which the target cannot be fused. Note that this restriction is geometrical and quite distinct from the physiological limitations usually discussed under the heading of Panum's fusional area.

The situation just discussed is different when the width of the hole in the near plane in Fig. 18A is equal to or wider than the intraocular separation (i.e., $h \geq i$). In that case, a finite width of the far plane is seen by both eyes, whatever the disparity of the far plane relative to the near plane.

Fig. 18C illustrates that the situation described above for uncrossed disparities is quite different for targets whose disparities are crossed in that geometry does not impose a limit on the largest crossed disparity that can be fused for a target of a given width. In Fig. 18C a restricted area of a near plane (N) occludes part of a far plane (F). The entire width of the near plane segment is seen by both eyes whatever the values of s, d, and the width of the near plane. The parts of the far plane that are seen by the right eye only or by the left eye only are marked *r* and *l* respectively. The parts of the near and far planes that are seen by both eyes in the geometrical situation illustrated are marked c_1, c_2, c_3 and c_4.

Results

Data points in Fig. 19A plot orientation discrimination thresholds for a constant-width bar. Bar detection threshold is indicated by the vertical arrows). The vertical dashed lines separate the disparity range over which the

Department of Psychology
FAX: (416) 736-5814

UNIVERSITÉ
YORK
UNIVERSITY

FACULTY OF ARTS
4700 KEELE STREET • NORTH YORK • ONTARIO • CANADA • M3J 1P3

bar and also the dots surrounding the bar were seen in binocular fusion (BF) from the disparity range over which the bar was diplopic (BD). Similar data were obtained for a bar that obeyed the geometrical constraints expressed in equation 5.

In the final experiment we carried out depth matching for the cyclopean bar. Results are shown in Fig. 20.

Conclusions

We report that matched depth increased smoothly with increasing uncrossed disparity through a range over which orientation discrimination threshold fell and then leveled out. In some instances orientation discrimination threshold remained approximately constant over a substantial range of disparities while depth continued to increase (note that the abscissae are logarithmic in Fig. 19). We conclude that the processing of the depth of a cyclopean form is dissociated from the processing of the orientation of that same cyclopean form.

We also report that the lowest values of threshold for crossed and uncrossed disparities are similar for cyclopean bars.

Morgan (1986) found that cyclopean vernier acuity is in the region of 0.7 min arc. He noted that this is roughly 10 times finer than the resolution limit for cyclopean gratings reported by Tyler (1974), and pointed out that this implies —in a way that hyperacuities for monocularly-visible form cannot do— that the precision of spatial grain in the cortex is less than 1 min arc

Department of Psychology
FAX: (416) 736-5814

UNIVERSITÉ
YORK
UNIVERSITY

FACULTY OF ARTS
4700 KEELE STREET • NORTH YORK • ONTARIO • CANADA • M3J 1P3

(Morgan, 1991). Along the same lines we reported previously that aspect ratio discrimination for cyclopean rectangles is consistent with a roughly 1.0 min arc precision of encoding the height or width of a cyclopean rectangle, again some 10 times finer than grating resolution (see above). In the present study, a 0.6 deg change in the orientation of a bar that is 2.3 deg long corresponds to a 1.4 min arc displacement of one end of the bar relative to the other end, thus providing a third illustration of cyclopean visual performance that substantially transcends the limit of cyclopean resolution.

The 0.7 to 1.5 min arc acuities for DD form discussed above are much inferior to the 2 to 5 sec arc acuities for LD form, just as the roughly 3 c/deg grating resolution for cyclopean form is much inferior to the 60 c/deg grating resolution for luminance-defined form. However, it is not the case that a given spatial discrimination for DD form is necessarily far inferior to that same discrimination for LD form, because orientation discrimination threshold for a cyclopean bar falls within the range of values previously reported for luminance-defined lines, bars or gratings (Andrews, 1967a, b; Thomas and Gille, 1979; Caelli et al., 1983; Ref. 127).

3.9 Orientation discrimination for texture-defined form

One Paper has been published D. Regan "Orientation discrimination for texture-defined bars" Perception (1995) 24, 1131-1138.

A texture pattern consisting of short (0.2 deg) lines contained a 5.0 deg x 1.4 deg texture-defined bar. The bar was rendered visible by the orientation

Department of Psychology
FAX: (416) 736-5814

UNIVERSITÉ
YORK
UNIVERSITY

FACULTY OF ARTS
4700 KEELE STREET • NORTH YORK • ONTARIO • CANADA • M3J 1P3

difference (2θ) between lines inside the bar and outside the bar (Fig. 21). Figure 22 shows photographs of the pattern. A luminance-defined bar was created by switching off all lines outside the bar. Orientation contrast was (β) equal to 2θ when 2θ was less than 90 deg, and was equal to (180 - 2θ) when 2θ was greater than 90 deg.

Orientation discrimination threshold for the texture-defined bar was a U-shaped function of 2θ over the range 2θ = 0 deg to 2θ = 180 deg (Fig. 23). The lowest threshold was at 2θ = 90 deg, and was 0.57 deg for both observers tested. Findings were similar when the mean orientation of the texture lines was horizontal rather than vertical. This orientation discrimination threshold was a little different for the lowest threshold for motion-defined bars (0.5 and 0.7 deg for two observers, Ref. 182) or for cyclopean bars (0.6, 0.9 and 0.9 deg for three observers, Ref. 238 and Section 3.8 above) or for chromatic gratings (0.99 deg, mean of two observers, Webster et al., 1990), though the value for luminance defined form in the present study (0.42 deg and 0.35 deg in Fig. 24) were a little lower than orientation discrimination thresholds for texture-defined bars and chromatic gratings.

Orientation discrimination threshold for the luminance-defined bar fell to a limiting value as the luminance contrast of the bar was progressively increased (Fig. 24, dashed lines). Threshold fell considerably more rapidly for the luminance-defined bar than for the texture-defined bar (Fig. 24, continuous line), though the asymptotic values were not greatly different.

Department of Psychology

FAX: (416) 736-5814

UNIVERSITÉ
YORK
UNIVERSITY

FACULTY OF ARTS

4700 KEELE STREET • NORTH YORK • ONTARIO • CANADA • M3J 1P3

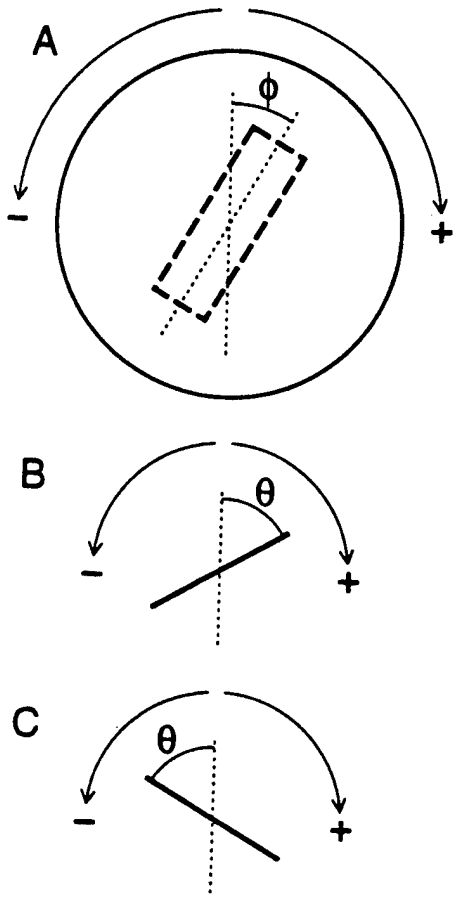

Figure 21 A: The texture-defined bar had an orientation ϕ that could be either clockwise (+) or anticlockwise (-) with respect to the vertical. B, C: Texture lines had one of two possible orientation (θ) that were symmetrical about the vertical.

Department of Psychology

FAX: (416) 736-5814

UNIVERSITÉ YORK UNIVERSITY

FACULTY OF ARTS

4700 KEELE STREET • NORTH YORK • ONTARIO • CANADA • M3J 1P3

Figure 22 Photographs of the stimulus display. A: Texture lines inside and outside the bar had orientations θ = -10 deg and θ = +10 deg, respectively, and the bar was oriented 5 deg anticlockwise of vertical (i.e., ϕ = -5 deg). B: Texture lines inside and outside the bar had orientations of θ = -80 and θ = +80 deg respectively, and the bar was oriented 5 deg clockwise of vertical (i.e., ϕ = +5 deg). Twelve new texture patterns were displayed while the camera shutter was open. The clumped black areas in the photograph could be seen as separated individual lines when the monitor was viewed by eye.

Department of Psychology
FAX: (416) 736-5814

UNIVERSITÉ
YORK
UNIVERSITY

FACULTY OF ARTS
4700 KEELE STREET • NORTH YORK • ONTARIO • CANADA • M3J 1P3

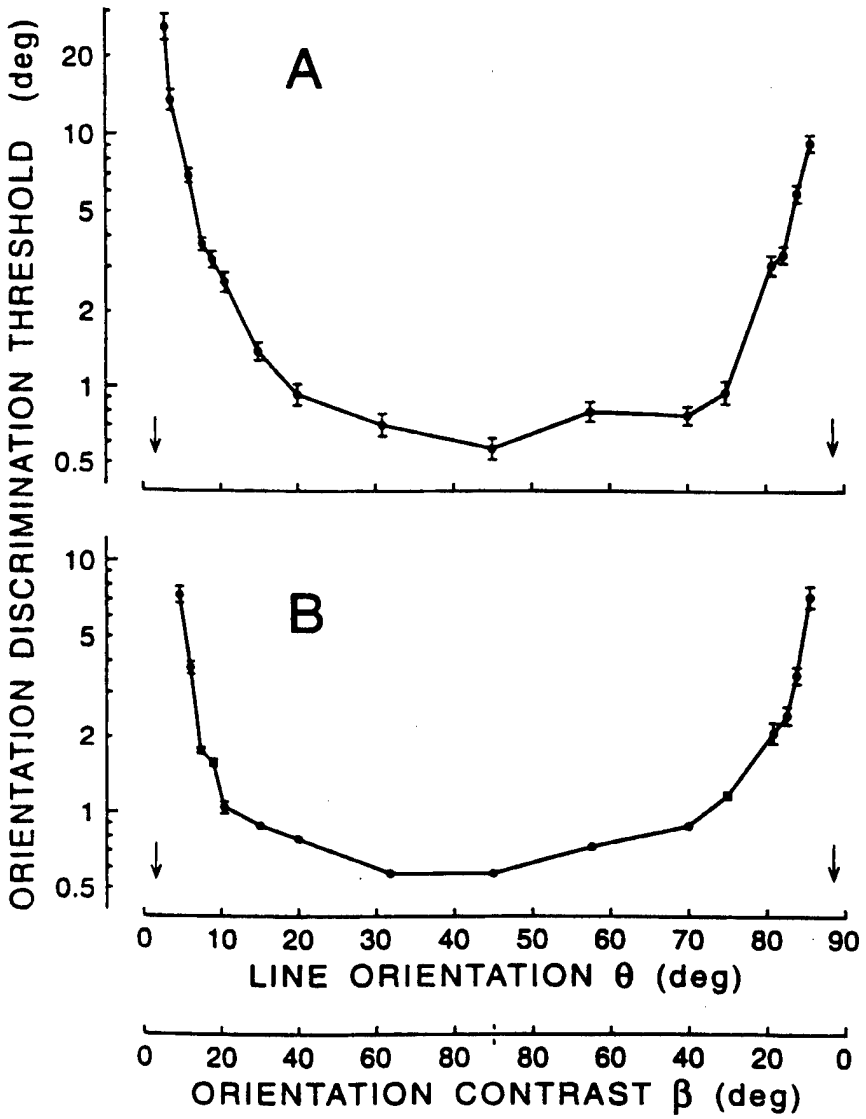

Figure 23 Orientation discrimination thresholds (ordinate) for a 5.0 x 1.4 deg texture-defined bar are plotted as ordinate versus the orientation contrast (β) and versus the orientation (θ) of the 0.2 x 0.03 deg texture lines. Error bars show ±1 SE. Where no error bar is visible the error bar was smaller than the data point. Vertical arrows indicate bar detection threshold. A and B are for observers 1 and 2 respectively.

Department of Psychology

FAX: (416) 736-5814

UNIVERSITÉ
YORK
UNIVERSITY

FACULTY OF ARTS

4700 KEELE STREET • NORTH YORK • ONTARIO • CANADA • M3J 1P3

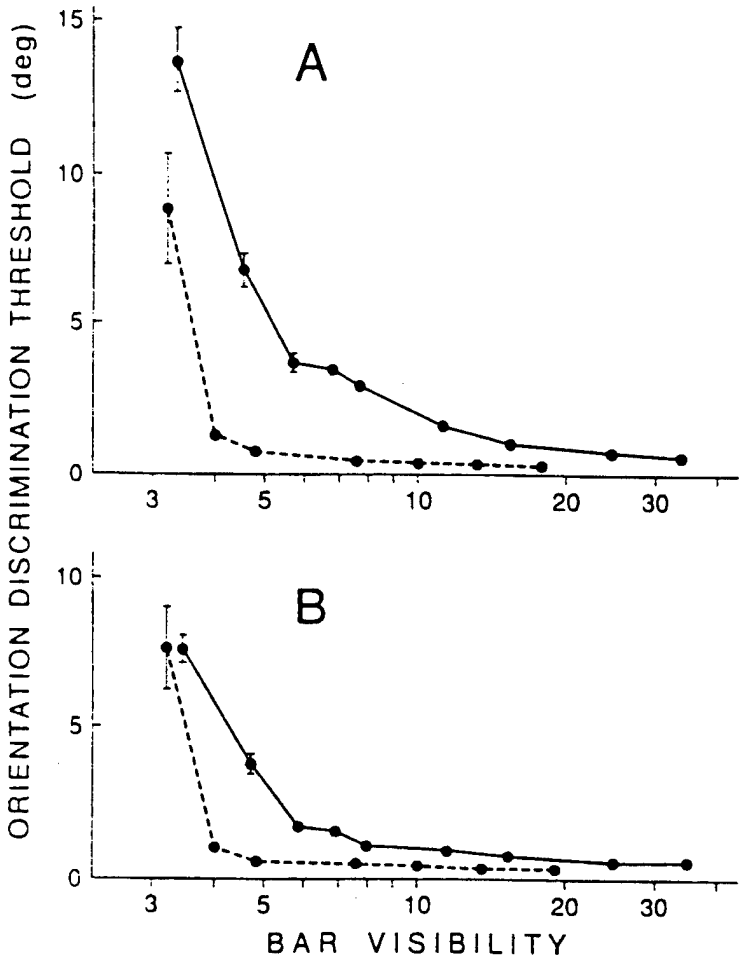

Figure 24 Orientation discrimination thresholds for a 5.0 x 1.4 deg texture-defined bar (continuous lines) and for a 5.0 x 1.4 deg luminance-defined bar (dashed lines) are plotted along the ordinates. Bar visibility (abscissa) is quantified as a multiple of bar detection threshold. For the texture-defined bar detection threshold is expressed as orientation contrast (β), and for the luminance-defined bar detection threshold is expressed as luminance contrast. A and B are for observers 1 and 2 respectively.

Department of Psychology
FAX: (416) 736-5814

UNIVERSITÉ YORK UNIVERSITY
FACULTY OF ARTS
4700 KEELE STREET • NORTH YORK • ONTARIO • CANADA • M3J 1P3

The orientation discrimination data shown in figure 23 can be discussed in terms of two hierarchical levels of processing, one operating on a considerably larger spatial scale than the other. At the first stage, each one of a parallel array of orientation-tuned neurons with small classical receptive fields is individually excited by one of the short (0.2 deg) lines that comprise the texture. At the second stage of processing the outputs of this parallel array of neurons are integrated spatially. This stage provides a basis for visually detecting the comparatively large (5 x 1.4 deg) OTD bar and for discriminating its orientation. So far as the spatially-integrative processing of bar orientation is concerned, the results of the first and also the second parts of experiment 1 indicate that spatial integration is not greatly different whether the integration is roughly parallel (e.g., Fig. 22A) or roughly perpendicular (e.g., Fig. 22B) to the orientations of the texture elements.

One possible explanation for the finding that the lowest values of orientation discrimination threshold are the same or not greatly different for OTD, LD, CD, MD and DD form is that the same neural mechanism determines orientation discrimination threshold for spatial form independently of which of the five kinds of contrast is responsible for the visibility of the form. An alternative hypothesis is that orientation discrimination threshold for the five kinds of form is determined by five different neural mechanisms, and that the similarity between the thresholds is a result of early visual development driven by the infant's persistent

Department of Psychology
FAX: (416) 736-5814

UNIVERSITÉ
YORK
UNIVERSITY

FACULTY OF ARTS
4700 KEELE STREET • NORTH YORK • ONTARIO • CANADA • M3J 1P3

attempts to achieve eye-limb coordination. Since an object is an object independently of how it is detected by the eye, the precision of orientation discrimination required of the organism would be the same for OTD, LD, CD, MD and DD form. These two hypotheses are discussed elsewhere (Refs. 155, 201, 211).

3.10 Texture-defined letter test

One paper has been published. D. Regan & X.H. Hong "Recognition and detection of texture-defined letters" Vision Research, 34, 2403-2407 (1994).

The broad issue is the ability to see and recognise an object such as a terrain feature. The experiment addresses a subject's ability to recognise an object whose visibility is created by texture contrast exclusively.

Methods

Stimulus textures were generated by an IBM 486PC clone with ATI VGA "Wonder plus XL24" graphics card, and displayed on a video monitor (Sony model CPD 1304). Resolution was 640 (horizontal) x 480 pixels. The screen measured 24 (horizontal) x 18 cm and, at the viewing distance of 2m, subtended 6.8 x 5.1 deg. so that one pixel subtended 0.64 min arc.

The screen was divided into 80 (horizontal) x 60 cells, each of 8 x 8 pixels. Any given cell contained one dotted bar. Each bar consisted of four dots as illustrated in Fig. 25A & B. (We used dotted lines to avoid the instrumental artifact that the luminance of a continuous line depended on its

Department of Psychology
FAX: (416) 736-5814

UNIVERSITÉ YORK UNIVERSITY
FACULTY OF ARTS
4700 KEELE STREET • NORTH YORK • ONTARIO • CANADA • M3J 1P3

orientation). In Fig. 25A & B the black squares represent illuminated pixels, and the crosses indicate other possible locations of illuminated pixels. Pixels that are not shown black or crossed were never illuminated. Fig. 25A shows one of the four possible positions of a vertical bar, and Fig. 25B shows one of the four possible positions of a horizontal bar. The texture could be degraded by noise by adding one dot to every cell, two dots to every cell, and so on up to 11 dots per cell. The placement of the noise dots within a cell was randomized from cell to cell. (A noise dot placed on top of a pre-existing dot had no effect). Thus, in every 8 x 8 pixel cell, there were 16 possible locations for a bar dot or noise dot and 48 forbidden locations.

A TD letter was created by placing one horizontal bar within every cell in the letter and one vertical bar within every cell outside the letter. With all bars horizontal or all bars vertical, the letter was perfectly camouflaged. Any vertical or horizontal stroke of the letter had a width of 5 cells. The letter was drawn within a square of 28 x 28 cells, so that at the viewing distance of 2m a letter subtended 2.4 x 2.4 deg. A reference texture was defined by having either one vertical bar or one horizontal bar in every cell. Fig. 26A is a photograph of the stimulus display for the letter H with zero noise dots per cell. In Fig. 26B & C the number of noise dots per cell were 2 and 4 respectively.

Department of Psychology

FAX: (416) 736-5814

UNIVERSITÉ YORK UNIVERSITY

FACULTY OF ARTS

4700 KEELE STREET • NORTH YORK • ONTARIO • CANADA • M3J 1P3

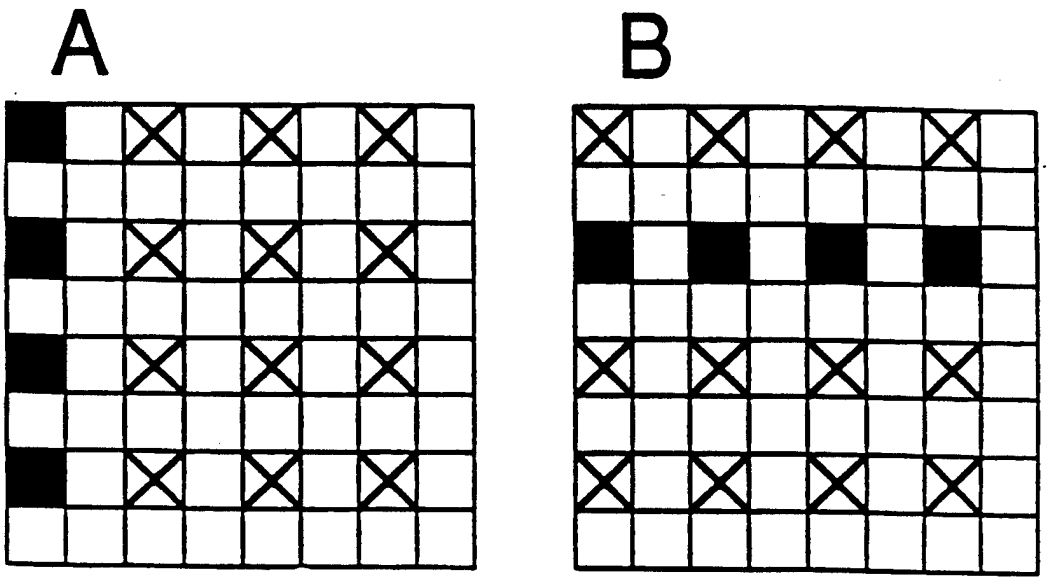

Figure 25 Each one of the 4800 cells comprised an array of 8 x 8 pixels . Only the pixels marked by a cross or a black square could be illuminated. Each cell contained a vertical bar in one of four possible positions [e.g. the black squares in (A)] or a horizontal bar in one of four possible positions [e.g. the black squares in (B)].

Department of Psychology

FAX: (416) 736-5814

UNIVERSITÉ
YORK
UNIVERSITY

FACULTY OF ARTS

4700 KEELE STREET • NORTH YORK • ONTARIO • CANADA • M3J 1P3

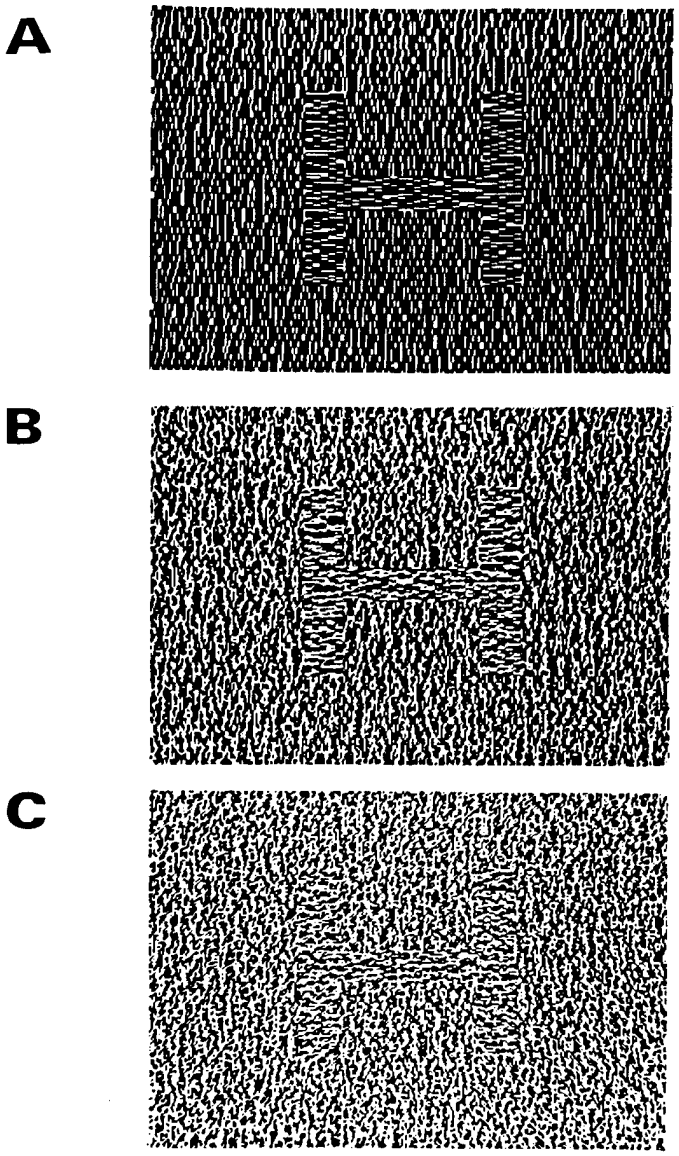

Figure 26 Photographs of a texture-defined letter (H) whose visibility is progressively degraded by adding 0, 2 & 4 noise dots per cell in panels A-D respectively.

Department of Psychology

FAX: (416) 736-5814

UNIVERSITÉ
YORK
UNIVERSITY

FACULTY OF ARTS

4700 KEELE STREET • NORTH YORK • ONTARIO • CANADA • M3J 1P3

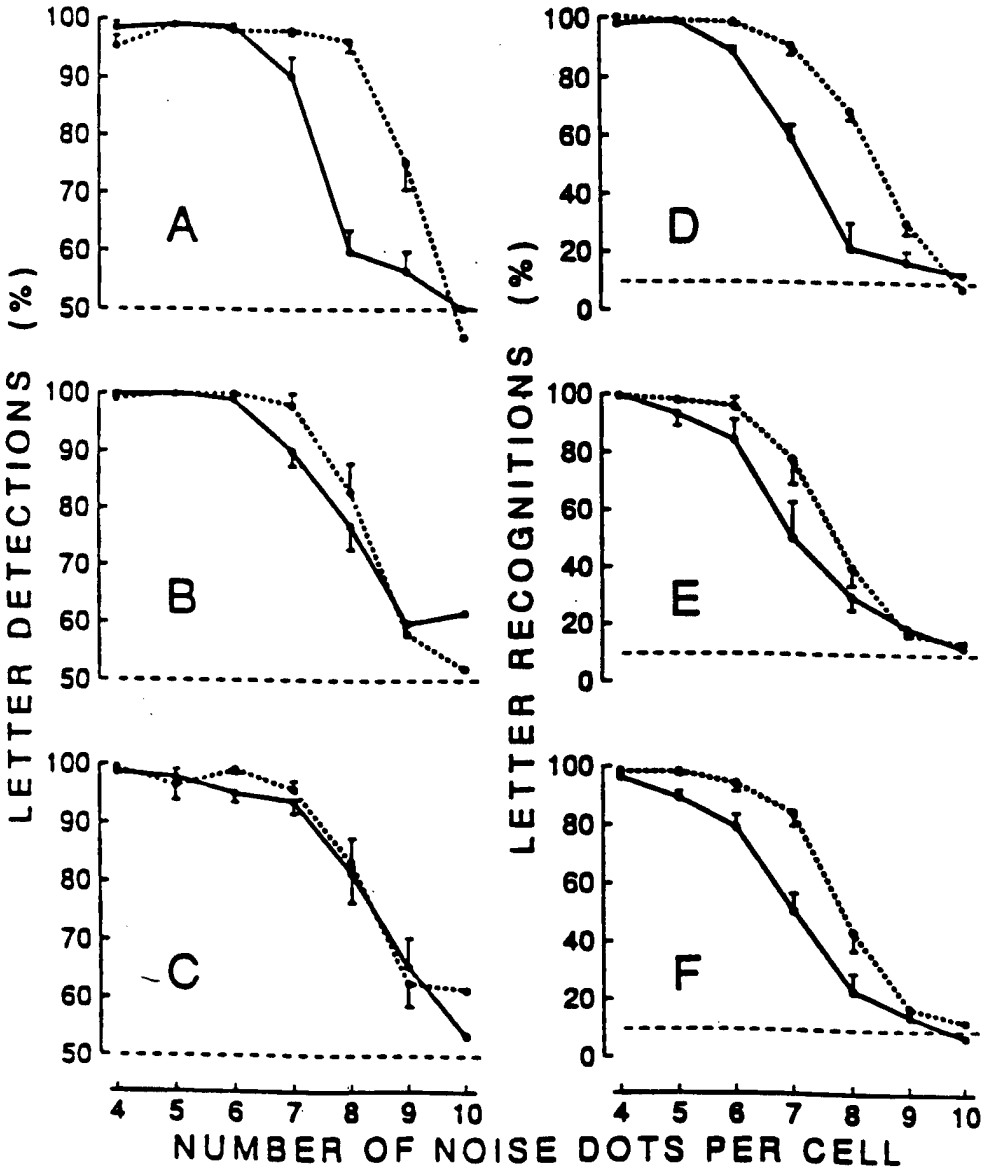

Figure 27 Percent correct detection (A-C) and recognition (D-F) of texture-defined letters. The horizontal dashed lines indicate chance level of performance. A, D, observer 1. B, E, observer 2. C, F, observer 3.

Department of Psychology

FAX: (416) 736-5814

UNIVERSITÉ
YORK
UNIVERSITY

FACULTY OF ARTS

4700 KEELE STREET • NORTH YORK • ONTARIO • CANADA • M3J 1P3

Each trial comprised two one-sec presentations, only one of which contained a letter. During the other presentation of a trial pair every 8 x 8 pixel cell contained either a vertical bar or a horizontal bar. There were 10 letters: H, C, D, K, N, O, R, S, V and Z. The number of noise dots per cell was identical in the two presentations. The monitor screen was blank except during presentations. The two presentations were separated by an interval of 0.5 sec. The order of the two presentations was randomised.

Subjects were instructed to state whether the letter was presented in the first or in the second trial (letter detection), and to name the letter (letter recognition).

Results

Detection of TD letters

For all subjects, percent correct detections remained at near-100% from zero up to 5 or 6 noise dots per cell, after which detection errors increased progressively, reaching chance (50% correct) at 9 or 10 noise dots per cell. After preliminary practice runs that established this pattern of scores, letters with from 0 to 3 noise dots per cell were omitted so as to focus on the portion of the psychometric function between 4 and 10 noise dots per cell. Detection scores averaged over all 10 letters for each of the three subjects are plotted in Fig. 27A-C. Dotted lines are for the case that the same texture pattern remained on the screen throughout any given presentation. Continuous lines are for dynamic texture.

Department of Psychology
FAX: (416) 736-5814

UNIVERSITÉ
YORK
UNIVERSITY

FACULTY OF ARTS
4700 KEELE STREET • NORTH YORK • ONTARIO • CANADA • M3J 1P3

Recognition of TD letters

Letter recognition scores averaged over all 10 letters for each of the three subjects are plotted in Fig. 27D-F. Dashed and solid lines have the same meaning as in Fig. 27A-D. Beyond 4 to 5 noise dots per cell, letter recognition scores fell off progressively, reaching chance (10% correct) at 8 to 10 noise dots per cell.

For all subjects, the curve for the dynamic texture was shifted to the right of the curve for the static texture.

One possible explanation for the difference between results for static and dynamic textures is as follows. The visibility of the letters was degraded by two sources of noise: variability of the texture across the pattern (Rubenstein & Sagi, 1990), and the dots that we added deliberately. In the dynamic pattern case, both of these noise components were, in general, different in every one of the 70 frames in one presentation. In contrast, every one of these 70 frames contained the same letter, and the relation between texture inside and outside the letter was the same. Thus, by analogy with the process of time domain averaging (reviewed in Regan, 1989, pp. 47-50), summation over multiple frames due to temporal integration within the visual pathway might have enhanced signal-to-noise ratio and hence improved subjects' scores.

3.11 Modelling the detection and recognition of texture-defined form

Department of Psychology

FAX: (416) 736-5814

UNIVERSITÉ YORK UNIVERSITY

FACULTY OF ARTS

4700 KEELE STREET • NORTH YORK • ONTARIO • CANADA • M3J 1P3

Results have been reported to the IEEE and a complete report has been published. D. Regan, S.J. Hamstra, X.H. Hong & S. Kaushal "Nonlinearities in the visual processing of motion and form". Proc. IEEE Conf. on Systems, Man & Cyberbetics, pp. 156-159, (1993). D. Regan & X.H. Hong (1994). "Two models of the recognition and detection of texture-defined letters compared. Biological Cybernetics, 72, 389-396.

Outline of Two Models

Both models comprise a sequence of physiologically-plausible filtering stages. The first three stages and the final stage are the same in both models. Model 1 has only one nonlinear stage, and this distinguishes it from model 2, which has a second nonlinear stage. The effect of the second nonlinear stage is to enhance the texture boundary by comparing texture at different locations on the texture pattern. The rationale is based on Nothdurft's (1991, 1992) demonstration that segregation between two orientation textures and also the perception of the texture boundary arise from local differences in orientation near the border rather than by global differences in the orientation statistics of the two textures.

Model 1, illustrated in Figure 28A, comprises the following sequence of processing stages: (1) parallel orientation-selective linear spatial filters; (2) full wave rectification; (3) low-pass spatial filtering (i.e. blurring); (4) subtraction of signals from filters tuned to different orientations; (5) either a letter detection or a letter recognition stage. Model 2, illustrated in Fig. 28B differs

Department of Psychology

FAX: (416) 736-5814

UNIVERSITÉ
YORK
UNIVERSITY

FACULTY OF ARTS

4700 KEELE STREET • NORTH YORK • ONTARIO • CANADA • M3J 1P3

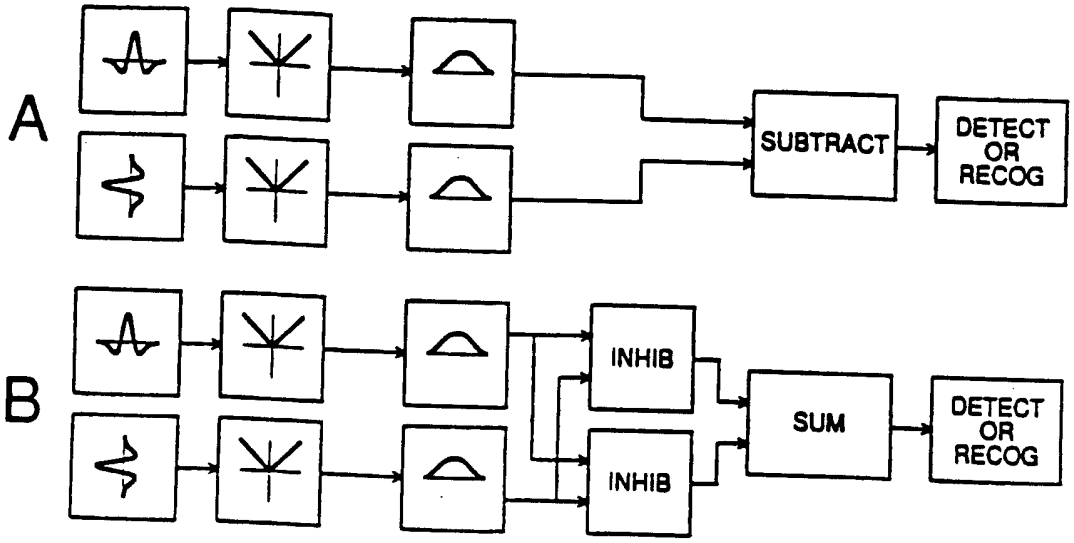

Figure 28 A, B: Block diagrams of models 1 and 2 respectively. The sequence of processing depicted is applied simultaneously to every pixel in the stimulus display.

Department of Psychology

FAX: (416) 736-5814

UNIVERSITÉ
YORK
UNIVERSITY

FACULTY OF ARTS

4700 KEELE STREET • NORTH YORK • ONTARIO • CANADA • M3J 1P3

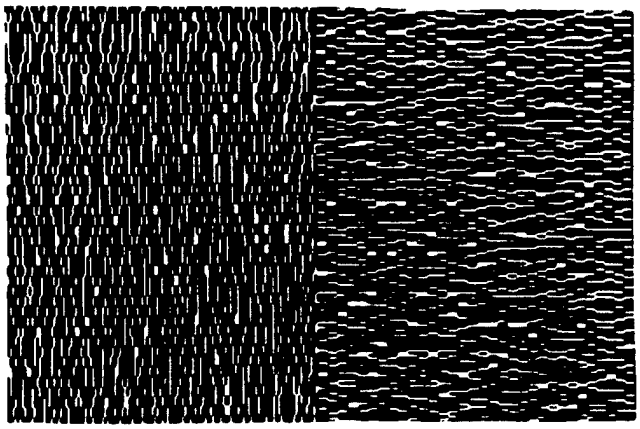

Figure 29 Photograph of segregating textures with a single boundary.

Department of Psychology

FAX: (416) 736-5814

UNIVERSITÉ
YORK
UNIVERSITY

FACULTY OF ARTS

4700 KEELE STREET • NORTH YORK • ONTARIO • CANADA • M3J 1P3

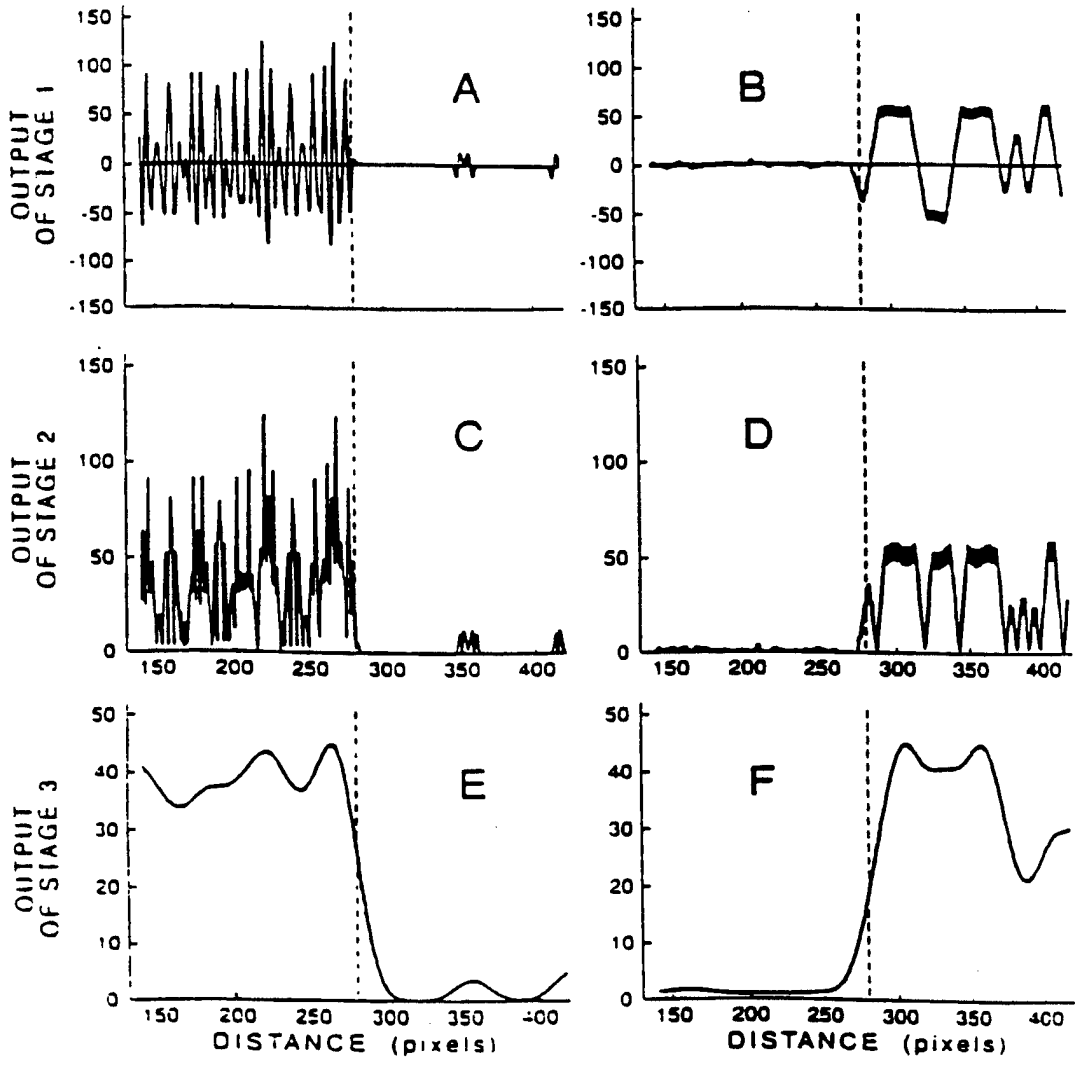

Figure 30 A: Result of convolving a vertically-oriented stage 1 DOG filter with the Fig. 3A pattern. B: As for A except that the filter was oriented horizontally. C and D: Rectified versions of A and B respectively. E and F: low-pass filtered versions of C and D.

Department of Psychology

FAX: (416) 736-5814

UNIVERSITÉ
YORK
UNIVERSITY

FACULTY OF ARTS

4700 KEELE STREET • NORTH YORK • ONTARIO • CANADA • M3J 1P3

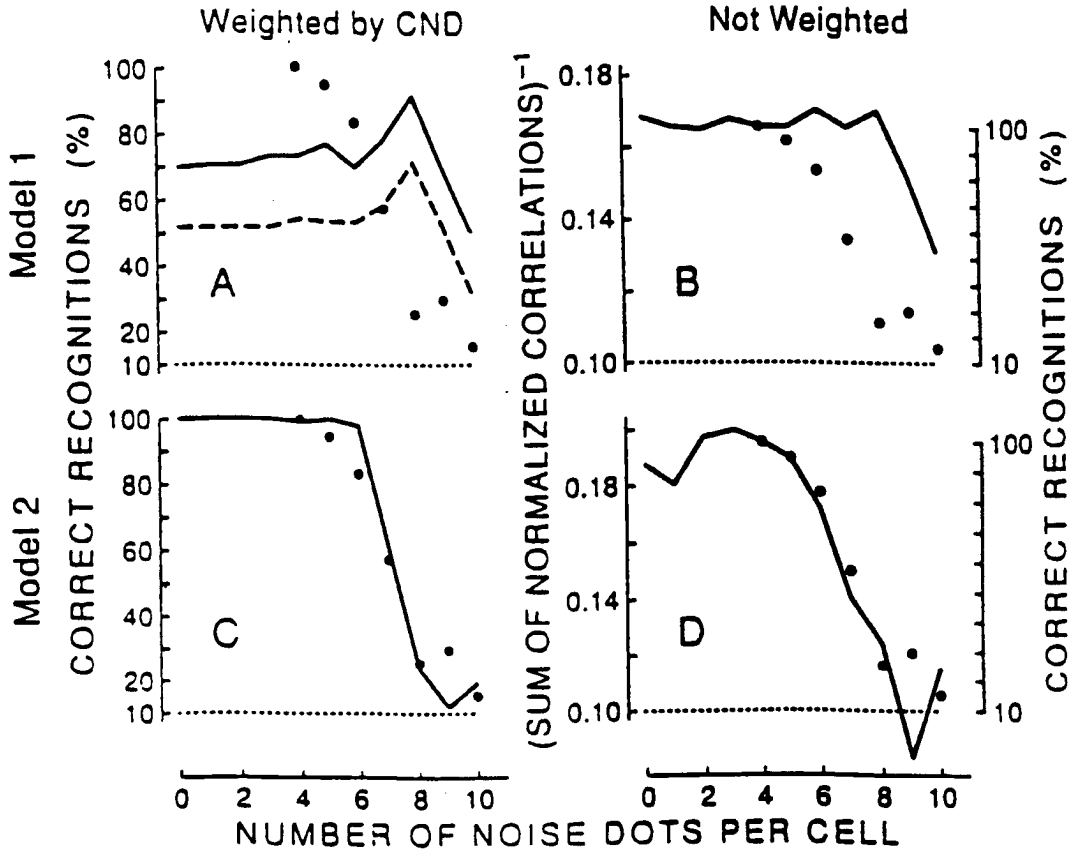

Figure 31 Filled circles plot percent correct reading accuracy for letter H averaged over all four observers (ordinate) versus the number of noise dots per cell. The curves in A and C plot the theoretical predictions of model 1 (A) and model 2 (C) obtained from cross correlations weighted by cumulative normal distributions. Continuous and dashed lines were obtained using different weighting functions. The continuous lines in B and D plot predictions obtained as in A and C except that the cross correlations were not weighted.

Department of Psychology

FAX: (416) 736-5814

UNIVERSITÉ
YORK
UNIVERSITY

FACULTY OF ARTS

4700 KEELE STREET • NORTH YORK • ONTARIO • CANADA • M3J 1P3

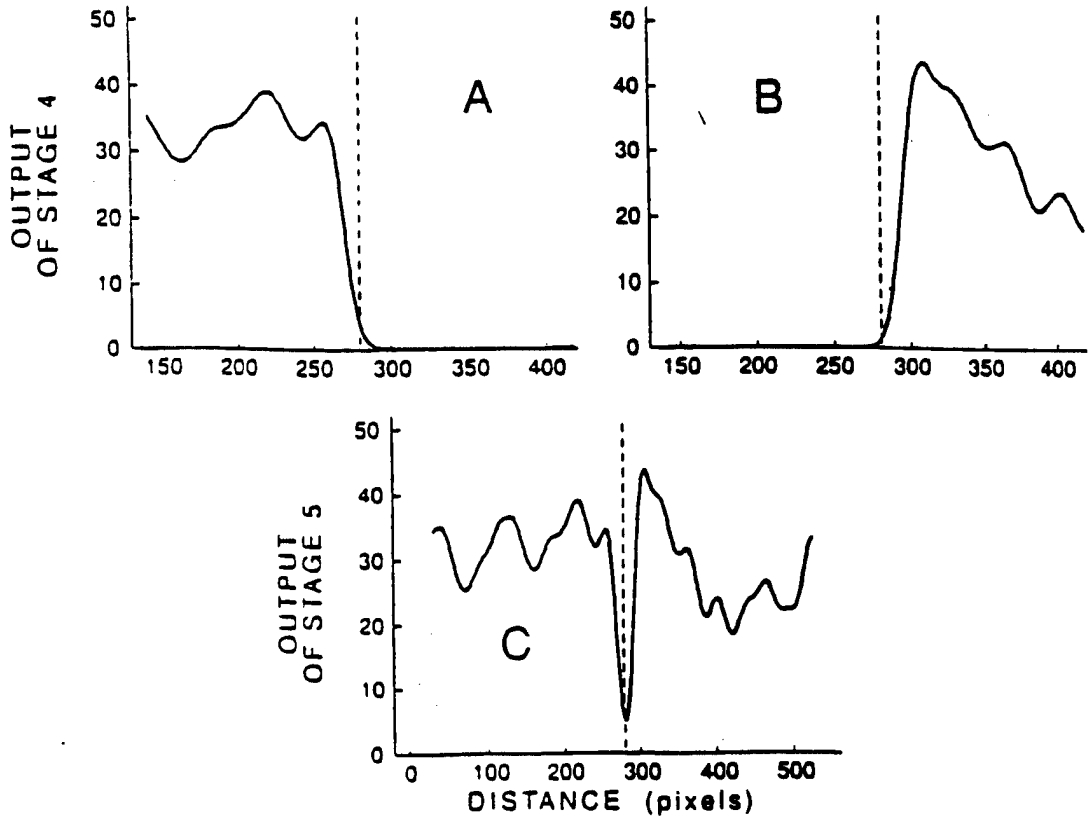

Figure 32 The first three stages of model 2 give the outputs shown in Fig. 4E and F. The output of the stage 4 inhibition is shown in A and B. Trace C is the sum of traces A and B. See text for details.

Department of Psychology

FAX: (416) 736-5814

UNIVERSITÉ
YORK
UNIVERSITY

FACULTY OF ARTS

4700 KEELE STREET • NORTH YORK • ONTARIO • CANADA • M3J 1P3

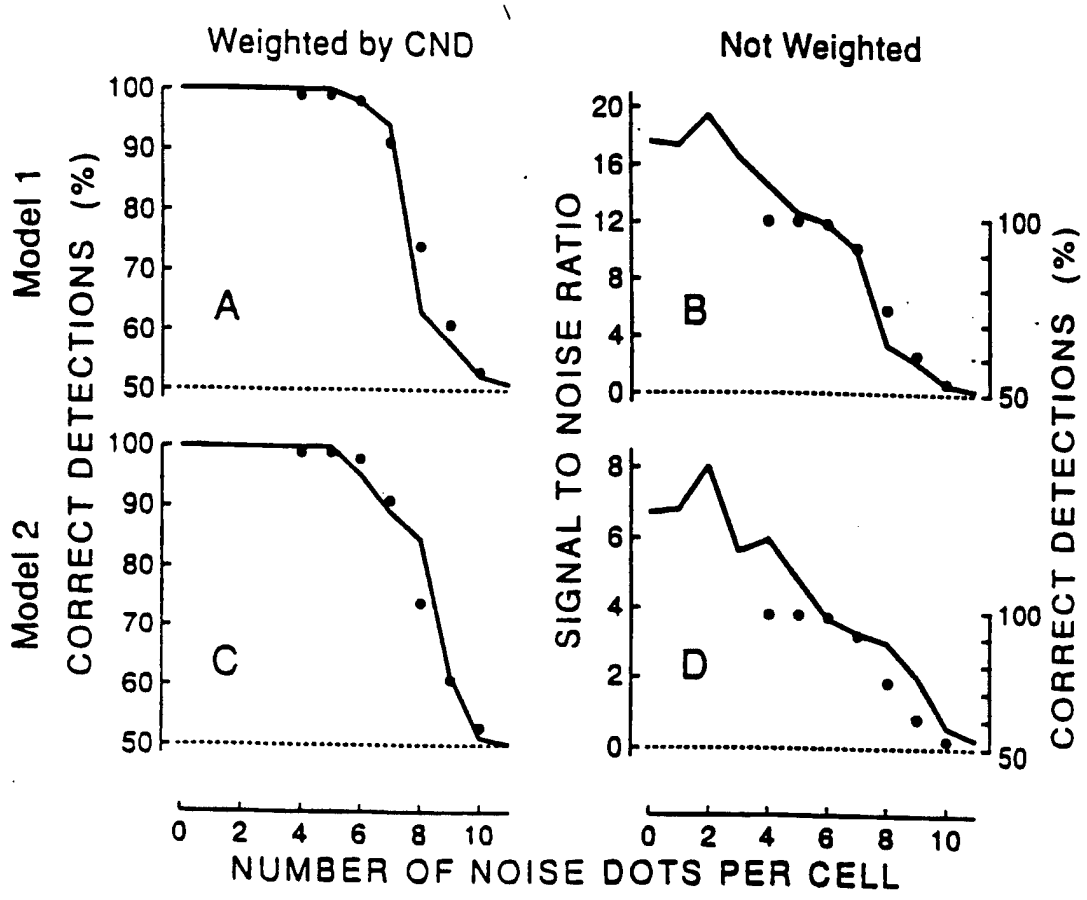

Figure 33 Filled circles plot percent correct letter detections averaged over all ten letters and all four observers (ordinate) versus the number of noise dots per cell. The continuous lines in A and C plot the theoretical predictions for models 1 and 2 respectively using the weighted signal-to-noise ratio of a letter-segment detector to model the letter detection stage. The continuous lines in B and D plot theoretical predictions based on the unweighted signal-to-noise ratios.

Department of Psychology
FAX: (416) 736-5814

UNIVERSITÉ
YORK
UNIVERSITY

FACULTY OF ARTS
4700 KEELE STREET • NORTH YORK • ONTARIO • CANADA • M3J 1P3

from model 1 in that nonlinear inhibition follows the stage 3 low-pass filtering.

Letter Recognition Predictions and Data

First we describe stage 1. The spatial filtering properties of visual pathway neurons have been modelled by several functions including Gabor functions and difference of Gaussians (Marceltja, 1980; Daugman, 1980; Rodieck & Stone, 1965; Parker & Hawken, 1988). We have chosen to use difference of Gaussians (DOG) filters in stage 1 on the basis of the good fit with physiological data and ease of computation. We believe that this is not a critical choice.

The DOG filter filled an 11 x 11 pixel square, and had a sensitivity curve such that the areas above and below zero were equal so that the filter would not respond to uniform illumination. The equation of the DOG filter was

$$y = 3 \exp(-(x/\sigma)^2) - 2 \exp(-0.44(x/\sigma)^2) \quad (15)$$

where x was distance expressed in pixels and σ was equal to 1.5 pixels. On the grounds that, experimentally, psychophysical performance on letter detection and also letter recognition were considerably affected when high spatial frequencies in the stimulus were attenuated by optical blur, the value of σ was chosen so that a single line in the texture pattern would strongly stimulate the DOG filter when centred on the filter. (This was not a critical choice however: our predictions were similar when σ was 1.0 and 3.0 pixels). First, a vertically-oriented filter was convolved with the stimulus illustrated in Fig.

Department of Psychology
FAX: (416) 736-5814

UNIVERSITÉ YORK UNIVERSITY

FACULTY OF ARTS

4700 KEELE STREET • NORTH YORK • ONTARIO • CANADA • M3J 1P3

29, giving the trace shown in Fig. 30A where the vertical dashed line indicates the vertical texture boundary. Then a horizontally-oriented filter was convolved with the stimulus illustrated in Fig. 29, giving the trace shown in Fig. 30B where the vertical dashed line indicates the same texture boundary.

Stage 2 was the first nonlinear stage. It follows Bergen and Adelson (1988), and is equivalent to summing the outputs of two half-wave rectifiers, one belonging to the ON system and one to the OFF system. (Rectification models the fact that a negative firing rate is impossible). The rectified outputs of stage 1 are shown in Fig. 30C and D respectively.

At stage 3 of model 1, the Fig. 30C and D traces were smoothed by a circularly-symmetric Gaussian filter (Fig. 30E and F). The standard deviation (σ) of the gaussian was 10.5 pixels, and it was truncated when the ordinate fell to 1.0% of its maximum value, giving a total filter diameter of 63 pixels.

We modelled the behavioural recognition of a stimulus letter in terms of cross-correlations with neural templates of the 10 possible letters. The procedure can be understood as follows. The letter H template was placed at the upper left corner of a central 304 x 304 pixel square, and the correlation coefficient was calculated. Then the template was translated one pixel rightwards, the correlation coefficient was calculated again, and so on until the rightmost edge of the template hit the right edge of the 304 x 304 pixel square. This entire procedure was repeated with the template displaced downwards by 9 pixels, and so on, giving a total of 9 left-to-right passes. We

Department of Psychology
FAX: (416) 736-5814

UNIVERSITÉ
YORK
UNIVERSITY

FACULTY OF ARTS
4700 KEELE STREET • NORTH YORK • ONTARIO • CANADA • M3J 1P3

noted the largest value of the resulting correlation coefficients. The same procedure was repeated with each one of the remaining 9 templates. To allow for the variability between one texture pattern and another we repeated this procedure for 5 different texture patterns and averaged the results. From the raw correlations we calculated normalized correlations (b). For example, for the H_7 stimulus (i.e., letter H with 7 noise dots per cell), b = (correlation between the output of stage 4 for the H_7 stimulus and the template of a given letter)/(correlation between the output of stage 4 for the H_7 stimulus and the H template).

Suppose that the b values for every template except the H template is zero. Clearly, letter recognition will be 100% correct. Now suppose that the b values are 1.0 for letters H and S, but are zero for the remaining 8 letters. Letter recognition will be 50% correct. Again, if the b values are 1.00 for letters H, S and R, but are zero for the remaining 7 letters, letter recognition will be 33% correct. If the visual system is noise-free, letter recognition will change abruptly from 33.3% to 50% correct if the b value for letter R falls from 1.00 to 0.99. But if the visual system is not noise-free, letter recognition will change smoothly and continuously from 33.3% to 50% correct as the b value for letter R falls progressively from 1.0 through lower values. We allowed for the effect of noise by weighting the values of b in such a way that b values were attenuated by a larger and larger factor as they fell below 1.0. Following Green and Swets (1966) we chose as a weighting function a

Department of Psychology
FAX: (416) 736-5814

UNIVERSITÉ YORK UNIVERSITY
FACULTY OF ARTS
4700 KEELE STREET • NORTH YORK • ONTARIO • CANADA • M3J 1P3

cumulative normal distribution on the assumption that the subject's task can be modelled as discriminating signal-plus-noise from noise.

We converted the ten weighted b values to a predicted percent correct letter recognition score ($100R_W$) by writing

$$100\ R_W = 100(1/\Sigma[b_W]) \text{ ---------- (16)}$$

where b_W was the weighted value of b. This procedure was used to predict the letter recognition score for all the letter H stimuli (i.e. H_0, H_1, H_2.....H_{10}).

The continuous line in Fig. 31A plots the predicted reading scores for letter H using a weighting function whose 50% and 75% points were respectively at b=0.88 and b=0.92. The fit with experimental data (filled circles) is poor. The dashed line in Fig. 31A plots predictions obtained with a different weighting function whose 50% and 75% points were respectively at b=0.84 and b=0.89, and illustrates the point that the fit with data cannot be made close by an appropriate choice of weighting function.

To indicate the effect of the cumulative normal weighting function, the continuous line in Fig. 31B plots R as left hand ordinate where

$$R = 1/\Sigma[b] \text{ ---------- (17)}$$

The only difference between the continuous lines in Fig. 31A and B is that no weighting function was used in Fig. 31B.

Now we will discuss the predictions of model 2. Model 2 is illustrated in Fig. 28B. The stage 3 low-pass filter is crucial in model 2, because, as

Department of Psychology
FAX: (416) 736-5814

UNIVERSITÉ
YORK
UNIVERSITY

FACULTY OF ARTS
4700 KEELE STREET • NORTH YORK • ONTARIO • CANADA • M3J 1P3

illustrated in Fig. 32A and B, it allows the cross-orientation inhibition to operate between different locations on the texture pattern by removing energy from the left of the texture boundary in Fig. 30E and from the right of the texture boundary in Fig. 30F. When the low-pass filter was omitted, the model's predictions fitted the psychophysical data very poorly. Furthermore, filters with a standard deviation of 3.5 pixels (diameter 23 pixels) or 13.5 pixels (diameter 81 pixels) gave a poorer fit with data than did the filter with 10.5 pixels standard deviation reported here. When the traces in Fig. 32A and B were summed (Fig. 32C), the texture boundary (vertical dashed line) was clearly marked by a sharp dip in the curve. In contrast, when the traces in Fig. 32E and F were summed (not shown), the texture boundary was not evident.

The rationale for choosing cross-orientation inhibition as a boundary-enhancing process is based on two physiological lines of evidence. First, in human subjects, stimulation by superimposed orthogonal gratings produces evoked potentials that show strong nonlinear inhibition(Morrone & Burr, 1986; Ref. 170). Second, cross-orientation inhibition is well established at single-cell level in visual cortical neurons of cat and monkey and cortical cells can show orientation-selective effects from stimuli outside the classic visual receptive field (Nelson & Frost, 1978; Burr et al., 1981; Toyama et al., 1981; Morrone et al., 1982).

Department of Psychology
FAX: (416) 736-5814

UNIVERSITÉ YORK UNIVERSITY
FACULTY OF ARTS
4700 KEELE STREET • NORTH YORK • ONTARIO • CANADA • M3J 1P3

At stage 4, for any given pixel, the output of stage 3 (ordinate in Fig. 30E) was transformed into the output of stage 4 (ordinate in Fig. 32A) by means of equation (18).

$$y'_v = y_v \exp(-ky_h) \quad \text{---------- (18)}$$

where y_v was the output of stage 3 and y'_v was the output of stage 4. Similarly, equation (23)

$$y'_h = y_h \exp(-ky_v) \quad \text{---------- (19)}$$

was used to transform the output of stage 3 (ordinate in Fig. 30F) into the output of stage 4 (ordinate in Fig. 32B), where y_h was the output of stage 3 and y'_h was the output of stage 4.

Letter Detection Predictions and Data

We assumed that the subject's detection strategy was to search for any part of a letter rather than to search for the entire letter. It was possible for subjects to adopt this strategy because they were told that the form to be detected was a letter and were shown high-visibility letters before they attempted to detect low-visibility letters. This prior knowledge allowed them to search for part of a letter because they already knew what a part of a letter looked like. In particular, the letters were composed of several elongated segments. We modelled this "to detect a part is to detect the whole" cognitive strategy as follows.

The letter-segment detector operated as follows. We took a bar-shaped region whose height was equal to the height of a letter and whose width was

Department of Psychology
FAX: (416) 736-5814

UNIVERSITÉ
YORK
UNIVERSITY

FACULTY OF ARTS
4700 KEELE STREET • NORTH YORK • ONTARIO • CANADA • M3J 1P3

equal to that of a letter stroke. Texture inside and outside the bar consisted, respectively, of horizontal and vertical lines. At the input to the letter-segment detector, a texture-defined bar with zero noise dots per cell was represented by a black bar of width 48 pixels surrounded by a white area of almost uniform luminance. As the number of noise dots was progressively increased, the luminance of the bar and its surroundings became progressively more patchy. We took a region 48 pixels wide whose height was equal to the height of a letter and placed it on the far left of the display at the input to the letter-segment detector. The value of DL was calculated. We defined DL as the difference between the highest and the lowest ordinate within the 48 pixel interval. Then we moved the interval one pixel to the right and calculated a second value for DL, and so on. We defined the signal-to-noise ratio of the letter-segment detector as equal to DL_S/s, where DL_S is the value of DL when the interval was centred on the texture-defined strip, and s was the standard deviation of all the values of DL across the display.

First we will discuss the predictions of model 1. The continuous line in Fig. 33A plots the detection scores predicted by weighting the signal-to-noise ratios with a cumulative normal distribution. Filled circles plot experimentally-measured detection scores averaged over both all 10 letters and all 4 subjects. Fig. 33A shows that the fit between prediction and data was close.

Department of Psychology
FAX: (416) 736-5814

UNIVERSITÉ
YORK
UNIVERSITY

FACULTY OF ARTS
4700 KEELE STREET • NORTH YORK • ONTARIO • CANADA • M3J 1P3

The continuous line in Fig. 33B plots unweighted signal-to-noise ratio versus the number of noise dots per cell. To compare these unweighted ratios with experimentally-measured letter detection scores we set the chance detection score (50%) on the right hand ordinate equal to a signal-to-noise ratio of zero on the left hand ordinate. We then set the signal-to-noise ratio for the stimulus with 6 noise dots per cell equal to the experimentally-measured detection score (98% correct) for that stimulus. A comparison of Fig. 33A and B brings out the effect of the weighting. The shape of the weighting function was almost irrelevant. Its only purpose was to create a saturation or ceiling effect so as to render all signal-to-noise ratios over about 12 equivalent to a 100% correct score.

The corresponding plots for model 2 (Fig. 33C and D) were similar. Just as for model 1, the shape of the weighting function was almost irrelevant; its chief function was to provide a saturation or ceiling effect.

Discussion

It is not difficult to predict letter detection data if we assume that the subject's detection strategy was to search for a part of the entire letter. Figure 33 indicates that the predictions of both models are a good fit with the data. Even the unweighted signal-to-noise ratios fit the data reasonably well for 6 noise dots per cell and upwards. We conclude that a model with no second nonlinearity (model 1) predicts letter detection data with as good accuracy as the model with a second nonlinearity.

Department of Psychology
FAX: (416) 736-5814

UNIVERSITÉ
YORK
UNIVERSITY

FACULTY OF ARTS
4700 KEELE STREET • NORTH YORK • ONTARIO • CANADA • M3J 1P3

It is more difficult to predict letter recognition than letter detection data. Model 1, lacking a second nonlinearity, fails badly whatever cumulative normal weighting function is chosen (Figure 31A). Recollect that the effect of the second nonlinear stage in model 2 is to enhance the boundary between different textures by comparing textures at different locations in the texture pattern. For model 2 the fit with data is good (Fig. 31C) even when the cross-correlations are not weighted (Fig. 31D). In view of the finding that some patients with multiple sclerosis (a demyelinating disease) show a selective loss of ability to detect and read texture-defined letters (see Section, 3.13 below) it may be significant that orientation-specific lateral interactions in monkey striate cortex are transmitted via myelinated horizontal connections (Gilbert et al., 1990).

3.12 Normally-sighted individuals: Intersubject variations in letter reading tests using texture-defined letters, motion-defined letters, low contrast luminance-defined letters and high contrast luminance-defined letters.

A paper has been published entitled "Test-retest variability and correlations between tests of texture processing, motion processing, visual acuity and contrast sensitivity" by T. L. Simpson & D. Regan in Optometry & Vision Science, (1995), 72, 11-16.

The broad issue is the ability to recognise a semi-camouflaged terrain feature by means of texture contrast.

Methods

Department of Psychology
FAX: (416) 736-5814

UNIVERSITÉ YORK UNIVERSITY
FACULTY OF ARTS
4700 KEELE STREET • NORTH YORK • ONTARIO • CANADA • M3J 1P3

In 20 normally-sighted subjects, monocular visual acuity, Regan 11% and 96% letter acuity, Pelli-Robson contrast sensitivity, and thresholds for recognising motion-defined letters (MD letters) and texture-defined letters (TD letters) were each measured twice on different days.

Results

Test-retest correlations were 0.75, 0.91, 0.61, 0.90 and 0.84 for high and low contrast acuity, contrast sensitivity, and motion and texture processing respectively.

Conclusions

Test-retest variability for the motion-defined and texture-defined letter tests were at least as low as for established clinical tests of high- and low-contrast acuity and contrast sensitivity. We conclude that the MD and TD letter tests offer behavioural and clinical information that not only complements, but is at least as reliable as, information provided by conventional visual acuity tests.

3.13 Selective loss in the ability of patients with multiple sclerosis to read texture-defined letters, motion-defined letters and luminance-defined letters

Results have been reported to ARVO in 1994 and a paper has been published. Simpson TL & D Regan. "Specific defects in the visual processing of texture in patients with multiple sclerosis". Presented at the Annual meeting of the Association for Research in Vision and Ophthalmology (ARVO), Sarasota. Invest. Ophthalmol. & Vis. Sci. 35, Suppl. 4, p. 1257 (1994). Regan D &

Department of Psychology
FAX: (416) 736-5814

UNIVERSITÉ
YORK
UNIVERSITY

FACULTY OF ARTS
4700 KEELE STREET • NORTH YORK • ONTARIO • CANADA • M3J 1P3

Simpson TL "Multiple sclerosis can cause visual processing deficits specific to texture-defined form". Neurology, 45, 809-815 (1995).

The broad issue is the ability to see and recognise a terrain feature by means of texture contrast. We performed the following tests in 25 patients with multiple sclerosis (MS) and 25 age-matched control subjects: recognition of texture-defined (TD) letters; recognition of motion-defined (MD) letters; recognition of luminance-defined (LD) letters of 96% and 11% contrasts. Six patients with normal visual acuity were abnormal on recognising TD letters, of whom one gave normal results on all other tests. Eleven patients were abnormal on MD letter recognition, of whom four gave normal results on all other tests. Visual acuity for letters of 11% contrast were abnormally low in seven patients, of whom two gave normal results on all other tests. We conclude that the neural mechanisms underlying recognition of TD, MD and low-contrast LD letters in subjects with normal visual acuity are sufficiently different that they can be differentially damaged by MS. Therefore, TD, MD and LD letter tests provide complementary information. We suggest that the detection of TD letters can be disrupted by demyelination of long-range horizontal connections between orientation-tuned neurons in striate cortex.

3.14 Parallel processing of three visual dimensions

One report has been published "Parallel independent encoding of orientation, spatial frequency and contrast" by A. Vincent & D. Regan Perception (1995) 24, 491-499.

Department of Psychology

FAX: (416) 736-5814

UNIVERSITÉ
YORK
UNIVERSITY

FACULTY OF ARTS

4700 KEELE STREET • NORTH YORK • ONTARIO • CANADA • M3J 1P3

These two experiments address the cognitive issue of attentional resources. A considerable body of experimental evidence supports the hypothesis that early visual processing of spatio-temporal information can be modelled in terms of parallel psychophysical channels. In such psychophysical models of early visual processing, retinal image information typically passes through an array of filters, each of which is tuned to temporal frequency, spatial frequency and orientation. The question of possible interactions between the processing of temporal and spatial information has been primarily investigated by using techniques of masking, adaptation or suprathreshold summation, all of which rely on an analysis of how the presence of one stimulus affects a subject's ability to detect a second stimulus. The weight of evidence does not support the idea that the orientation, spatial frequency and temporal tuning of these early visual filters is separable (i.e. independent).

However, the majority of the studies cited above focused on the detection of gratings of different spatial modulation frequencies, spatial frequencies and orientations, and there is evidence that the results of experiments on discrimination cannot necessarily be predicted from the results of experiments on detection. For example, in spite of the evidence just cited that the orientation and spatial frequency tuning of early visual filters are not independent, we have shown that orientation discrimination thresholds for pairs of gratings differ widely in spatial frequency are as low as

Department of Psychology
FAX: (416) 736-5814

UNIVERSITÉ YORK UNIVERSITY
FACULTY OF ARTS
4700 KEELE STREET • NORTH YORK • ONTARIO • CANADA • M3J 1P3

orientation discrimination thresholds for pairs of gratings of the same spatial frequency, and spatial frequency discrimination threshold for pairs of orthogonal gratings are as low as for pairs of parallel gratings (Ref. 127).

A limitation of earlier discrimination studies is that they did not involve the temporal dimension. As well, most of these studies have required the subject to discriminate the orientation of two considerably different spatial frequencies or to discriminate the spatial frequency of two considerably different orientations. This experimental design requires subjects to process only one dimension at a time, and to filter out changes in the task— irrelevant dimension. Such experiments fail to address the further question whether there are interactions between the processing of orientation and spatial frequency when they are processed simultaneously. I report here two empirical studies. One was on the extent to which observers can unconfound simultaneous changes in the temporal frequency, spatial frequency and orientation of a grating when they are required to encode all three visual dimensions simultaneously. In a second study we measured the extent to which observers can unconfound simultaneous changes in the contrast, spatial frequency and orientation of a grating when they are required to encode all three visual dimensions simultaneously.

The method of constant stimuli was used in both studies. Trial stimuli were organized as a cube of 6 x 6 x 6 cells. Each of the 216 cells represented a different grating. The three visual dimensions varied orthogonally along the

Department of Psychology
FAX: (416) 736-5814

UNIVERSITÉ
YORK
UNIVERSITY

FACULTY OF ARTS
4700 KEELE STREET • NORTH YORK • ONTARIO • CANADA • M3J 1P3

x-axis, y-axis and z-axis of the stimulus cube. The 216 test stimuli were presented in random order, one per trial. After each trial the observers were required to make three judgements. For each of the visual dimensions in turn the observer judged whether the test value was greater or smaller than the mean of the set of 216 stimuli. In subsidiary experiments only one visual dimension at a time was varied so that observers made only one rather than three discriminations after each trial.

The task required of our subjects involved memory and selective attention as well as visual perception. Variations of the three dimensions were totally confounded within the set of 216 stimuli. The subject's task was to unconfound and to discriminate the simultaneous variations of all three variables with respect to reference values stored in memory. Following a previous line of argument (Ref. 150) we can model this task as follows: (1) build up a memory of the mean values of all three variables for the set of 216 gratings; (2) neurally encode and store in memory the values of the three variables presented in any given test grating; (3) selectively attend to the newly-stored representation of variable 1, and compare it with the stored representation of the mean value of variable 1 of the set of 216 gratings; (4) selectively attend to the newly-stored representation of variable 2, and compare it with the stored representation of the mean value of variable 2 for the set of 216 gratings; (5) selectively attend to the newly-stored representation

Department of Psychology
FAX: (416) 736-5814

UNIVERSITÉ
YORK
UNIVERSITY

FACULTY OF ARTS
4700 KEELE STREET • NORTH YORK • ONTARIO • CANADA • M3J 1P3

of variable 3 and compare it with the stored representation of the mean value of variable 3 for the set of 216 gratings.

Using multiple stepwise regression analysis we found that observers could almost perfectly unconfound simultaneous variations in three variables.

Figs. 34 and 35 show the results of a different kind of analysis of the same data in which we obtained nine psychometric functions simultaneously.

However, even though subjects were able to ignore variations in the two task-irrelevant variables, it does not necessarily follow that discrimination threshold for the task-relevant variable was unaffected by the simultaneous changes in the task-irrelevant variables. A plausible possibility is that orientation discrimination threshold would be lower when the only trial-to-trial variations were in the task-relevant variable than when all three variables changed simultaneously. In the first case the reference value of only one variable would need to be stored in memory, and in addition subjects could focus their entire attentional resources on the task-relevant variable alone, while in the second case the reference values of the three variables would need to be stored in memory, and in addition subjects must distribute their attentional resources among three variables. If we consider only the memory aspect, there is reason to

Department of Psychology

FAX: (416) 736-5814

UNIVERSITÉ
YORK
UNIVERSITY

FACULTY OF ARTS

4700 KEELE STREET • NORTH YORK • ONTARIO • CANADA • M3J 1P3

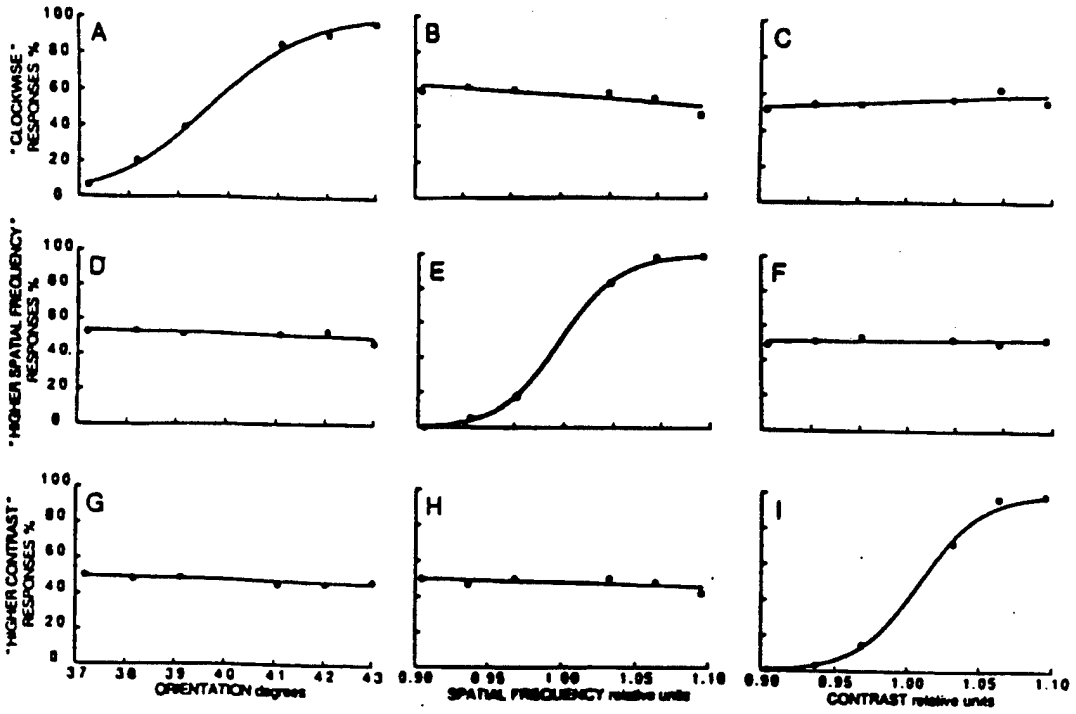

Figure 34 *Simultaneous encoding of spatial frequency, orientation and contrast.* Nine psychometric functions were obtained simultaneously. A, B, C: Orientation discrimination task. The percentage of "test grating orientation clockwise with respect to the mean of the stimulus set" responses are plotted as ordinate vs test grating orientation (A), spatial frequency (B) and contrast (C). D, E, F: Spatial frequency discrimination task. The percentage of "test grating spatial frequency higher than the mean of the stimulus set" is plotted as ordinate vs test grating orientation (D), spatial frequency (E) and contrast (F). G, H, I: Contrast discrimination task. The percentage of "test grating contrast higher than the mean of the stimulus set" is plotted as ordinate vs test grating orientation (G), spatial frequency (H) and contrast (I). The mean orientation of the stimulus set was 40 deg clockwise of vertical. On the spatial frequency axis, 1.0 corresponds to the mean spatial frequency of 5.0 c/deg. On the contrast axis, 1.0 corresponds to the mean contrast of 0.5.

Department of Psychology

FAX: (416) 736-5814

UNIVERSITÉ
YORK
UNIVERSITY

FACULTY OF ARTS

4700 KEELE STREET • NORTH YORK • ONTARIO • CANADA • M3J 1P3

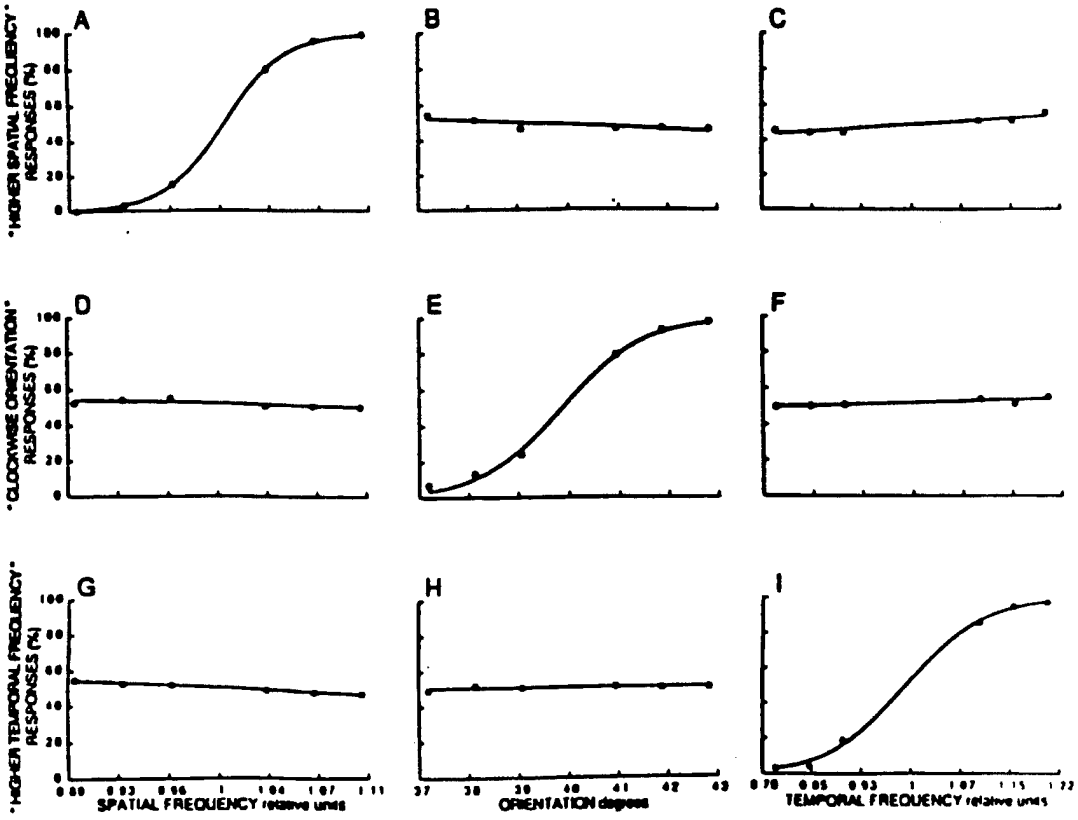

Figure 35 *Simultaneous encoding of spatial frequency, orientation and temporal frequency.* The observer was presented, one by one, with 216 stimulus gratings, each of which had a different combination of spatial frequency, orientation and temporal frequency and instructed to signal how spatial frequency (A-C), orientation (D-F) and temporal frequency (G-I) differed from the mean values for the set of 216 stimuli. Each of the three sets of responses are plotted versus normalized spatial frequency (A, D, G), orientation (B, E, H) and normalized temporal frequency (C, F, I).

Department of Psychology
FAX: (416) 736-5814

UNIVERSITÉ
YORK
UNIVERSITY

FACULTY OF ARTS
4700 KEELE STREET • NORTH YORK • ONTARIO • CANADA • M3J 1P3

expect some interaction of spatial and temporal components of the memory trace (Dutta & Nairne, *Memory & Cognition*, 1993, 21, 440-448).

Nevertheless, however plausible it might seem, this possibility was ruled out empirically. Our finding that thresholds were approximately the same whether trial-to-trial changes occurred in the values of only one or all three variables leads us to conclude that the possible limitations of memory and attentional resources just described are not evident, and also that interactions between the processing of temporal frequency, spatial frequency and orientation are, at most, very small even when the three visual dimensions are processed simultaneously—at least near discrimination threshold.

On the grounds that the three visual dimensions varied simultaneously and subjects made their responses after the test presentation, we suggest that the temporal frequency, spatial frequency and orientation of any given grating are encoded in parallel as are contrast, spatial frequency and orientation.

One implication of our conclusion that both sets of variables are encoded independently in parallel and with negligible cross talk can be understood as follows. Cells in primary visual cortex are in general not selectively sensitive to one visual dimension only. Rather, they respond to temporal frequency, contrast, spatial frequency and orientation — though the balance of sensitivities varies from cell to cell. As discussed previously (Refs.

Department of Psychology
FAX: (416) 736-5814

UNIVERSITÉ
YORK
UNIVERSITY

FACULTY OF ARTS
4700 KEELE STREET • NORTH YORK • ONTARIO • CANADA • M3J 1P3

147, 155), our proposed physiological explanation for these psychophysical findings is that information about these four dimensions, though confounded at single-cell level in striate cortex, is unconfounded by different connectivities within the cell population.

3.15 Psychophysical evidence for a neural mechanism that encodes angles

Results have been reported to ARVO (1995) and a report has been published "Evidence for a neural mechanism that encodes angles" by D. Regan, R. Gray & S. Hamstra Vision Research (1996) 36, 323-330.

It is well known that the orientation of a line is a variable so important that it merits the anatomical substrate of orientation columns, a substrate so gross that it can be rendered visible to naked-eye examination of the visual cortex. Here we report a search for evidence that there is a neural mechanism for angle that is distinct from the mechanism for orientation.

We measured the discrimination threshold $(\Delta\theta)_{Th}$ for angle θ, where θ was either the angle of a Vee composed of two straight lines contained within the frontoparallel plane or the angle of intersection of two straight lines contained within the frontoparallel plane. The two-line pattern was rotated bodily through a random angle between trials with the aim of eliminating the absolute orientation of one or the other line as a reliable cue to the task. We demonstrated that this aim was achieved by showing that orientation discrimination threshold for a single line was very high in our situation of jitter rotation. Our main conclusion is that the ability to discriminate a

Department of Psychology
FAX: (416) 736-5814

UNIVERSITÉ
YORK
UNIVERSITY

FACULTY OF ARTS
4700 KEELE STREET • NORTH YORK • ONTARIO • CANADA • M3J 1P3

change in angle θ cannot entirely be explained in terms of the ability to discriminate changes in the orientations of the individual lines that comprise the Vee. We propose that the human visual pathway contains a neural mechanism that encodes the difference in the orientations of two simultaneously-presented straight lines. Discrimination threshold for angle ($\Delta\theta_{Th}$) is roughly twice orientation discrimination threshold for an isolated line when mean orientation is near-vertical. When subjects cannot use the orientation of one or other line as a cue to the task, the plot of $(\Delta\theta)_{Th}$ versus θ is approximately flat between θ = 20 deg and θ = 160 deg: although discrimination threshold at a reference angle of 90 deg is significantly lower than at an arbitrary reference angle, the difference is small (<30%).

At first sight our failure to find that a right angle is special seems out of line with one's intuitions. However, our finding can be stated as "when feedback is provided and observers are given time to learn the task, discrimination threshold is only a little lower at 90 deg than at other angles". When we required observers to set angles without feedback and with no preliminary display of the designated angle, performance was much better at 90 deg than at other angles. However, angle-dependent differences were almost abolished when there was a preliminary display of the designated angle or when feedback was provided.

3.16 *"Accuracy of reproducing angles: is a right angle special" by R. Gray & D. Regan* Perception *(1996) 25, 531-542.*

Department of Psychology
FAX: (416) 736-5814

UNIVERSITÉ
YORK
UNIVERSITY

FACULTY OF ARTS
4700 KEELE STREET • NORTH YORK • ONTARIO • CANADA • M3J 1P3

We compared the ability to set the angle of a Vee to a designated value in the following three conditions: (a) verbal designation of Vee angle; (b) initial 30-sec visual demonstration of the designated Vee angle; (c) verbal designation of Vee angle plus feedback after every setting. The designated angles were 90 deg and 45 deg plus three arbitrary angles (65 deg, 125 deg and 145 deg). Each run comprised thirty consecutive settings. To ensure that our observers based their settings entirely on Vee angle we arranged that line orientation did not provide a reliable cue to Vee angle. In condition (a), accuracy of setting Vee angle was significantly worse when the designated angle was other than 90 deg or 45 deg. This was not the case in condition (b), indicating that observers maintained a memory of the initial demonstration throughout a run of 30 settings. Setting error was not significant in condition (c) for any of the five angles. However, even in condition (c), setting-to-setting variability was significantly lower for the 90 deg angle than for the other angles.

3.17 MEG study on colour-defined form

This experiment was completed during the 1993-96 funding period, but most of the work was carried out during the 1990-93 funding period, and reported in the 1991-93 Final Report for grant # AFOSR-91-0080, so the present report will be restricted to noting that a paper has been published entitled "Magnetic and electrical responses to chromatic contrast in human" by D. Regan & P. He Vision Research (1996) 36, 1-18.

Department of Psychology
FAX: (416) 736-5814

UNIVERSITÉ YORK UNIVERSITY
FACULTY OF ARTS
4700 KEELE STREET • NORTH YORK • ONTARIO • CANADA • M3J 1P3

3.18 MEG study on texture-defined form

This experiment was completed during the 1993-96 funding period, but most of the work was carried out during the 1990-93 funding period and reported in the 1990-93 Final Report for grant # AFOSR-91-0080, so the present report will be restricted to noting that a paper has been published entitled "Magnetic and electrical responses of the human brain to texture-defined form and to textons" by D Regan & P He Journal of Neurophysiology (1995) 74, 1167-1178.

3.19 MEG evidence for an audio-visual convergence area in the human brain

A report has been published entitled "An audio-visual convergence area in human brain" by M. P. Regan, D. Regan, & P. He ,Experimental Brain Research, (1995) 106, 485-487.

The purpose of this experiment was to find an area in the human brain where visual and auditory information are integrated.

Rationale

Suppose a subject views a light flickering at frequency F_V Hz while listening to a sound whose amplitude is modulated at frequency F_A Hz. Neural processing within the visual pathway can generate responses at F_V, $2F_V$, $3F_V$, $4F_V$-----Hz, and neural processing within the auditory pathway can generate responses at F_A, $2F_A$, $3F_A$, $4F_A$, ----Hz but combination frequencies cannot be generated until visual and auditory signals converge. Therefore, combination frequencies are a "signature" of an audio-visual convergence

Department of Psychology
FAX: (416) 736-5814

UNIVERSITÉ
YORK
UNIVERSITY

FACULTY OF ARTS
4700 KEELE STREET • NORTH YORK • ONTARIO • CANADA • M3J 1P3

area of the brain. [Combination frequencies are ($nF_1 \pm mF_2$), where n and m are nonzero integers)].

Methods and Results

Subject fixated the centre of a uniform circular patch of light whose luminance was sinusoidally modulated at frequency F_V =10.304 Hz. A 1000 Hz sinewave was multiplied by a sinewave of frequency F_A = 5.054 Hz and the resulting waveform was transduced into an amplitude-modulated (AM) tone and fed into the subject's ear.

Magnetic fields produced by brain cells in response to sensory stimulation were recorded using an array of 7 coils placed close to the subject's head. Because the amplitude of the brain's magnetic field is exceedingly small, the recording coils were immersed in liquid helium to reduce thermally-generated noise in the coils, and both the subject and the recording equipment were placed in a magnetically-shielded room. During a recording session, the subject remained still, while the array of recording coils was moved to different locations on the head (typically, 49 coil locations in all). Our major technical problem was that the power of the audio-visual cross-modulation response was some thousands of times less than the total power of the brain's magnetic field. We countered this problem by analysing the brain's magnetic field into a power spectrum at the theoretical limit of frequency resolution (Gabor, 1946) using the "nondestructive zoom-FFT" technique whose theoretical basis and practical implementation we have

Department of Psychology
FAX: (416) 736-5814

UNIVERSITÉ
YORK
UNIVERSITY

FACULTY OF ARTS
4700 KEELE STREET • NORTH YORK • ONTARIO • CANADA • M3J 1P3

described elsewhere (Refs. 167, 177, 178). In the present case, each recording had a duration of 160 sec and the spectrum had a resolution of 0.0078 Hz over the recording bandwidth of 1 to 50 Hz. This technique cleanly extracts very small signals from noise by capitalising on the finding that the magnetic (and electrical) responses of the brain to repetitive stimulation are sufficiently constant in both amplitude and delay that the bandwidth of a harmonic or cross-modulation sensory response component can be as narrow as 0.002 Hz or less. In our case the noise was distributed across the 6274 lines of the 1-50 Hz spectrum while the audio-visual response was concentrated into a single 0.0078 Hz frequency interval in a relatively noise-free part of the spectrum, so that the signal-to-noise enhancement was several thousand times. Because this technique is very dependent on the stability of the stimulation modulation frequencies, the modulation frequencies of both visual and auditory stimuli were generated by crystal-controlled synthesizers.

Stimulation was as follows. Subjects fixated the centre of a uniform circular area of green light whose luminance was modulated sinusoidally at F_V = 10.304 Hz to a depth of 100%. A 1000 Hz sinewave tone was amplitude-modulated at a frequency F_A = 5.054 Hz, and fed into the subject's left ear while the subject viewed the flickering light. (The choice of stimulus frequencies was not crucial within broad limits, but 0.001 Hz stability was essential). Fig. 43A is a contour map over the skull of the $2F_V$ Hz component of the brain's magnetic field. The contour lines join locations over the skull

Department of Psychology
FAX: (416) 736-5814

UNIVERSITÉ
YORK
UNIVERSITY

FACULTY OF ARTS
4700 KEELE STREET • NORTH YORK • ONTARIO • CANADA • M3J 1P3

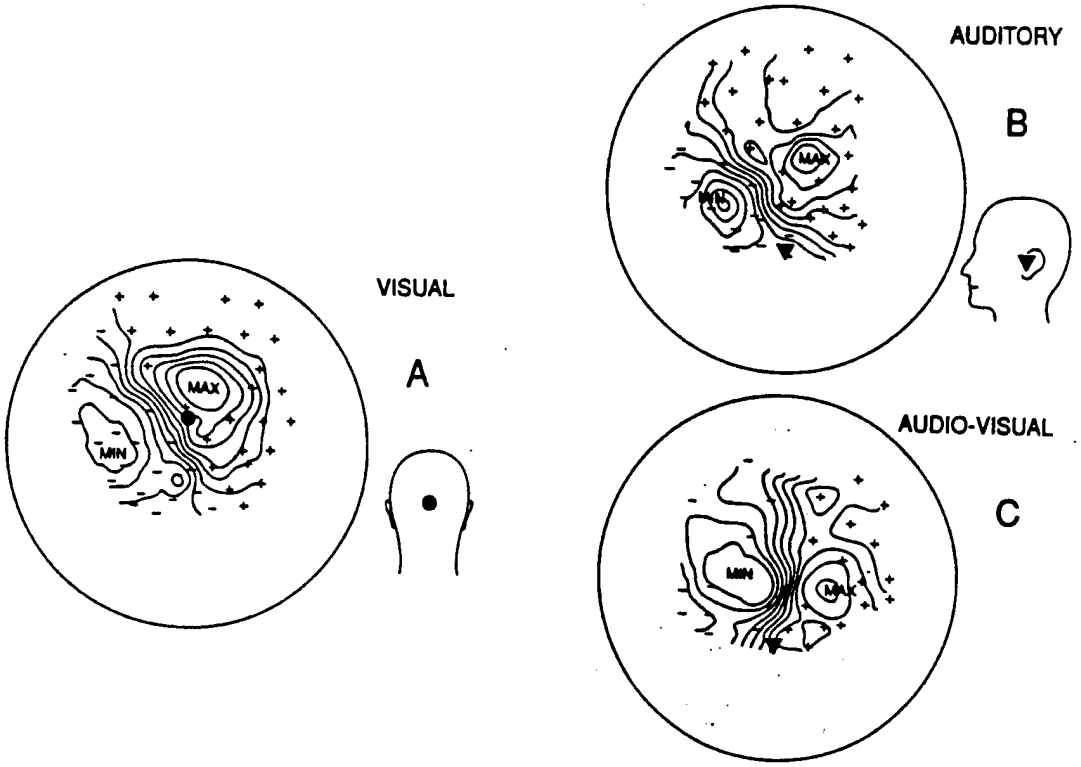

Figure 36 Contour maps of magnetic response amplitude recorded from the human brain during simultaneous visual and auditory stimulation. A: responses generated in visual cortex. B: responses generated in auditory cortex. C: responses generated in an audio-visual convergence area. The circle round the map is a best fit to fit the curvature of the skull over the region of the head from which recordings were made, as illustrated in the heads at the far right. Recording sites are marked + and - according to the phase of the response. The viewpoint was from the left side of the head in A & B and from directly behind the head in C. The dots and arrows in the small stylized heads mark the location and magnetic field direction of the source of the brain response from three different viewpoints. The inion is marked in A. The left periauricular point is marked in A & B.

Department of Psychology
FAX: (416) 736-5814

UNIVERSITÉ
YORK
UNIVERSITY

FACULTY OF ARTS
4700 KEELE STREET • NORTH YORK • ONTARIO • CANADA • M3J 1P3

where response amplitude was constant. As expected from the fact that the recording coils emphasize the contributions of shallow nearby sources, the response to visual stimulation is concentrated near the primary visual cortex of the brain over the occipital region at the back of the head. Fig. 36B maps the amplitude of the $2F_A$ component of the magnetic field. The field distribution is a reasonable fit to that of a single dipole ($r = 0.92$). The location of the dipole is illustrated in the three small stylized heads. As expected, the estimated location of this auditory response source is close to the location of primary auditory cortex in human (Galabarda & Sandies, 1980).

The coordinates of the equivalent dipoles in Fig. 36B & C were as follows (X, Y & Z in cm). B: X = 1.83; Y = 4.73; Z = 6.82; Ψ = -154 deg. C: X = -0.22; Y = 4.31; Z = 6.56; Ψ = 170 deg. The coordinate system has been described previously (Williamson & Kaufman, 1989; Williamson et al., 1991). In brief, a sensor position indicator was used not only to record coil locations but also to encode head dimensions and shape. The multiple recordings were translated into a map of the magnetic field over a spherical surface computed to be a best fit to the skull from which the recordings were made. Source location was computed in terms of Cartesian coordinates defined by the nasion and periauricular points. The origin is the mid-point between left and right periauricular points. The X-axis passes through the origin to emerge from the head at the nasion. The Z-axis is oriented perpendicular to both the X-axis and the line between the periauricular points, and passes through to emerge

Department of Psychology
FAX: (416) 736-5814

UNIVERSITÉ
YORK
UNIVERSITY

FACULTY OF ARTS
4700 KEELE STREET • NORTH YORK • ONTARIO • CANADA • M3J 1P3

near the vertex. The Y-axis is perpendicular to both the X- and Z-axes, and passes through the origin to emerge from the left hemisphere. The orientation of the equivalent dipole's moment is given by angle Ψ measured counterclockwise from the plane containing the Z-axis and the location of the dipole.

Our main finding is shown in Fig. 36C where the contours join scalp locations at which the amplitude of an audio-visual ($2F_A + F_V$) Hz cross-modulation response had constant amplitude. These cross-modulations responses are the first objective evidence for an audio-visual convergence area in human brain cortex. Since the recording coils emphasize nearby sources, we conclude that this convergence area is far from visual cortex and close to the source of the auditory response (compare the viewpoints of the maps in Fig. 36A, B & C). The entire experiment was repeated two months later and gave very similar results. Similar results to those shown in Fig. 36 were obtained from a second subject.

In the absence of previous data on audio-visual convergence areas in human brain we can compare our data only with the known locations of sensory convergence area in the cortex of macaque monkey. The field distribution in Fig. 36C is a close ($r = 0.92$) fit to that of a single dipole whose location is depicted graphically in the three stylized heads in Fig. 36C. Bearing in mind that the magnetic field that we recorded is largely generated within the bodies of cortical neurons aligned parallel to the skull (Hari and

Department of Psychology
FAX: (416) 736-5814

UNIVERSITÉ
YORK
UNIVERSITY

FACULTY OF ARTS
4700 KEELE STREET • NORTH YORK • ONTARIO • CANADA • M3J 1P3

Lounasna, 1989; Williamson et al., 1991), this equivalent dipole location corresponds to a known cortical audio-visual convergence area in macaque monkey (Tigges and Tigges, 1985).

Studies on the auditory processing of complex waveforms

It is widely accepted that a considerable proportion of the information transmitted in speech is transmitted via changes in the frequencies and amplitude of formants (formants are well-defined peaks or concentrations of power in the frequency spectrum). Much of the research on speech processing and comprehension compares psychophysical or cognitive responses with the auditory waveform or spectrum that reaches the ear. We propose that further insights might be possible by comparing psychophysical responses, not with the auditory stimulus that reaches the ear, but rather with the signal that is available to the brain, i.e. the output of the hair cells. The force of this point is that the hair cell transducer function resembles a saturating rectifier and, therefore, distorts and changes the incoming waveform very strongly, and in a way that is far from intuitively obvious.

The problem of calculating the distortions to a speech waveform produced by the hair cell transducer function is not simple. Therefore we have proceeded in a series of steps as described in Section 3.20 - 3.21.

3.20 This study provides a theoretical method for calculating the distortion of a pure tone that occurs when sound is transduced into current by hair cells in the inner ear.

Department of Psychology
FAX: (416) 736-5814

UNIVERSITÉ YORK UNIVERSITY
FACULTY OF ARTS
4700 KEELE STREET • NORTH YORK • ONTARIO • CANADA • M3J 1P3

One report has been published entitled "A method for calculating the spectral response of a hair cell to a pure tone" by M. P. Regan (1994) Biological Cybernetics, 71, 13-16.

Hubbard et al. (1979) recorded the CM potential in guinea-pigs while presenting a pure tone stimulus to the ear. The tone frequency ranged from 120 to 160 Hz, and the time-averaged CM waveforms were Fourier analysed to obtain the amplitudes and phases of the fundamental and the first five harmonics. The sound-pressure level (SPL) was progressively increased up to levels of 122 db. Figure 37 shows the plots of the magnitude and phase of the six harmonics versus the SPL of the stimulus for turn II of the cochlea.

First we will calculate the amplitude and the phase of the first six harmonics in the output of this function for a sinusoidal input.

Consider the input function $e(t)$ where

$$e(t) = k \cos(2\pi f t + \theta_f) \quad \text{---------- (20)}$$

where k is the maximum amplitude of the input function, and f is the frequency with phase θ_f, and $e(t)$ is the input voltage.

This can be expressed more simply as

$$f(x) = k \cos x \quad \text{---------- (21)}$$

taking $x = 2\pi f t + \theta_f$. If $f(x)$ is the input to a hair cell whose characteristic , $H(r)$, is shown in Fig. 38, then the output is given by

$$F(x) = H[f(x)] \quad \text{---------- (22)}$$

Department of Psychology

FAX: (416) 736-5814

UNIVERSITÉ
YORK
UNIVERSITY

FACULTY OF ARTS

4700 KEELE STREET • NORTH YORK • ONTARIO • CANADA • M3J 1P3

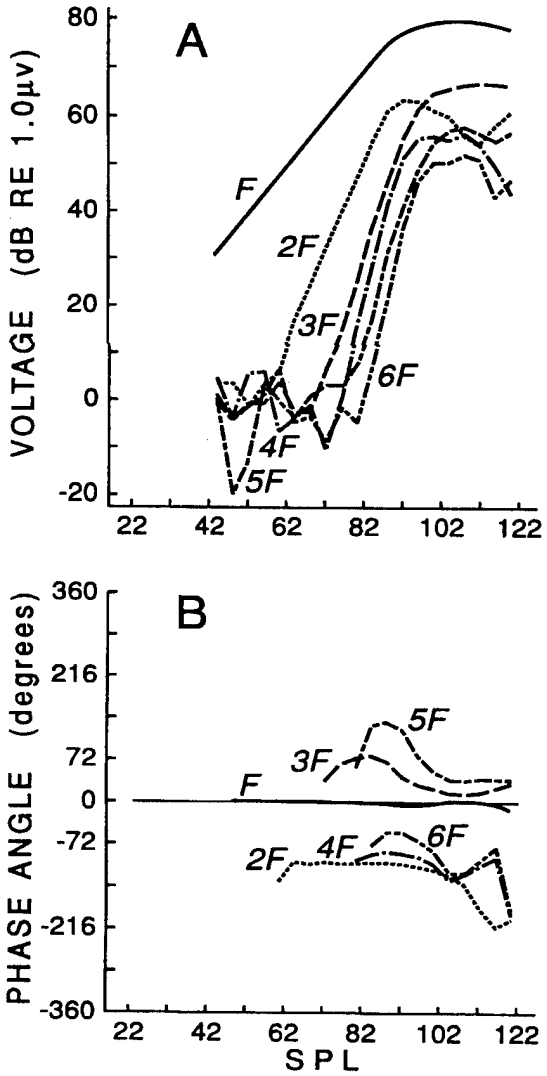

Figure 37 A: Magnitudes of turn II cochlear microphonic (CM) harmonics as a function of the sound-pressure level (SPL) in the guinea-pig. B: Phases of turn II CM harmonics versus SPL corresponding to magnitudes in A. Note the grouping of the phase curves for even and odd harmonics. Redrawn from Hubbard et al. (1979).

Department of Psychology
FAX: (416) 736-5814

UNIVERSITÉ
YORK
UNIVERSITY

FACULTY OF ARTS
4700 KEELE STREET • NORTH YORK • ONTARIO • CANADA • M3J 1P3

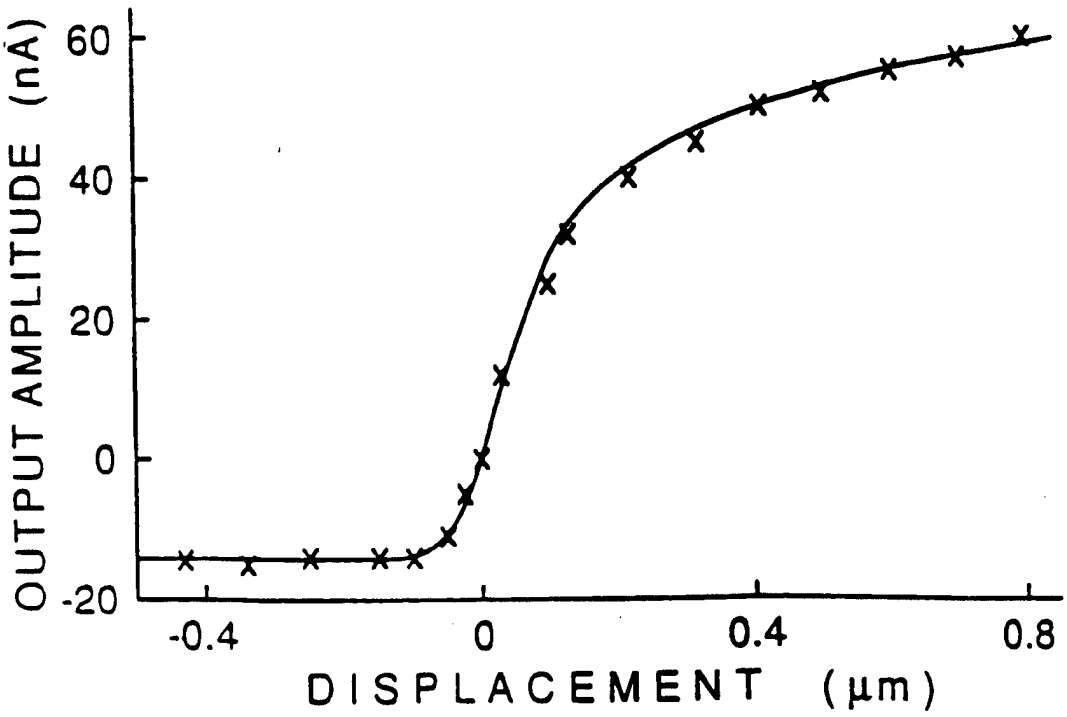

Figure 38 Experimentally measured response characteristics of hair cells: transduction from sound to neural signals. Hair cell displacement in microns is plotted on the abscissa, and the output amplitude in nanoamperes (nA) is plotted as the ordinate. The solid line plots the curve used in the text. (From Corey and Hudspeth 1983).

Department of Psychology
FAX: (416) 736-5814

UNIVERSITÉ
YORK
UNIVERSITY

FACULTY OF ARTS
4700 KEELE STREET • NORTH YORK • ONTARIO • CANADA • M3J 1P3

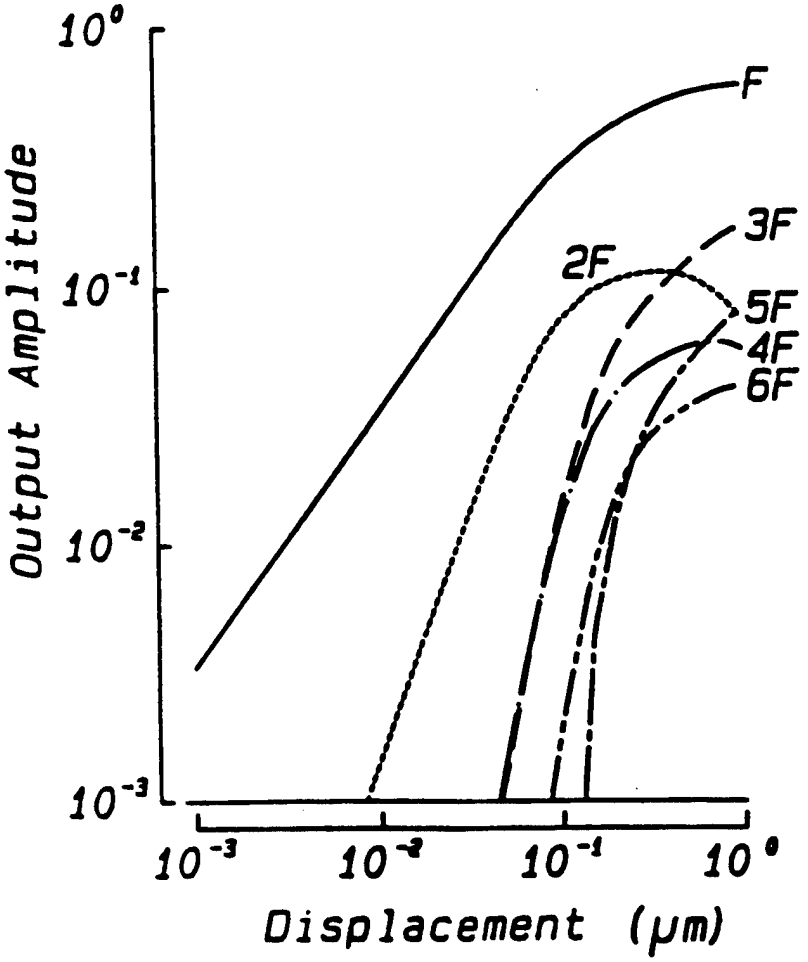

Figure 39 Calculated amplitude in arbitrary units of the output of the Fig. 38 transducer function is plotted as ordinate on a logarithmic scale where the input was k cos(2πFt). Values of k from 0.001 to 1 μm are plotted along the abscissa on a logarithmic scale

Department of Psychology
FAX: (416) 736-5814

UNIVERSITÉ
YORK
UNIVERSITY

FACULTY OF ARTS
4700 KEELE STREET • NORTH YORK • ONTARIO • CANADA • M3J 1P3

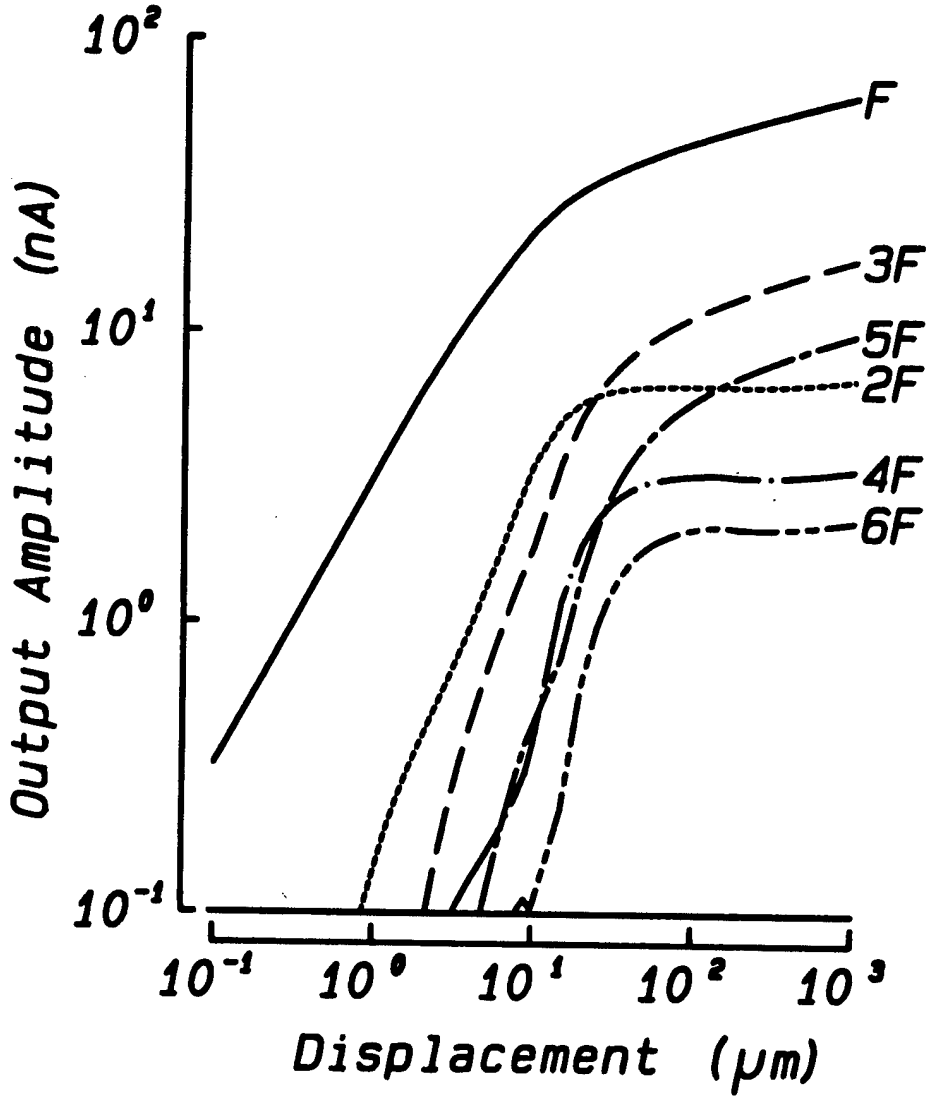

Figure 40 Calculated amplitude in arbitrary units of the output of the Assad & Corey transducer function is plotted along the ordinate on a logarithmic scale where the input was $k\cos(2\pi Ft)$. Values of k from 0.001 to 1 μm are plotted along the abscissa on a logarithmic scale.

Department of Psychology

FAX: (416) 736-5814

UNIVERSITÉ
YORK
UNIVERSITY

FACULTY OF ARTS

4700 KEELE STREET • NORTH YORK • ONTARIO • CANADA • M3J 1P3

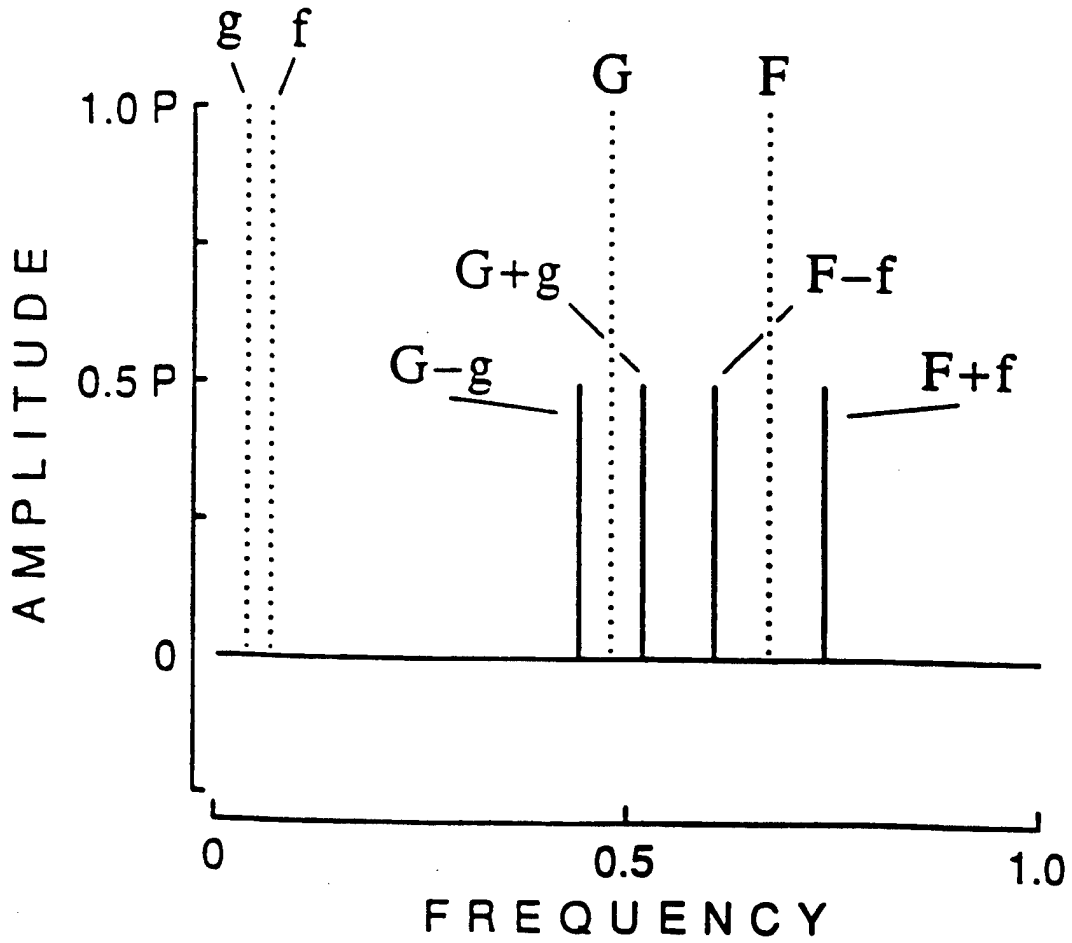

Figure 41 The spectrum of the auditory stimulus waveform f (x, y, z, w) = P(cos x cos y + cos z cos w) where $x = 2\pi ft + \theta_f$, $y = 2\pi Ft + \theta_F$, $z = 2\pi gt + \theta_g$, and $w = 2\pi Gt + \theta_G$. Amplitude in units of P is plotted as the ordinate on a linear axis. Frequency is plotted as the abscissa on a linear axis in arbitrary units. The only frequency components in the spectrum are those shown at (F ± g), (F ± f), (G ± g), and (G ± f). The dotted lines emphasize that frequencies f, g, F, and G have zero amplitude in the spectrum.

Department of Psychology
FAX: (416) 736-5814

UNIVERSITÉ
YORK
UNIVERSITY

FACULTY OF ARTS
4700 KEELE STREET • NORTH YORK • ONTARIO • CANADA • M3J 1P3

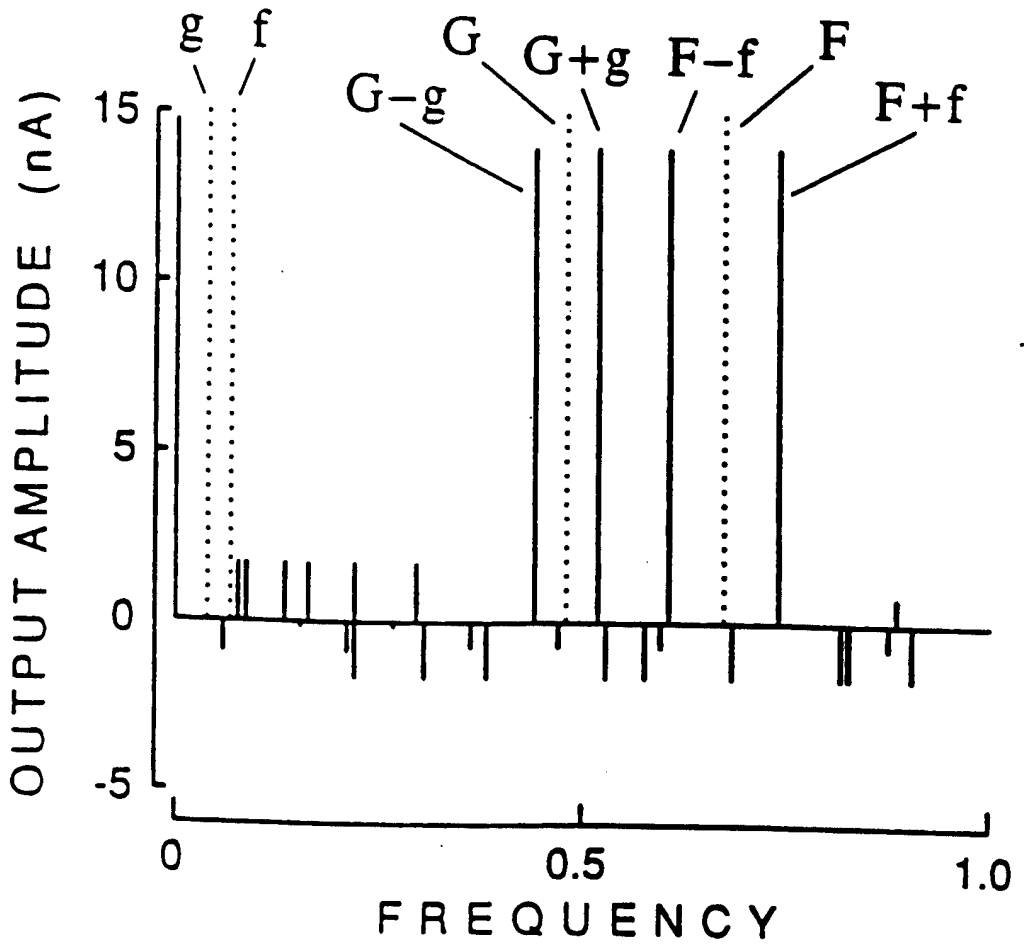

Figure 42 Calculated amplitude of the output of the Fig. 38 transducer function (in nanoamperes) is plotted as the ordinate on a linear axis. The input was the Fig. 48 input waveform with P equal to 0.2 μm hair cell displacement. Output frequency is plotted as the abscissa on a linear axis in arbitrary units. Only some of the combination frequencies are shown. The dotted lines emphasize that there is zero amplitude at frequencies *f*, g, F, and G.

Department of Psychology

FAX: (416) 736-5814

UNIVERSITÉ
YORK
UNIVERSITY

FACULTY OF ARTS

4700 KEELE STREET • NORTH YORK • ONTARIO • CANADA • M3J 1P3

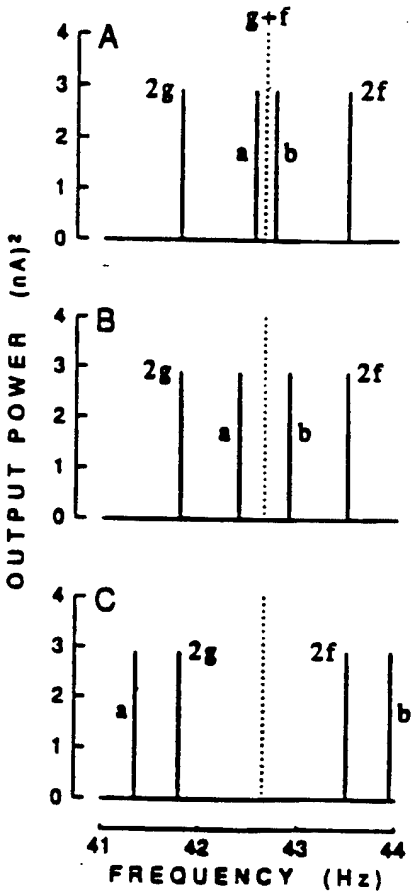

Figure 43 A-C: A section of the Fig. 42 response spectrum (two-carrier case) for different values of the two carrier frequencies F and G. The [(f + g) - (F - G)] component is marked as a and the [(f + g) + (F - G)] component as b (compare with Fig. 44E-G). Theoretical predictions of output power (in nanoamperes squared) for the Fig. 38 transducer function are plotted as the ordinate on a linear axis. Frequency (in hertz) is plotted as the abscissa on a linear axis. The frequency component (f + g), indicated by the dotted line, has zero amplitude.

A: (F - G) = 0.1 Hz. B: (F - G) = 0.25 Hz. C: (F - G) = 1.3 Hz. Compare with the experimental data of Fig. 44E-G.

Department of Psychology

FAX: (416) 736-5814

UNIVERSITÉ
YORK
UNIVERSITY

FACULTY OF ARTS

4700 KEELE STREET • NORTH YORK • ONTARIO • CANADA • M3J 1P3

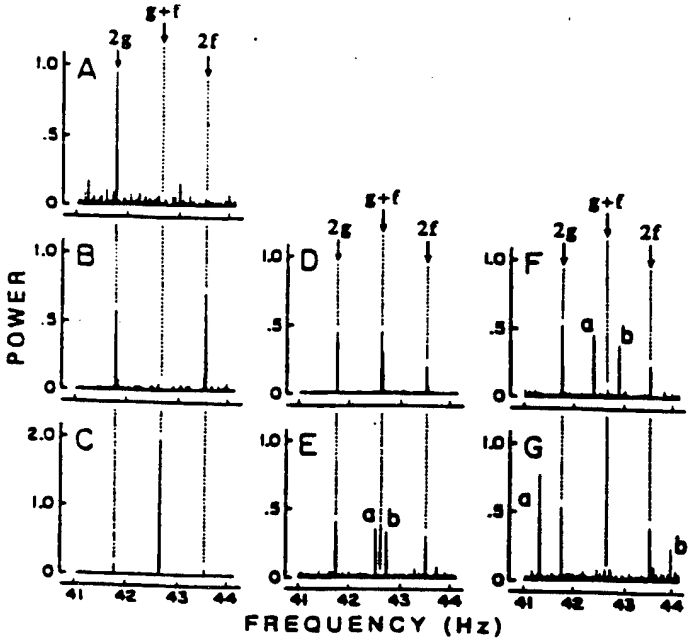

Figure 44 A-G: Experimentally measured response spectra of field potentials recorded in humans. Three auditory stimulus waveforms were used: S1, an F Hz audio carrier amplitude-modulated at *f* Hz; S2, an F Hz audio carrier amplitude-modulated at g Hz; S3, a G Hz audio carrier amplitude-modulated at g Hz. A: S1 to left ear. B: S1 to left ear and S2 to right. C: S1 plus S2 to left ear; a is the [(*f* + g) + (F - G)] component and b is the [(*f* + g) + (F - G)] component. D-G: S1 plus S3 to the left ear. D: (F - G) = 0.01 Hz. E: (F - G) = 0.10 Hz. F: (F - G) = 0.25 Hz. G: (F - G) = 1.3 Hz. Ordinates indicate power; 1.0 on the ordinate corresponds to an amplitude of 1.0 mV. The EEG was amplified over a 1-100 Hz bandwidth and analyzed using zoom-FFT by a Bruel & Kjaer model 2032 spectral analyzer at 0.0078 Hz frequency resolution. Auditory stimuli of 50 db sensation level were generated by earphones coupled to the ears via 1-m plastic tubes. Carrier waves were generated by analog electronics that added the difference in frequency (F - G) Hz to the F Hz sinusoid.

Department of Psychology

FAX: (416) 736-5814

UNIVERSITÉ YORK UNIVERSITY

FACULTY OF ARTS

4700 KEELE STREET • NORTH YORK • ONTARIO • CANADA • M3J 1P3

This output is a periodic function of x. The period is 2π, and F(x) is bounded and continuous in the region ($-\pi \leq x \leq \pi$) so that F(x) can be expressed as a Fourier series. Since F(x) is an even function, its Fourier expansion will be cosine series given by

$$F(x) = \frac{1}{2}A_0 + \sum_{m=1}^{\infty} A_m \cos mx \qquad (23)$$

where

$$A_m = \frac{1}{\pi}\int_{-\pi}^{\pi} F(x)\cos mx\, dx, m = 0, 1, 2, \ldots.$$

Since the region is symmetrical for x, it follows that the amplitude of the mth harmonic is

$$A_m = \frac{2}{\pi}\int_{0}^{\pi} F(x)\cos mx\, dx, \qquad (24)$$

and the phase Θ_m of each harmonic is $[m\theta_f]$, where $\theta_f = \frac{\pi}{2}$.

Using (23) and (24) we can calculate the amplitude of the fundamental frequency (A_1) and the next five harmonics, A_2, A_3, A_4, A_5 and A_6. When the input amplitude, k, of the sinusoid is progressively increased, we obtain a family of curves (shown in Fig. 39) by plotting output amplitude versus input amplitude for the different harmonic frequencies. For input amplitudes expressed as SPL, k = 1 is equivalent to a SPL of 120 db in the bullfrog hair cell. Then the calculations described above for the Assad and Corey transducer

Department of Psychology
FAX: (416) 736-5814

UNIVERSITÉ
YORK
UNIVERSITY

FACULTY OF ARTS
4700 KEELE STREET • NORTH YORK • ONTARIO • CANADA • M3J 1P3

function were carried out. Their transducer function fits the theoretical equation.

$$P_0 = 1/(1 + \exp[g_2 - z_2x)/kT] \times \{1 + \exp[g_1 - z_1x)/kT] \quad \text{-------} \quad (25)$$

with $g_1 = 6.1E - 21$, $z_1 = 1.09E - 22$, $g_2 = 7E - 22$, $z_2 = 2.7E - 14$.

Figure 40 plots the predicted amplitudes of the fundamental and next five harmonics. For both transducer functions we obtain a phase of -90 deg for odd harmonics and -180 deg for even harmonics at moderate to high values of SPL. At very low values of SPL the phase changes only for the fifth harmonic component at these low values.

Conclusions

The harmonic distortion reported by Hubbard et al. (1979) in the CM response to a pure tone can be described in terms of a hair cell transducer function modelled as an asymmetric rectifier with no memory and based on the data of Corey and Hudspeth (1983) or (a little more closely) on the data of Assad and Corey (1992).

3.21 This experimental and theoretical study addresses the distortion produced by passing multiple amplitude-modulated sinusoidal tones through the hair cell transducer function.

Two reports have been published M.P. Regan & D. Regan "Nonlinear terms produced by passing amplitude-modulated sinusoids through Corey & Hudspeth's hair cell transducer function". Biological Cybernetics, (1994) 69,

Department of Psychology
FAX: (416) 736-5814

UNIVERSITÉ
YORK
UNIVERSITY

FACULTY OF ARTS
4700 KEELE STREET • NORTH YORK • ONTARIO • CANADA • M3J 1P3

439-446 and M.P. Regan "Linear half-wave rectification of modulated sinusoids". Applied Mathematics and Computation, (1994) 62, 61-79.

Background

Sound energy is transduced into electrical current by hair cells whose transducer function is illustrated in Fig. 38. Frequencies not present in the sound input are created when a pure tone or amplitude-modulated (AM) tone are passed through this a nonlinear function.

Methods

The sum of two AM tones can be written as

$$e(t) = P[\cos(2\pi ft + \theta_f)\cos(2\pi Ft + \theta_F) + (\cos(2\pi gt + \theta_g)\cos(2\pi Gt + \theta_G)] \text{ ------ } (26)$$

Using (26) expressed in the simpler form as

$$f(x, y, z, w) = P(\cos x \cos y + \cos z \cos w) \text{ ---------- } (27)$$

where $x = 2\pi ft + \theta_f$, $y = 2\pi Ft + \theta_F$, $z = 2\pi gt + \theta_g$, and $w = 2\pi Gt + \theta_G$). Figure 41 shows the spectrum of the time series given by (27). The vertical dotted lines bring out the point that the input frequencies f, g, F, and G have zero amplitude in the spectrum.

If f (x, y, z, w) is the input to a hair cell whose characteristic, H(X), is shown in Fig. 38, then the output F (x, y, z, w) is given by

$$F(x, y, z, w) = H[F(x, y, z, w)] \text{ ---------- } (28)$$

and the amplitudes $A_{\pm mnpq}$ of the output frequencies ($mf \pm ng \pm \pi F \pm \theta G$) can be found from

Department of Psychology
FAX: (416) 736-5814

UNIVERSITÉ
YORK
UNIVERSITY

FACULTY OF ARTS
4700 KEELE STREET • NORTH YORK • ONTARIO • CANADA • M3J 1P3

$$A_{\pm mnpq} = \frac{2}{\pi^4} \int_0^{\pi} \cos qw\, dw \int_0^{\pi} \cos pz\, dz \int_0^{\pi} \cos ny\, dy \int_0^{\pi} F(x,y,z,w) \cos mx\, dx. \quad (29)$$

Thus, the spectrum of the output is as shown in Figure 42, and it contains many more frequency components than the Figure 41 input spectrum, but the four input frequencies, f, g, F and G still have zero amplitude in the output.

Fig. 43A-C shows a section of the theoretically-calculated response spectrum. Note that the frequency terms marked a, b and 2g & 2f do not exist in input sound waveform (Fig. 41).

Next, we compare this theoretical work with experiment. We stimulated one ear with two separate waveforms. The first waveform used was that of two summed sinusoids modulating a single carrier sinusoid given by the input function e(t) in (16), where f =20.886 Hz and g=21.778 Hz were the two modulating frequencies with phase θ_f and θ_g, and F=1048.5 Hz was the carrier frequency with phase θ_F. Using this waveform as the input to the left ear, we measured the auditory evoked potential to this steady-state stimulus. The modulating frequencies had been chosen to give the maximum response in the AEP and we subjected the EEG to spectral analysis by ultra-high resolution zoom-FFT. The technique achieves the Heisenberg-Gabor theoretical limit of frequency resolution in the spectrum ($\Delta F = 1/T$ Hz), where T is the recording duration. For the recording duration of 320 sec this

Department of Psychology
FAX: (416) 736-5814

UNIVERSITÉ
YORK
UNIVERSITY

FACULTY OF ARTS
4700 KEELE STREET • NORTH YORK • ONTARIO • CANADA • M3J 1P3

technique can be regarded as providing, in effect, 25,000 filters in parallel each of bandwidth 0.0078 Hz within the 1-200 Hz bandwidth of the EEG amplifier.

Figure 44C shows that the recorded response contained power at 42.664 Hz [i.e. at $(f + g)$] with a high signal-to-noise ratio, but comparatively little power at the second harmonics of the two modulating frequencies (indicated by the vertical dotted lines). When we used two different carrier frequencies, the $(f + g)$ term split into two (Fig. 44E-F). Note the similarity between Figure 44E-F and the corresponding theoretical Figure 43A-C. The agreement between theory and experiment described above might seem surprising, because we were attempting to describe responses recorded at the scalp in terms of distortions arising at the level of the hair cells. We conclude that in our experimental situation peripheral processing largely determined a property of a central response.

3.22 Distortion produced by the hair cell transducer function on a frequency-modulated tone

The first part of this study has been completed and published. M. P. Regan (1966). Applied Mathematics & Computation, 62, 61-79.

As a first step to obtaining a general expression for the distortion produced on a frequency-modulated (FM) tone by the hair cell transducer function we have calculated the output of a linear and noise-free rectifier in the cases the input is : (a) an FM tone; (b) a quasi-FM tone; (c)an amplitude-modulated (AM) tone.

Department of Psychology

FAX: (416) 736-5814

UNIVERSITÉ YORK UNIVERSITY

FACULTY OF ARTS

4700 KEELE STREET • NORTH YORK • ONTARIO • CANADA • M3J 1P3

Here, we should note that an FM tone is, in general, represented in the frequency domain by a carrier frequency with multiple sidebands, while a quasi-FM tone is represented by a carrier with only two sidebands. A quasi-FM tone approximates an FM tone of very low modulation index (The modulation index is F_M / F_C where F_M is the modulation frequency and F_C is the carrier frequency). An AM tone has exactly the same power spectrum as quasi-FM (i.e. a carrier with two sidebands), but the phase spectrum is different for AM and quasi-FM.

Just as in the case of AM, the rectifier characteristic produces frequency components that are not present in FM or quasi-FM. The main finding, however, is that although the power spectra of quasi-FM and AM are identical, after passing though the rectifier they are different: rectification converts a difference in phase spectra into a difference in power spectra.

The possible significance of this finding is that differences in psychophysical responses to quasi-FM and AM that have been attributed to auditory sensitivity to a difference in phase spectra might be in fact due to a difference in power spectra produced by nonlinear transduction.

We are currently extending these calculations to model hair cell transducer functions with added noise.

4 REFERENCES

Department of Psychology

FAX: (416) 736-5814

UNIVERSITÉ YORK UNIVERSITY

FACULTY OF ARTS

4700 KEELE STREET • NORTH YORK • ONTARIO • CANADA • M3J 1P3

Andrews DP (1967a) Perception of contour orientation in the central fovea. Part I: Short lines. *Vision Research*, 7, 1975-1977.

Andrews DP (1967b). Perception of contour orientation in the central fovea. Part II: Spatial integration. *Vision Research*, 7, 999-1013.

Assad JA & Corey DP (1992) An active motor model for adaptation by vertebrate hair cells. *Neuroscience* 12, 3291-3309.

Bergen JR, Adelson E (1988) Early vision and texture perception. Nature (Lond), 333: 363-364

Burr D, Morrone C, Maffei L (1981) Intra-cortical inhibition prevents simple cells from responding to textured visual patterns. Exp Brain Res 43: 455-458

Caelli T, Brettel H, Rentschler I and Hilz R (1983) Discrimination thresholds in the two-dimensional spatial frequency domain. *Vision Research*, 23, 129-133.

Corey DP & Hudspeth AJ (1983) Kinetics of the receptor current in bullfrog sccular hair cells. *Neuroscience* , 3, 962-967.

Daugman JG (1980) Two dimensional spectral analysis of cortical receptive field profiles. Vis Res 25: 671-684

Gabor D, Theory of communication. *J. IEEE.*, 93, (1946) 429-456.

Galaburda, A. and Sandies, F., Cytoarchitectonic organization of the human auditory cortex. *J.Comp. Neurol.*, 190 (1980) 597-610.

Gilbert CD, Hirsch JA, Weisel TN (1990) Lateral interactions in visual cortex. In Cold Spring Harbor Sym Quan Biol 55: 663-667

Green, D. M. & Swets, J. A. (1960) *Signal detection Theory and Psychophysics*.. New York, Wiley.

Hari R, Lounasna A. (1989) Recording and interpretation of cerebral magnetic fields. Science 244: 432-436.

Hoyle, F. (1957). *The Black Cloud*. (pp. 26-27). London: Penguin Books.

Hubbard AE, Geisler CD & Mountain DC (1979) The spectral content of the cochlear microphonic measured in scala media of the guinea pig cochlea. *J. Acoust. Soc Am* 66, 415-430.

Julesz B (1971) *Foundations of Cyclopean Perception*.. University of Chicago Press, Chicago.

Marceltja S (1980). Mathematical descriptions of the responses of simple cortical cells. J Opt Soc Amer 70: 1297-1300

McKee SP (1981) A local mechanism for differential velocity discriminations. *Vision Res.* 21, 491-500.

Department of Psychology

FAX: (416) 736-5814

UNIVERSITÉ YORK UNIVERSITY

FACULTY OF ARTS

4700 KEELE STREET • NORTH YORK • ONTARIO • CANADA • M3J 1P3

Morgan MJ (1986) Positional acuity without monocular cues. *Perception*, 15, 157-162.

Morgan MJ (1991) Hyperacuity. In Regan, D. (Ed) *Spatial Vision*, London: Macmillan pp. 87-113.

Morrone MC, Burr D, Maffei L (1982) Functional implications of cross-orientation inhibition of cortical visual cells: I. Neurophysiological evidence. Proc Royal Soc, B 216: 335-354

Morrone MC, Burr D (1986) Evidence for the existence and development of visual inhibition in humans. Nature 321: 235-237

Nelson JI, Frost B (1978) Orientation selective inhibition from beyond the classic visual receptive field. Brain Res 139: 359-365

Nothdurft HC, (1991) Texture segmentation and pop-out from orientation contrast. Vis Res 31:1073-1078

Nothdurft HC (1992) Feature analysis and the role of similarity in preattentive vision. Percep and Psychophys 52: 355-375

Parker A, Hawken MJ (1988) Two-dimensional spatial structure of receptive fields in monkey striate cortex. J Opt Soc Amer A5: 598-605

Regan D, Regan MP (1987) Nonlinearity in human visual responses to two-dimensional patterns and a limitation of Fourier methods. Vis Res 27: 2181-2183

Regan D (1989) *Human brain electrophysiology: Evoked potentials and evoked magnetic fields in science and medicine.* New York: Elsevier, pp.95-96 and p.107.

Rodieck RW, Stone J (1965) Analysis of receptive fields of cat retinal ganglion cells. J Neurophysiol 28: 833-849

Rubenstein BS & Sagi D. (1990) Spatial variability as a limiting factor in texture-discrimination tasks: implications for performance asymetrics. *J. Opt. Soc. Amer.* A7, 1632-1643.

Thomas JP and Gille J (1979) Bandwidths of orientation channels in human vision. *Journal of the Optical Society of America*, 69, 652-660.

Tigges J, Tigges M. (1985) Subcortical sources of direct projections to visual cortex. In Peters A, Jones EG (eds) Cerebral Cortex Vol. 3. M. I. T. Press, Cambridge, Mass., pp. 351-378

Toyama K, Kimura M, Tanaka K (1981) Organization of cat visual cortex as investigated by cross-correlation techniques. J Neurophysiol 46: 202-214

Tyler CW (1974) Depth perception in disparity gratings. *Nature*, 251, 140-142.

Department of Psychology

FAX: (416) 736-5814

UNIVERSITÉ
YORK
UNIVERSITY

FACULTY OF ARTS

4700 KEELE STREET • NORTH YORK • ONTARIO • CANADA • M3J 1P3

VanEssen DC, Felleman DJ, DeYoe EA, Olavarria J & Knierem J (1990) Modular and hierarchical organization of extrastriate visual cortex in the macaque monkey. In *The Brain* Cold Spring Harbour Press, 679-696.

Webster. (1990).

Williamson SJ, Lu L, Karron Z, Kaufman L. (1991) Advantages and limitations of magnetic source imaging. Brain Topog 4: 169-180.

Zeki S (1990) Parallelism and functional specialization in human visual cortex. In *The Brain* Cold Spring Harbour Press, 651-661.

4 CUMULATIVE LIST OF PUBLICATIONS STEMMING FROM RESEARCH EFFORT

Science Citation Index 887 (1975-79), 1107 (1980-84), 1097 (1985-89), 1112 (1990-1994),329(1995).

Books

1.Regan D (1972) *Evoked potentials in psychology, sensory physiology and clinical medicine.* London: Chapman & Hall; New York: Wiley, 328 pp, rpt 1975.

2.Regan D (1989) *Human brain electrophysiology: Evoked potentials and evoked magnetic fields in science and medicine.* New York: Elsevier, 672 pp.

3.Regan D, Shapley RM & Spekreijse H (Eds) (1985) *Systems approach in vision.* New York: Pergamon, 219 pp.

4.Regan D (Ed) (1991) *Binocular Vision* (Vol 9, "Vision and visual dysfunction" series). London: Macmillan.

5.Regan D (Ed) (1991) *Spatial Vision* (Vol 10, "Vision and visual dysfunction" series). London: Macmillan.

Papers

1966

1. Regan D (1966) Some characteristics of average steady-state and transient responses evoked by modulated light. *Electroenceph clin Neurophysiol* 20, 238-48.
2. Regan D (1966) An apparatus for the correlation of evoked potentials and repetitive stimuli. *Med Biol Engng* 4, 168-77.
3. Regan D (1966) An effect of stimulus colour on average steady-state potentials evoked in man. *Nature* 210, 1056-7.

1968

4. Regan D (1968) A high frequency mechanism which underlies visual evoked potentials. *Electroenceph clin Neurophysiol* 25, 231-7.
5. Regan D (1968) Chromatic adaptation and steady-state evoked potentials. *Vision Res* 8, 149-58.
6. Regan D (1968) Evoked potentials and sensation. *Percept Psychophys* 4, 347-50.

1969

7. Regan D (1969) Evoked potentials and colour vision. *7th ISCERG Symp*, Istanbul. Univ of Istanbul, 37-50.

Department of Psychology

FAX: (416) 736-5814

UNIVERSITÉ YORK UNIVERSITY

FACULTY OF ARTS

4700 KEELE STREET • NORTH YORK • ONTARIO • CANADA • M3J 1P3

8. Regan D (1969) Chapters 3 & 4 in DM MacKay (Ed), Evoked potentials and Psychophysics. *Neurosci Res Bull* 7, N° 3.
9. Regan D & Heron JR (1969) Clinical investigation of lesions of the visual pathway: a new objective technique. *J Neurol Neurosurg Psychiat* 32, 479-83.
10. Tweel LH van der, Regan D & Spekreijse H (1969) Some aspects of potentials evoked by changes in spatial brightness contrast. *7th ISCERG Symp*, Istanbul. Univ of Istanbul, 1-11.

1970

11. Regan D (1970) Evoked potential and psychophysical correlates of changes in stimulus colour and intensity. *Vision Res* 10, 163-78.
12. Regan D (1970) Objective method of measuring the relative spectral luminosity curve in man. *J Opt Soc Am* 60, 856-9.
13. Regan D & Heron JE (1970) Simultaneous recording of visual evoked potentials from the left and right hemispheres in migraine. In AL Cochrane (Ed), *Background to migraine*. London: Heinemann, 66-77.
14. Regan D & Cartwright RF (1970) A method of measuring the potentials evoked by simultaneous stimulation of different retinal regions. *Electroenceph clin Neurophysiol* 28, 314-9.
15. Regan D & Spekreijse H (1970) Electrophysiological correlate of binocular depth perception in man. *Nature* 255, 92-4.

1971

16. Regan D & Sperling HG (1971) A method of evoking contour-specific scalp potentials by chromatic checkerboard patterns. *Vision Res* 11, 173-6.
17. Regan D & Tyler CW (1971) Wavelength-modulated light generator. *Vision Res* 11, 43-56.
18. Regan D & Tyler CW (1971) Some dynamic features of colour vision. *Vision Res* 11, 1307-24.
19. Regan D & Tyler CW (1971) Temporal summation and its limit for wavelength changes: an analog of Bloch's law for color vision. *J Opt Soc Am* 61, 1414-21.
20. Regan D & Richards W (1971) Independence of evoked potentials and apparent size. *Vision Res* 11, 679-84.

1972

21. Regan D (1972) Evoked potentials to changes in the chromatic contrast and luminance contrast of checkerboard stimulus patterns. In GB Arden (Ed), *The visual system*. New York: Plenum, 171-87.
22. Regan D (1972) Evoked potentials to changes in chromatic contrast. Proc GAIN symp on EPs to spatial contrast. *Trace* 6, 20-8.
23. Regan D (1972) Cortical evoked potentials. *Adv Behav Biol* 5, 177-92.
24. Spekreijse H, van der Tweel LH & Regan D (1972) Interocular sustained suppression: correlations with evoked potential amplitude and distribution. *Vision Res* 12, 521-6.
25. Milner BA, Regan D & Heron JR (1972) Theoretical models of the generation of steady-state evoked potentials, their relation to neuroanatomy and their relevance to certain clinical problems. *Adv Med Biol* 24, 157-69.

1973

Department of Psychology

FAX: (416) 736-5814

UNIVERSITÉ YORK UNIVERSITY

FACULTY OF ARTS

4700 KEELE STREET • NORTH YORK • ONTARIO • CANADA • M3J 1P3

26. Regan D (1973) Parallel and sequential processing of visual information in man: investigation by evoked potential recording. In *Photophysiology*, Vol 8. New York: Academic, 185-208.
27. Regan D (1973) An evoked potential correlate of colour: evoked potential findings and single-cell speculations. *Vision Res* 13, 1933-41.
28. Regan D (1973) Evoked potentials specific to spatial patterns of luminance and colour. *Vision Res* 13, 2381-2402.
29. Regan D (1973) Rapid objective refraction using evoked brain potentials. *Invest Ophthalmol* 12, 669-79.
30. Regan D & Richards W (1973) Brightness contrast and evoked potentials. *J Opt Soc Am* 63, 606-11.
31. Regan D & Beverley KI (1973) Disparity detectors in human depth perception: evidence for directional selectivity. *Science* 18, 877-9.
32. Regan D & Beverley KI (1973) Some dynamic features of depth perception. *Vision Res* 13, 2369-79.
33. Regan D & Beverley KI (1973) The dissociation of sideways movements from movements in depth: psychophysics. *Vision Res* 13, 2403-15.
34. Beverley KI & Regan D (1973) Evidence for the existence of neural mechanisms selectively sensitive to the direction of movement in space. *J Physiol* 235, 17-29.
34a. Beverley KI & Regan D (1973) Selective adaptation in stereoscopic depth perception. *J Physiol* 232, 40-41P.
35. Regan D & Beverley KI (1973) Relation between the magnitude of flicker sensation and evoked potential amplitude in man. *Perception* 2, 61-5.
36. Regan D & Beverley KI (1973) Electrophysiological evidence for the existence of neurones sensitive to the direction of depth movement. *Nature* 246, 504-6.
37. Richards W & Regan D (1973) A stereo field map with implications for disparity processing. *Invest Ophthalmol* 12, 904-9.

1974

38. Cartwright RF & Regan D (1974) Semi-automatic, multi-channel Fourier analyser for evoked potential analysis. *Electroenceph clin Neurophysiol* 36, 547-50.
39. Regan D (1974) Electrophysiological evidence for colour channels in human pattern vision. *Nature* 250, 437-49.
40. Regan D & Spekreijse H (1974) Evoked potential indications of colour blindness. *Vision Res* 14, 89-95.
41. Heron JR, Regan D & Milner BA (1974) Delay in visual perception in unilateral optic atrophy after retrobulbar neurities. *Brain* 97, 69-78.
42. Beverley KI & Regan D (1974) Temporal integration of disparity information in stereoscopic perception. *Exp Brain Res* 19, 228-32.
43. Beverley KI & Regan D (1974) Visual sensitivity to disparity pulses: evidence for directional selectivity. *Vision Res* 14, 357-61.
44. Regan D (1974) Visually evoked potential methods with clinical application. Proc 11th ISCERG Symp, Bad Neuheim (1973). *Docum Ophthal Proc Series* 4, 285-301.
45. Milner BA, Regan D & Heron JR (1974) Differential diagnosis of multiple sclerosis by visual evoked potential recording. *Brain* 97, 755-72.

1975

Department of Psychology

FAX: (416) 736-5814

UNIVERSITÉ YORK UNIVERSITY

FACULTY OF ARTS

4700 KEELE STREET • NORTH YORK • ONTARIO • CANADA • M3J 1P3

46. Regan D (1975) Colour coding of pattern responses in man investigated by evoked potential feedback and direct plot techniques. *Vision Res* 15, 175-83.
47. Heron JR, Milner BA & Regan D (1975) Measurement of acuity variations within the central visual field caused by neurological lesions. *J Neurol Neurosurg Psychiat* 38, 356-62.
48. Regan D, Schellart NAM, Spekreijse H & van den Berg TJTP (1975) Photometry in goldfish by electrophysiological recording: comparison of criterion response method with heterochromatic flicker photometry. *Vision Res* 15, 799-807.
49. Beverley KI & Regan D (1975) The relation between discrimination and sensitivity in the perception of motion in depth. *J Physiol* 249, 387-98.
50. Regan D (1975) Recent advances in electrical recording from the human brain. *Nature* 253, 401-07.

1976

51. Regan D, Milner BA & Heron JR (1976) Delayed visual perception and delayed visual evoked potentials in the spinal form of multiple sclerosis and in retrobulbar neuritis. *Brain* 99, 43-66.
52. Regan D, Varney P, Purdy J & Kraty N (1976) Visual field analyser: assessment of delay and temporal resolution of vision. *Med Biol Engng* 14, 8-14.
53. Regan D (1976) Latencies of evoked potentials to flicker and to pattern speedily estimated by simultaneous stimulation method. *Electroenceph clin Neurophysiol* 40, 654-60.
54. Galvin RJ, Regan D & Heron JR (1976) A possible means of monitoring the progress of demyelination in multiple sclerosis: effect of body temperature on visual perception of double light flashes. *J Neurol Neurosurg Psychiat* 39, 861-65.
55. Galvin RJ, Regan D & Heron JR (1976) Impaired temporal resolution of vision after acute retrobulbar neuritis. *Brain* 99, 255-68.

1977

56. Regan D (1977) Fourier analysis of evoked potentials: some methods based on Fourier analysis. In JE Desmedt (Ed), *Visual evoked potentials in man: new developments*. Oxford: Oxford Univ Press, 110-17.
57. Regan D (1977) Rapid methods for refracting the eye and for assessing visual acuity in amblyopia, using steady-state visual evoked potentials. In JE Desmedt (Ed), *Visual evoked potentials in man: new developments*. Oxford: Oxford Univ Press, 418-26.
58. Regan D (1977) Evoked potential indications of the processing of pattern, colour, and depth information. In JE Desmedt (Ed), *Visual evoked potentials in man: new developments*. Oxford: Oxford Univ Press, 234-49.
59. Regan D, Milner BA & Heron JR (1977) Slowing of visual signals in multiple sclerosis, measured psychophysically and by steady-state evoked potentials. In JE Desmedt (Ed), *Visual evoked potentials in man: new developments*. Oxford: Oxford Univ Press, 461-69.
60. Regan D (1977) Speedy assessment of visual acuity in amblyopia by the evoked potential method. *Ophthalmologica* 175, 159-64.
61. Regan D & Spekreijse H (1977) Auditory-visual interactions and the correspondence between perceived auditory space and perceived visual space. *Perception* 6, 133-38.
62. Galvin RJ, Heron JR & Regan D (1977) Subclinical optic neuropathy in multiple sclerosis. *Arch Neurol* 34, 666-70.

Department of Psychology

FAX: (416) 736-5814

UNIVERSITÉ YORK UNIVERSITY

FACULTY OF ARTS

4700 KEELE STREET • NORTH YORK • ONTARIO • CANADA • M3J 1P3

63. Regan D (1977) Steady state evoked potentials. Proc Symp Electrophysiological Techniques in Man. *J Opt Soc Am* 67, 1475-89.
64. Regan D, Silver R & Murray TJ (1977) Visual acuity and contrast sensitivity in multiple sclerosis - hidden visual loss. *Brain* 100, 563-79.
65. Regan D, Murray TJ & Silver R (1977) Effect of body temperature on visual evoked potential delay and visual perception in multiple sclerosis. *J Neurol Neurosurg Psychiat* 40, 1083-91.
66. Arden GB, Bodis-Wollner I, Halliday AM, Jeffreys A, Kulikowski JJ, Spekreijse H & Regan D (1977) Methodology of patterned visual stimulation. In JE Desmedt (Ed), *Visual evoked potentials in man: new developments*. Oxford: Oxford Univ Press, 3-15.
67. Regan D (1977) Visual evoked potentials and visual perception in multiple sclerosis. *Proc San Diego Biomed Symp*, Vol 16. New York: Academic, 87-95.
68. Regan D (1977) New methods for neurological assessment: overview. *Proc San Diego Biomed Symp*, Vol 16. New York: Academic, 55-62.
69. Regan D (1977) Evoked potentials in basic and clinical research. In A Rémond (Ed), *EEG informatics: a didactic review of methods and applications of EEG data processing*. Amsterdam: Elsevier, 319-46.
70. Regan D (1977) Colour and contrast. In H Spekreijse & LH van der Tweel (Eds), *Spatial contrast: report of a workshop*. Publ for Netherlands Royal Academy of Sciences. Amsterdam: North-Holland, 75-9.

1978

71. Regan D & Milner BA (1978) Objective perimetry by evoked potential recording: limitations. *Electroenceph clin Neurophysiol* 44, 393-7.
72. Regan D & Beverley KI (1978) Looming detectors in the human visual pathway. *Vision Res* 18, 415-21.
73. Cynader M & Regan D (1978) Neurones in cat parastriate cortex sensitive to the direction of motion in three-dimensional space. *J Physiol* 274, 549-69.
74. Regan D & Beverley KI (1978) Illusory motion in depth: aftereffect of adaptation to changing size. *Vision Res* 18, 209-12.
75. Hillyard SA, Picton TW & Regan D (1978) Sensation, perception and attention: analysis using ERPs. In E Callaway, P Tueting & SH Koslow (Eds), *Event-related brain potentials in man*. New York: Academic, 223-321.
76. Regan D (1978) Assessment of visual acuity by evoked potential recording: ambiguity caused by temporal dependence of spatial frequency selectivity. *Vision Res* 18, 439-45.
77. Regan D (1978) Investigations of normal and defective colour vision by evoked potential recording. *Mod Probl Ophthal* 19, 19-28.
78. Regan D, Beverley KI & Cynader M (1978) Stereoscopic depth channels for position and for motion. In SJ Cool & EL Smith (Eds), *Frontiers in visual science*. New York: Springer, 351-72.

1979

79. Regan D, Beverley KI & Cynader M (1979) Stereoscopic subsystems for position in depth and for motion in depth. *Proc R Soc Lond* B 204, 485-501.
80. Regan D & Tansley BW (1979) Selective adaptation to frequency-modulated tones: evidence for an information-processing channel selectively sensitive to frequency changes. *J Acoust Soc Am* 65, 1249-57.

Department of Psychology

FAX: (416) 736-5814

UNIVERSITÉ YORK UNIVERSITY

FACULTY OF ARTS

4700 KEELE STREET • NORTH YORK • ONTARIO • CANADA • M3J 1P3

81. Regan D & Beverley KI (1979) Visually guided locomotion: psychophysical evidence for a neural mechanism sensitive to flow patterns. *Science* 205, 311-13.
82. Beverley KI & Regan D (1979) Separable aftereffects of changing-size and motion-in-depth: different neural mechanisms? *Vision Res* 19, 727-32.
83. Beverley KI & Regan D (1979) Visual perception of changing-size: the effect of object size. *Vision Res* 19, 1093-1104.
84. Regan D & Cynader M (1979) Neurons in area 18 of cat visual cortex selectively sensitive to changing size: nonlinear interactions between responses to two edges. *Vision Res* 19, 699-711.
85. Regan D & Beverley KI (1979) Binocular and monocular stimuli for motion in depth: changing-disparity and changing-size feed the same motion-in-depth stage. *Vision Res* 19, 1331-42.
86. Regan D, Beverley KI & Cynader M (1979) The visual perception of motion in depth. *Scient Am* 241, 136-51.
87. Tansley BW & Regan D (1979) Separate auditory channels for unidirectional frequency modulation and unidirectional amplitude modulation. *Sensory Proc* 3, 132-40.
88. Regan D (1979) Electrical responses evoked from the human brain. *Scient Am* 241, 134-46.

1980

89. Regan D, Whitlock J, Murray TJ & Beverley KI (1980) Orientation-specific losses of contrast sensitivity in multiple sclerosis. *Invest Ophthalmol Vis Sci* 19, 324-28.
90. Regan D & Beverley KI (1980) Visual responses to changing size and to sideways motion for different directions of motion in depth: linearization of visual responses. *J Opt Soc Am* 11, 1289-96.
91. Beverley KI & Regan D (1980) Temporal selectivity of changing-size channels. *J Opt Soc Am* 11, 1375-77.
92. Beverley KI & Regan D (1980) Visual sensitivity to the shape and size of a moving object: implications for models of object perception. *Perception* 9, 151-60.
93. Beverley KI & Regan D (1980) Device for measuring the precision of eye-hand coordination while tracking changing size. *Aviat Space Environ Med* 51, 688-93.
94. Regan D (1980) Speedy evoked potential methods for assessing vision in normal and amblyopic eyes: pros and cons. *Vision Res* 20, 265-69.
95. Regan D (1980) New visual tests in multiple sclerosis. In HS Thompson (Ed), *Topics in neuro-ophthalmology*. Baltimore: Williams & Wilkins, 219-42.
96. Regan D (1980) Detection and quantification of neuroophthalmological abnormalities using psychophysical measures of visual delay and temporal resolution. In S Sokol (Ed), *Electrophysiology and psychophysics: their use in ophthalmic diagnosis*. Intl Ophthal Clinics. Boston: Little, Brown, 185-204.
97. Regan D (1980) Control system and physiological monitoring applications of steady-state evoked potentials. In FE Gomer (Ed), *Biocybernetic applications for military systems*. DARPA Conf, Chicago (1978). St Louis: McDonnell-Douglas. Report MDC E2191, 175-202.

1981

98. Regan D & Beverley KI (1981) Motion sensitivity measured by a psychophysical linearizing technique. *J Opt Soc Am* 71, 958-65.
99. Raymond J, Regan D & Murray TJ (1981) Abnormal adaptation of visual contrast sensitivity in multiple sclerosis patients. *Can J Neurol Sci* 8, 221-34.

Department of Psychology

FAX: (416) 736-5814

UNIVERSITÉ YORK UNIVERSITY

FACULTY OF ARTS

4700 KEELE STREET • NORTH YORK • ONTARIO • CANADA • M3J 1P3

100. Noseworthy J, Miller J, Murray TJ & Regan D (1981) Auditory brainstem responses in postconcussion syndrome. *Arch Neurol* 38, 275-78.
101. Regan D, Raymond J, Ginsburg A & Murray TJ (1981) Contrast sensitivity, visual acuity and the discrimination of Snellen letters in multiple sclerosis. *Brain* 104, 333-50.
102. Petersik JT, Beverley KI & Regan D (1981) Contrast sensitivity of the changing-size channel. *Vision Res* 21, 829-32.
103. Regan D (1981) Psychophysical tests of vision and hearing in patients with multiple sclerosis. In SG Waxman & JM Ritchie (Eds), *Demyelinating disease: basic and clinical electrophysiology*. Proc Vail Conf MS Soc of USA. New York: Raven, 217-37.
104. Kruk R, Regan D, Beverley KI & Longridge T (1981) Correlations between visual test results and flying performance on the Advanced Simulator for Pilot Training (ASPT). *Aviat Space Environ Med* 52, 455-60.
105. Regan D (1981) Visual psychophysical tests in multiple sclerosis as an aid to diagnosis, localization of pathology, and assessment of experimental therapy. In *Clinical applications of visual psychophysics* (Proc NAS/NRC Symp). New York: Cambridge Univ Press.
106. Regan D (1981) Electrophysiology and psychophysics of motion in depth. Proc 18th ISCERG Symp, Amsterdam (1981). *Docum Ophthal Proc Series* 27, 271-81.
107. Regan D (1981) Evoked potential studies of visual perception. *Can J Psychol* 35, 77-112.
108. Regan D, Kruk R, Beverley KI & Longridge T (1981) The relevance of channel theory for the design of simulator imagery. *Proc Image II conf*, Arizona, 307-44.

1982

109. Regan D (1982) Comparison of transient and steady-state methods. *Proc NY Acad Sci* 388, 46-71.
110. Beverley KI & Regan D (1982) Adaptation to incomplete flow patterns: no evidence for "filling in" the perception of flow patterns. *Perception* 11, 275-78.
111. Cynader M & Regan D (1982) Neurons in cat visual cortex tuned to the direction of motion in depth: effect of positional disparity. *Vision Res* 22, 967-82.
112. Regan D & Cynader M (1982) Neurons in cat visual cortex tuned to the direction of motion in depth: effect of stimulus speed. *Invest Ophthalmol Vis Sci* 22, 535-50.
113. Tansley BW, Regan D & Suffield JB (1982) Measurement of the sensitivities of information-processing channels for frequency change and for amplitude change by a titration method. *Can J Psychol* 36, 723-30.
114. Regan D & Beverley KI (1982) How do we avoid confounding the direction we are looking with the direction we are moving? *Science* 215, 194-96.
115. Regan D (1982) Visual information channeling in normal and disordered vision. *Psychol Rev* 89, 407-44.
116. Regan D, Regal DM & Tibbles JAR (1982) Evoked potentials during recovery from blindness recorded serially from an infant and his normally sighted twin. *Electroenceph clin Neurophysiol* 54, 465-68.
117. Regan D, Bartol S, Murray TJ & Beverley KI (1982) Spatial frequency discrimination in normal vision and in patients with multiple sclerosis. *Brain* 105, 735-54.
118. Regan D (1982) Visual sensory aspects of simulation. In W Richards & K Dismukes (Eds), *Vision research for flight simulator*. Washington: National Academy Press, 65-71.

1983

Department of Psychology

FAX: (416) 736-5814

UNIVERSITÉ
YORK
UNIVERSITY

FACULTY OF ARTS

4700 KEELE STREET • NORTH YORK • ONTARIO • CANADA • M3J 1P3

119. Kruk R, Regan D, Beverley KI & Longridge T (1983) Flying performance on the Advanced Simulator for Pilot Training and laboratory tests of vision. *Human Factors* 25, 457-66.
120. Regan D (1983) Visual psychophysical tests in demyelinating disease. *Bull Soc Belge Ophtal* 208-I, 303-21.
121. Regan D & Beverley KI (1983) Visual fields described by contrast sensitivity, by acuity and by relative sensitivity to different orientations. *Invest Ophthalmol Vis Sci* 24, 754-59.
122. Regan D & Beverley KI (1983) Visual fields for frontal plane motion and for changing size. *Vision Res* 23, 673-76.
123. Regan D (1983) Spatial frequency mechanisms in human vision investigated by evoked potential recording. *Vision Res* 23, 1401-08.
124. Quine DB, Regan D & Murray TJ (1983) Delayed auditory tone perception in multiple sclerosis. *Can J Neurol Sci* 10, 183-86.
125. Beverley KI & Regan D (1983) Texture changes versus size changes as stimuli for motion in depth. *Vision Res* 23, 1387-1400.
126. Kruk R & Regan D (1983) Visual test results compared with flying performance in telemetry-tracked aircraft. *Aviat Space Environ Med* 54, 906-11.
127. Burbeck CA & Regan D (1983) Independence of orientation and size in spatial discriminations. *J Opt Soc Am* 73, 1691-94.
128. Regan D & Beverley KI (1983) Spatial frequency discrimination and detection: comparison of postadaptation thresholds. *J Opt Soc Am* 73, 1684-90.
129. Regan D & Neima D (1983) Low-contrast letter charts as a test of visual function. *Ophthalmology* 90, 1192-1200.

1984

130. Regan D & Beverley KI (1984) Figure-ground segregation by motion contrast and by luminance contrast. *J Opt Soc Am* 1, 433-42.
131. Quine DB, Regan D, Beverley KI & Murray TJ (1984) Patients with multiple sclerosis experience hearing loss specifically for shifts of tone frequency. *Arch Neurol* 41, 506-08.
132. Quine DB, Regan D & Murray TJ (1984) Degraded discrimination between speech-like sounds by patients with multiple sclerosis and Friedreich's ataxia. *Brain* 107, 1113-22.
133. Neima D & Regan D (1984) Pattern visual evoked potentials and spatial vision in retrobulbar neuritis and multiple sclerosis. *Arch Neurol* 41, 198-201.
134. Neima D, LeBlanc R & Regan D (1984) Visual field defects in ocular hypertension and glaucoma. *Arch Ophthalmol* 102, 1042-45.
135. Regan D & Neima D (1984) Visual fatigue and VEPs in multiple sclerosis, glaucoma, ocular hypertension and Parkinson's disease. *J Neurol Neurosurg Psychiat* 47, 673-78.
136. Wilson HR & Regan D (1984) Spatial frequency adaptation and grating discrimination predictions of a line-element model. *J Opt Soc Am* A 1, 1091-96.
137. Regan D & Neima D (1984) Balance between pattern and flicker sensitivities in the visual fields of ophthalmological patients. *Br J Ophthalmol* 68, 310-15.
138. Regan D & Neima D (1984) Low contrast letter charts in early diabetic retinopathy, ocular hypertension, glaucoma and Parkinson's disease. *Br J Ophthalmol* 68, 885-89.
139. Regan D (1984) Visual psychophysical tests in the diagnosis of multiple sclerosis. In CM Poser (Ed), *The diagnosis of multiple sclerosis*. New York: Thieme-Stratton, 64-75.

Department of Psychology

FAX: (416) 736-5814

UNIVERSITÉ YORK UNIVERSITY

FACULTY OF ARTS

4700 KEELE STREET • NORTH YORK • ONTARIO • CANADA • M3J 1P3

140. Regan D (1984) Chapters 11 & 12 in E Donchin (Ed), Cognitive psychophysiology. Hillsdale, NJ: Erlbaum, 303-38.
141. Regan D & Beverley KI (1984) Psychophysics of visual flow patterns and motion in depth. In L Spillman & BR Wooten (Eds), *Sensory experience, adaptation and perception*. Hillsdale, NJ: Erlbaum, 215-40.
142. Regan D (1984) Visual factors in flying performance. Proc TARP, NAMRL Monograph 33, 3-10.
143. Regan D, Beverley KI & Macpherson H (1984) Pattern visual evoked potentials in amblyopic children. In RH Nodar & C Barber (Eds) *Evoked potentials II.* Boston: Butterworth, 293-301.
144. Regan D (1984). Spatial vision: VEP evidence for mechanisms tuned to spatial frequency. In RH Nodar & C Barber (Eds) *Evoked potentials II.* Boston: Butterworth, 287-89.

1985

145. Regan D & Beverley KI (1985) Postadaptation orientation discrimination. *J Opt Soc Am* A 2, 147-55.
146. Regan D (1985) Visual flow and direction of locomotion.*Science* 227, 1063-65.
147. Regan D & Beverley KI (1985) Visual responses to vorticity and the neural analysis of optic flow. *J Opt Soc Am* A 2, 280-83.
148. Regan D (1985) Evoked potentials in diagnosis. In M Swash & C Kennard (Eds), *Scientific basis of clinical neurology.* Edinburgh: Churchill Livingstone.
149. Regan D (1985) Masking of spatial frequency discrimination. *J Opt Soc Am* A 2, 1153-59.
150. Regan D (1985) Storage of spatial-frequency information and spatial-frequency discrimination. *J Opt Soc Am* A 2, 619-21.
151. Regan D (1985) Evoked potentials and their application to neuro-ophthalmology. *Neuro-ophthalmology* 5, 73-108.
152. Regan D (1985) New visual sensory tests in neurology and ophthalmology. In A Starr (Ed), *Proc 7th evoked potential workshop*, Univ of California, Irvine (1984). Milan: Amplifon, 101-19.
153. Spekreijse H, Dangelie G, Maier J & Regan D (1985) Flicker and movement constituents of the pattern reversal response. *Vision Res* 25, 1297-1304.

1986

154. Regan D (1986) Visual processing of four kinds of relative motion. *Vision Res* 26, 127-45.
155. Regan D & Price P (1986) Periodicity in orientation discrimination and the unconfounding of visual information. *Vision Res* 26, 1299-1302.
156. Regan D & Spekreijse H (1986) Evoked potentials in vision research: 1961-1985. *Vision Res* 26, 1461-80.
157. Regan D (1986) Form from motion parallax and form from luminance contrast: vernier discrimination. *Spatial Vision* 1, 305-18.
158. Regan D, Collewijn H & Erkelens CJ (1986) Necessary conditions for the perception of motion in depth . *Invest Ophthalmol Vis Sci* 27, 584-97.
159. Regan D, Erkelens CJ & Collewijn H (1986) Visual field defects for vergence eye movements and for stereomotion perception. *Invest Ophthalmol Vis Sci* 27, 806-19.
160. Regan D & Maxner C (1986) Orientation-dependent loss of contrast sensitivity for pattern and flicker in multiple sclerosis. *Clin Vision Sci* 1, 1-23.

Department of Psychology

FAX: (416) 736-5814

UNIVERSITÉ YORK UNIVERSITY

FACULTY OF ARTS

4700 KEELE STREET • NORTH YORK • ONTARIO • CANADA • M3J 1P3

161. Erkelens CJ & Regan D (1986) Human ocular vergence movements induced by changing size and disparity. *J Physiol* 379, 145-69.
162. Collewijn H, Erkelens CJ & Regan D (1986) Absolute and relative disparity: a re-evaluation of their significance in perception and oculomotor control. In E Keller & DS Zee (Eds), *Adaptive processes in visual and oculomotor systems*. Pergamon.
163. Regan D (1986) The eye in ballgames: hitting and catching. *Sport en zien*. Haarlem: De Vrieseborch, pp 7-32.
164. Regan D., Kaufman, L. and Lincoln, J (1986) Motion in depth and visual acceleration. In KR Boff, L. Kaufman & JP Thomas (Eds) *Handbook of perception and human performance*. New York: Wiley, pp.19-1 to 19-46.
165. Regan D (1986) Binocular vision. In *Encyclopaedia of physics in medicine and biology*. Pergamon, pp 33-4.

1987

166. Regan D & Maxner C (1987) Orientation-selective visual loss in patients with Parkinson's disease. *Brain* 110, 239-71.
167. Regan D & Regan MP (1987) Nonlinearity in human visual responses to two-dimensional patterns and a limitation of Fourier methods. *Vision Res* 27, 2181-83.
168. Regan D (1987) Human visual evoked potentials. In T Picton (Ed), *Human event-related potentials*. Amsterdam: Elsevier, pp 159-243.
169. Regan D (1987) Evoked potentials and color-defined categories. In S Harnad (Ed), *Categorical perception*. New York: Cambridge Univ Press, 443-51.
170. Regan D & Regan MP (1987) Spatial frequency tuning, orientation tuning and spatial discrimination investigated by nonlinear analysis of pattern evoked potentials. In C Barber & T Blum (Eds) *Evoked potentials III*. Stoneham, MA: Butterworths.
171. Morgan MJ & Regan D (1987) Opponent model for line interval discrimination: interval and vernier performance compared. *Vision Res* 27, 107-18.
172. Apkarian P, Tijssen R, Spekreijse H & Regan D (1987) Origin of notches in CSF: optical or neural? *Invest Ophthalmol Vis Sci* 28, 607-12.
173. Regan D & Regan MP (1987) "Dissecting" the visual and auditory pathways by means of the two-input technique. Proc Conf on Electric and Magnetic Activity of the Central Nervous System, Trondheim, Norway. AGARD Conf Proc. 432, 6, 1-9.
174. Regan D & Neima D (1987) Relation between VEP and visual function in lesions of the optic nerve and visual pathway. Proc Conf on Electric and Magnetic Activity of the Central Nervous System, Trondheim, Norway. AGARD Conf. Proc. 432, 38, 1-8.

1988

175. Regan D (1988) Low contrast letter charts and sinewave grating tests in ophthalmological and neurological disorders. *Clin Vision Sci* 2, 235-50.
176. Regan D (1988) Low-contrast visual acuity test for paediatric use. *Can J Ophthalmol* 23, 224-27.
177. Regan D & Regan MP (1988) The transducer characteristic of hair cells in the human ear: a possible objective measure. *Brain Res* 438, 363-65.
178. Regan D & Regan MP (1988) Objective evidence for phase-independent spatial frequency analysis in the human visual pathway. *Vision Res* 28, 187-91.
179. Regan MP & Regan D (1988) A frequency domain technique for characterizing nonlinearities in biological systems. *J Theoret Biol* 133, 293-317.

Department of Psychology

FAX: (416) 736-5814

UNIVERSITÉ YORK UNIVERSITY

FACULTY OF ARTS

4700 KEELE STREET • NORTH YORK • ONTARIO • CANADA • M3J 1P3

180. Regan D (1988) Visual sensory loss in patients with Parkinson's disease. In I Bodis-Wollner & M Piccolino (Eds), *Dopaminergic mechanisms in vision*. Neurology & Neurobiology 43. New York: AR Liss, pp 221-26.

1989

181. Hong X & Regan D (1989) Visual field defects for unidirectional and oscillatory motion in depth. *Vision Res* 29, 809-19.
182. Regan D (1989) Orientation discrimination for objects defined by relative motion and objects defined by luminance contrast. *Vision Res* 29, 1389-1400.
183. Regan MP & Regan D (1989) Objective investigation of visual function using a nondestructive zoom-FFT technique for evoked potential analysis. *Can J Neurol Sci* 16, 168-79.
184. Regan D (1989) Magnetic fields generated by the human brain. *Can Res* 22, 11-15.
185. Regan D (1989) To what extent can visual defects caused by multiple sclerosis be understood in terms of parallel processing? In B Cohen (Ed), *Vision and the brain: The organization of the central visual system*. New York: Raven, 317-29.
186. Regan D (1989) Acute spatial discriminations and the unconfounding of visual information. In JJ Kulikowski (Ed), *Seeing contour and colour*, 333-339.
187. Regan MP & Regan D (1989) Evoked potential investigation of nonlinear processing stages in human spatial vision. In JJ Kulikowski (Ed), *Seeing contour and colour*, 513-18.
188. Regan D & Regan MP (1989) Ultra-high resolution analysis of auditory and visual brain responses using zoom-FFT. In SJ Williamson, M Hoke, G Stroink & M Kotani (Eds), *Advances in biomagnetism*. New York: Plenum, 205-07.
189. Regan MP & Regan D (1989) A frequency domain technique for using evoked magnetic fields to test multi-stage models of sensory processing. In SJ Williamson, M Hoke, G Stroink & M Kotani (Eds), *Advances in biomagnetism*. New York: Plenum, 201-04.

1990

190. Regan D & Hong X (1990) Visual acuity for optotypes made visible by relative motion. *Optom & Vision Science* 67, 49-55.
191. Kothe A. & Regan D (1990) The component of gaze selection/control in the development of visual acuity in children. *Optom & Vision Science* 67, 770-778.
192. Kothe AC & Regan D (1990) Crowding depends on contrast. *Optom & Vis Sci* 4, 283-86.
193. Regan D (1990) High and low contrast acuity. *Optom & Vis Sci* 67, 650-53.
194. Regan D, Frisby J, Poggio G, Schor C & Tyler CW (1990) The perception of stereodepth and stereomotion. In L Spillman and JS Werner (Eds), *Neurophysiological foundations of visual perception*. Academic, 317-47.

1991

195. Regan D (1991) Specific tests and specific blindness: keys, locks and parallel processing. Prentice Medal Lecture. *Optom & Vis Sci* 68, 489-512.
196. Regan D & Hamstra S (1991) Shape discrimination for motion-defined and contrast-defined form: Squareness is special. *Perception* 20, 315-36.
197. Regan D, Kothe AC & Sharpe JA (1991) Recognition of motion-defined shapes in patients with multiple sclerosis and optic neuritis. *Brain* 114, 1129-55.
198. Regan D (1991) Do letter charts measure contrast sensitivity? *Clin Vis Science* 6, 401-08.

Department of Psychology

FAX: (416) 736-5814

UNIVERSITÉ YORK UNIVERSITY

FACULTY OF ARTS

4700 KEELE STREET • NORTH YORK • ONTARIO • CANADA • M3J 1P3

199. Regan D (1991) A brief review of some of the stimuli and analysis methods used in spatiotemporal vision research. In D Regan (Ed), *Spatial vision*. London: Macmillan, 1-42.
200. Regan D (1991) Spatiotemporal abnormalities of vision in patients with multiple sclerosis. In D Regan (Ed), *Spatial vision*. London: Macmillan, 239-49.
201. Regan D. (1991) Detection and spatial discriminations for objects defined by colour contrast, binocular disparity and motion parallax. In D Regan (Ed), *Spatial vision*. London: Macmillan, 135-78.
202. Bodis-Wollner I & Regan D (1991) Spatiotemporal contrast vision in Parkinson's disease and MPTP treated monkeys: the role of dopamine. In D Regan (Ed), *Spatial vision*. London: Macmillan, 250-60.
203. Regan D (1991) Depth from motion and motion in depth. In D Regan (Ed), *Binocular vision*. London: Macmillan, 37-69.
204 Collewjjn H, Steinman RM, Erkelens CJ & Regan D (1991) Binocular fusion, stereopsis and stereoacuity with a moving head. In D Regan (Ed.) *Binocular vision*. London, Macmillan, 121-36.
205. Regan D & Hong XH (1991) Motion-defined letter reading test. *Opt Soc of Amer Tech Digest*.
206. Regan D (1991) A sensitive method for quantifying functional loss caused by veiling glare in patients and in elderly nonpatients. *Opt Soc of Amer Tech Digest*.
207. Regan D, Hong XH & Hamstra (1991) Visual sensitivity to camouflaged motion-defined objects and the limits of safety in nap-of-the-Earth helicopter navigation. In Proc. Symp. on *Aeromedical Aspects of Vision*, Toronto, 161-66.
208. Regan D (1991) Procedures for establishing low-contrast vision and glare susceptibility standards for pilots and drivers, and the selection of personnel for visual search and surveillance. In Proc. Symp. on *Aeromedical Aspects of Vision*, Toronto, 34-56.
209. Karnavas WJ, Bahill AT and Regan D (1991) Sensitivity analysis of a model for the rising fastball and breaking curveball. *Proc IEEE Syst Man & Cybernet*, Los Angeles.

1992

210. Regan D & Hamstra S (1992) Dissociation of orientation discrimination from form detection for motion-defined bars and luminance-defined bars: effects of dot lifetime and presentation duration. *Vision Res.*,32,1655-1666.
211. Regan D & Hamstra S (1992) Shape discrimination and the judgement of perfect symmetry: dissociation of shape from size. *Vision Res.* 32,1845-1864.
212. Regan D, Giaschi D, Sharpe JA & Hong XH (1992) Visual processing of motion-defined form: selective failure in patients with parieto-temporal lesions. *J. Neurosci.*, 12, 2198-2210.
213. Giaschi D, Regan D, Kothe AC, Hong XH & Sharpe JA (1992) Motion-defined letter detection and recognition in patients with multiple sclerosis. *Ann. Neurol.* 31, 621-628.
214. Giaschi D, Regan D, Kraft S & Hong XH (1992) Defective processing of motion in the fellow eye of unilateral amblyopes. *Invest Ophthal. Vis. Sci.*, 33, 2483-2489.
215. Regan D, Giaschi D, Kraft S & Kothe AC (1992) A method for identifying amblyopes whose reduced line acuity is caused by defective selection and/or control of gaze. *Opthalmic & Physiological Optics.* 12, 425-432.

Department of Psychology

FAX: (416) 736-5814

UNIVERSITÉ YORK UNIVERSITY

FACULTY OF ARTS

4700 KEELE STREET • NORTH YORK • ONTARIO • CANADA • M3J 1P3

216. Regan D (1992) Visual judgements and misjudgements in cricket, and the art of flight. *Perception*. 21, 91-115.
217. Regan D (1992) Nonlinearities in psychophysical models of the processing of spatial form and motion. In R. Pinter (Ed) *Nonlinear Vision* pp 293-307
218. Regan MP & Regan D (1992) A frequency domain method for testing nonlinear multi-neuron models against data. In R. Pinter (Ed) *Nonlinear Vision* ..pp 265-291
219. Regan D, Hamstra S & Kaushal S (1992) Visual factors in the avoidance of front-to-rear end highway collisions. *Proc. Human Factors Soc. 36th Annual meeting.*

1993

220. Regan D, Hamstra S (1993) Dissociation of discrimination thresholds for time to contact and for rate of angular expansion *Vision Res.*,33, 447-462.
221. Regan D (1993) Detection and discrimination of motion-defined and luminance-defined two-dimensional form.In L.Harris and M.Jenkins(Eds.)*Spatial Vision in Humans and Robots*,Cambridge Univ.Press. (pp. 281-312).
222. Regan D & Lee BB (1993) A comparison of the human 40 Hz response with the properties of macaque ganglion cells. *Visual Neuroscience*, 10, 439-445.
223. Regan.D.(1993) Detection and discrimination of spatial form in patients with eye or visual pathway disorders.Fifth Annual Retina Research Foundation Symposium. *Contrast Sensitivity:From Receptors to Clinic*, M.I.T.Press, (pp. 309-337).
224. Regan D, Giaschi D & Fresco B (1993) Measurement of glare sensitivity in cataract patients using low-contrast letter charts. *Ophthalmic & Physiological Optics* 13, 115-123.
225. Regan D.,Kaiser P.K. & Nakano Y.(1993) Dissociation of chromatic and achromatic processing of spatial form by the titration method. *J. Opt. Soc. Amer.* 10, 1314-1323.
226. Giaschi D, Regan D, Kraft S & Kothe AC (1993) Crowding and contrast in amblyopia. *Optom. Vis. Sci.*. 70, 969-975.
227. Regan MP & Regan D (1993) Nonlinear terms produced by passing amplitude-modulated sinusoids through Corey & Hudspeth's hair cell transducer function.*Biological Cybernetics* 69, 439-446.
228. Regan D, Hamstra SJ, Hong, XH & Kaushal, S (1993) Nonlinearities in the visual processing of motion and form. Proc. IEEE Conf. on Systems, Man & Cyberbetics, 156-159.
229. Regan MP & Regan D (1993) Rectification of amplitude-modulated sinusoids with particular reference to a hair cell transducer function. Proc. IEEE Conf. on Systems, Man & Cyberbetics, 495-500.
230. Regan D (1993) The divergence of velocity and visual processing. *Perception*, 22, 497-499
231. Regan D (1993) Binocular correlates of the direction of motion in depth. *Vision Res.*, 33, 2359-2360.
232. Regan D, Giaschi D & Fresco B (1993) Measurement of glare sensitivity in cataract patients using low-contrast letter charts. *Ophthalmic & Physiological Optics* 13, 115-123.

1994

233. Regan D ,Kaushal S (1994) Monocular judgement of the direction of motion in depth. *Vision Res.*, 34, 163-177.
234. Regan D & Hamstra S (1994) Shape discrimination for rectangles defined by disparity alone, disparity plus luminance and by disparity plus motion. *Vision Res.*, 34, 2277-2291.

Department of Psychology

FAX: (416) 736-5814

UNIVERSITÉ
YORK
UNIVERSITY

FACULTY OF ARTS

4700 KEELE STREET • NORTH YORK • ONTARIO • CANADA • M3J 1P3

235. Regan D.& Hong X.H.(1994) Recognition and detection of texture-defined letters. *Vision Res.*, 34, 2403-2407
236. Regan MP (1994). A method for calculating the spectral response of a hair cell to a pure tone. *Biological Cybernetics*, 71, 13-16

1995

237. Regan D.(1995) Spatial vision in children and adults: A tribute to Russel Harter *Internat.J.Neurosci.* 80, 153-172.
238. Hamstra, SJ & Regan, D (1995) Orientation discrimination in cyclopean vision. Vision Res., 35, 365-374.
239. Regan D & Vincent A (1995) Visual processing of looming and time to contact throughout the visual field. Vision Research, 35, 1845-1857.
240. Regan D, Hamstra SJ, Kaushal S, Vincent A, Gray R & Beverley KI (1995) Visual processing of an object's motion in three dimensions for a stationary or a moving observer. Perception, 24, 87-103.
241. Regan D & Simpson TL (1995) Multiple sclerosis can cause visual processing deficits specific to texture-defined form. *Neurology*, 45, 809-815.
242. Regan D & Hong XH (1995) Two models of the recognition and detection of texture-defined letters compared. *Biological Cybernetics*, 72, 389-396.
243. Simpson T & Regan D (1995) Test-retest variability and correlations between tests of texture processing, motion processing, visual acuity and contrast sensitivity. *Optometry & Vision Science*, 72, 11-16.
244. Regan D (1995) Orientation discrimination for texture-defined form. *Perception*, 24, 1131-1138.
245. Regan D & He P (1995) Magnetic and electrical responses of the human brain to texture-defined form and to textons. *J Neurophysiol*, 74, No.3, 1167-1178.
246. Regan MP, He P & Regan D (1995) An audio-visual convergence area in human brain. *Exp. Brain Res.*, 106, 485-487.
247. Vincent A, & Regan D. (1995) Parallel independent encoding of orientation, spatial frequency and contrast. *Perception.* 24, 491-499.
248. Regan, D (1995) Spatial orientation in aviation: Visual contributions. *J Vestibular Research*, 5, 455-471.
249. Simpson, T. L. (1995). Vision thresholds from psychometric analyses: alternatives to Probit analysis. *Optometry & Vision Science*, 72, 371-377.
250. Regan MP (1995) Linear half-wave rectification of amplitude-modulated sinusoids. *Applied Mathematics & Computation*, 62, 61-79.

1996

251. Regan D & He P (1996) Magnetic and electrical brain responses to chromatic contrast in human. *Vision Research*, 36, 1-18.
252. Regan, D, Gray, R & Hamstra, SJ (1996) Evidence for a neural mechanism that encodes angles. *Vision Research* 36, 323-330.
253. Gray R & Regan D (1996) Cyclopean motion perception produced by oscillations of size, disparity and location. *Vision Res* 35,655-666.
254. Kruk, R. & Regan, D. (1996) Collision avoidance: A helicopter simulator study. *Aviat., Space & Environ. Med.* 67, 111-114.

Department of Psychology

FAX: (416) 736-5814

UNIVERSITÉ YORK UNIVERSITY

FACULTY OF ARTS

4700 KEELE STREET • NORTH YORK • ONTARIO • CANADA • M3J 1P3

255. Gray, R. & Regan, D. (1996) Accuracy of reproducing angles: is a right angle special? *Perception*, 25, 531-542.
256. Giaschi, D. E., Trope, G. E., Kothe, A. C. & Hong, X. H. (1996). Loss of sensitivity to motion-defined form in patients with primary open angle glaucoma and ocular hypertension. *Journal of the Optical Society of America*, 13, 707-716.
257. Regan, M. P. (1996) Half-wave rectification of a frequency modulated sinusoid. *Jour. of Applied Math. and Computation*, 79, 137-162.

1997

258. Regan, D. (1997) Perceptual motor skills and human motion analysis. In *Handbook Of Human Factors And Ergonomics*, G. Salvendy (Ed.) New York: Wiley.
259. Portfors-Yeomans, C. V. & Regan, D. (1997) Discrimination of the direction and speed of motion in depth from binocular information alone. *J. Exp. Psychol.: Hum. Percept & Perform.* in press.
260. Regan, D (1997) Visual factors in catching and hitting. *J Sports Sciences*, in press.
261. Vincent, A. & Regan, D. (1997) Judging the time to collision with a simulated textured object: effect of mismatching rates of expansion of size and of texture elements. *Perception and Psychophysics* in press.

Patents

Regan, D. & Parr, N. "Improvement in paramedical instrumentation" (Joule-Thomson effect cataract surgery probe). U.K. patent application 4964 (1972). Wilkinson Sword Research.

Regan, D. "Improvements in paramedical instrumentation" (visual acuity measurement). U.K. patent application 4866 (1972). Accepted in U.K. , U.S.A., Germany, E. Europe, Japan. Wilkinson Sword Research.

Regan, D. "Improvements in paramedical instrumentation" (multiple sclerosis diagnosis). U.K. patent application 4865(1972). U.S.A. patent N^{o} 3,837,734; West German Patent N^{o} 2,304,808. Wilkinson Sword Research.

Regan, D. "Improvements in signal analysis". U.K. patent application 59921 (1972).

Regan, D. "Improved apparatus and methods for optometry" (1972). U.K. patent application 15246/72, 49241/72, 9934/73. U.S.A., E. Europe, W. Germany, U.K. National Research Development Corporation.

Regan, D. "Paramedical apparatus and method" (multiple sclerosis diagnosis). U.K. patent application 25,532 (1964). Wilkinson Sword Research.

Department of Psychology

FAX: (416) 736-5814

UNIVERSITÉ YORK UNIVERSITY

FACULTY OF ARTS

4700 KEELE STREET • NORTH YORK • ONTARIO • CANADA • M3J 1P3

Regan D. and Beverley, K.I. "Methods and apparatus for measuring hand-eye coordination while tracking a changing-size image". U.S. patent N^{o} 4,325,697 (1982). U.S. Air Force.

Regan, D. "Paramedical apparatus and method" (eye test chart). U.K. provisional patent 8521775 (1985).

Presentations and abstracts

1993

1. Hamstra, S. & Regan, D. (1993). Shape discrimination for form defined by binocular disparity, luminance contrast and relative motion. 16th European Conference on Visual Perception, Edinburgh.
2. Regan, M. P. & Regan, D. (1993). Visual processing of two-dimensional patterns. Nonlinear interactions between orthogonal contours. 16th European Conference on Visual Perception, Edinburgh.
3. Regan, D., Hamstra, S. J., Hong, X. H. & Kaushal, S. (1993). Nonlinearities in the visual processing of motion and form. Presented at IEEE, France 1993.
4. Regan, D. & Kaushal, S. (1993). Monocular discrimination of the direction of motion in depth. Canadian Society for Brain, Behaviour and Cognitive Science, Toronto.
5. Regan, D. & He, P. (1993). Magnetic brain responses to chromatic contrast in human. Canadian Society for Brain, Behaviour and Cognitive Science, Toronto.
6. He, P., Regan, M. P. & Regan, D. (1993). Audio-visual integration area in human brain: identification and localization. Canadian Society for Brain, Behaviour and Cognitive Science, Toronto.

1994

7. Simpson, T. L. & Regan, D. (1994). Specific deficits in visual processing of texture in patients with multiple sclerosis. Presented at the Annual meeting of the Association for Research in Vision and Ophthalmology (ARVO), Sarasota.
8. Regan, D. & Hong, X. H. (1994). Recognition and detection of texture-defined letters. Presented at the Annual meeting of the Association for Research in Vision and Ophthalmology (ARVO), Sarasota.
9. Vincent, A. & Regan, D. (1994). Visual processing of motion in depth and time to contact throughout the visual field. Presented at the Annual

Department of Psychology

FAX: (416) 736-5814

UNIVERSITÉ YORK UNIVERSITY

FACULTY OF ARTS

4700 KEELE STREET • NORTH YORK • ONTARIO • CANADA • M3J 1P3

meeting of the Association for Research in Vision and Ophthalmology (ARVO), Sarasota.

10. Hamstra, S. J. & Regan, D. (1994). Orientation discrimination for cyclopean bars and edges.
11. Regan, D. (1994). Vision in sport, aviation and highway driving. Keynote Lecture, Biannual Conference of Canadian Optometrists, Waterloo, 1994.

1995

12. Regan, D. (1995). "Psychophysical methods for analyzing visual processing into parallel and sequential sub units." International Conference on Visual Coding, York University.
13. Gray, R. & Regan, D. (1995). "Cyclopean motion perception produced by oscillations of size, disparity and location". *Investigative Ophthalmology and Visual Science,*, 36, No. 4, S369. Presented to the Annual meeting of the Association for Research in Vision and Ophthalmology (ARVO), Sarasota, April 1995.
14. Regan, D. & Gray, R. (1995). "Evidence for a neural mechanism that encodes angles". *Investigative Ophthalmology and Visual Science,*, 36, No. 4, S465. Presented to the Annual meeting of the Association for Research in Vision and Ophthalmology (ARVO), Sarasota, April 1995.
15. Portfors-Yeomans, C. V. & Regan, D. (1995). "Direction discrimination and speed discrimination of motion in depth using binocular cues only". *Investigative Ophthalmology and Visual Science,*, 36, No. 4, S813. Presented to the Annual meeting of the Association for Research in Vision and Ophthalmology (ARVO), Sarasota, April 1995.
16. Giaschi, D. E. & Regan, D. (1995). "Dissociated visual development in the processing of motion-defined form". *Investigative Ophthalmology and Visual Science,*, 36, No. 4, S443. Presented to the Annual meeting of the Association for Research in Vision and Ophthalmology (ARVO), Sarasota, April 1995.
17. Vincent, A. & Regan, D. (1995). "Parallel processing of spatial frequency, temporal frequency, orientation and contrast". *Investigative Ophthalmology and Visual Science,*, 36, No. 4, S438. Presented to the Annual meeting of the Association for Research in Vision and Ophthalmology (ARVO), Sarasota, April 1995.
18. Regan, D. "Methods for testing visual functions that are important in aviation and driving". DCIEM Vision in Aviation Workshop, Toronto, 1995.

Department of Psychology

FAX: (416) 736-5814

UNIVERSITÉ YORK UNIVERSITY

FACULTY OF ARTS

4700 KEELE STREET • NORTH YORK • ONTARIO • CANADA • M3J 1P3

19. Regan, D. "Applying psychophysical research to the design of stereo flight simulators". TORON-NIHON Workshop on Virtual Reality, Toronto, 1995.

1996

20. Regan, D., Hajdur, L. V. & Hong, X. H. (1996). Orientation discrimination and aspect ratio discrimination for texture-defined form. Presented to the Annual meeting of the Association for Research in Vision and Ophthalmology (ARVO), Ft. Lauderdale, April 1996.
21. Gray, R. & Regan, D. (1996). Estimates of time to collision based on binocular and monocular visual information. Presented to the Annual meeting of the Association for Research in Vision and Ophthalmology (ARVO), Ft. Lauderdale, April 1996.
22. Portfors-Yeomans, C. V. & Regan, D. (1996). Speed discrimination of cyclopean motion in depth. Presented to the Annual meeting of the Association for Research in Vision and Ophthalmology (ARVO), Ft. Lauderdale, April 1996.
23. Vision in aviation and sport" University of Alabama at Birmingham, June, 1996.
24. Regan, D. (1996). "Visual factors in aviation". Workshop, Hollerman AFB, New Mexico. January, 1996.
25. Regan, D. (1996). "New avenues in clinical tests of functional vision". Eye Research Institute of Canada, Toronto Western Hospital, February 1996.
26. Regan, D. (1996). "Visual factors in low level flight and collision avoidance". Workshop, Wright-Pattersosn AFB, Ohio, 1996.

9. HONOURS/AWARDS (Lifetime achievement)

Charles F. Prentice Medal, (highest honour, American Academy of Optometry). 1990.

Fellow of the Royal Society of Canada, 1989.

D.Sc. (London University, 1974).

Distinguished Research Professor, York University, 1991.

I.W. Killam Fellow, 1991.

I.W. Killam Research Professor, 1978.

Max Forman Prize for Medical Research.

Fellow of the Optical Society of America.

Fellow of the American Academy of Optometry.

Department of Psychology

FAX: (416) 736-5814

UNIVERSITÉ YORK UNIVERSITY

FACULTY OF ARTS

4700 KEELE STREET • NORTH YORK • ONTARIO • CANADA • M3J 1P3

Listed in "Who's Who in America" ,"Canadian Who's Who" ,"Who's Who in the World", "Who's Who in Engineering", Dictionary of International Biography, "American Men and Women of Science", "International Who's Who in Medicine".

5. PARTICIPATING PROFESSIONALS

M.P. Regan (Ph.D.) (Applied Mathematics), M..Sc. (mathematics), B.Sc. (Mathematics).
X.H. Hong Ph.D. (Biophysical Engineering), M.Sc. (Biophysical Engineering), B.Sc. (Electronic Engineering).
S. Hamstra Ph.D. (Psychology), M.A. (Psychology), B.A.(Psychology)
A. Vincent Ph.D. (Psychology), M.A. (Psychology), B.A.(Psychology)
D. Giaschi Ph.D. (Psychology), M.A. (Psychology), B.A.(Psychology)
T. Simpson Ph.D. (Vision Science), O.D. (Optometry)
G. A. Trope M.D. , F.R.C.S. Head, Dept. of Ophthalmology, University of Toronto.
A. Lang M.D. , F.R.C.P.
R. Gray M.A. (Psychology), B.A.(Psychology
R. Kohly B.A.(Psychology
L. Hajdur Biology undergraduate
S. Hajdur Biology undergraduate

6. INTERACTIONS

6.1 Collaborations

Collaborative research on collision avoidance and on the terrain texturing requirements for nap-of-the-Earth (NOE) flight in helicopters using the Simulator Training Research Advanced Testbed for Aviation (STRATA) at the Army Research Institute (ARI) at Fort Rucker, Alabama. Collaboration is with Dr. C. Gainer, Chief, Aviation Research and Development Activity, U. S. Army Research Institute, Fort Rucker. Data collection was organized by Dr. R. Kruk of CAE who installed the Fort Rucker stereo simulator. Dr. Kruk's travel and living expenses for his visits to Fort Rucker were paid entirely by CAE. Subjects on the simulator studies, apart from Dr. Kruk, were pilot instructors from Fort Rucker who volunteer their time gratis.

Department of Psychology
FAX: (416) 736-5814

UNIVERSITÉ YORK UNIVERSITY
FACULTY OF ARTS
4700 KEELE STREET • NORTH YORK • ONTARIO • CANADA • M3J 1P3

Collaboration with Dr. R. M. Steinman of the University of Maryland on a proposed study on eye-hand coordination.

6.2 Advisory Functions

Editorial Board: *Spatial Vision*

Editorial Board: *Ophthalmic and Physiological Optics*

Grant Reviewer (during 1993-1996): National Eye Institute (NIH); National Science Foundation (USA); Wellcome Trust (UK); Medical Research Council (UK); Medical Research Council of Canada; Natural Sciences & Engineering Research Council (NSERC)(Canada).

6.3 Meetings organized

Co-organized (with Drs. I. Howard and B. Rogers) an International meeting on "Parallel Processing in Vision", York University, June 1995.

Co-organized (with Drs. I. Howard and B. Rogers) an International meeting on "Vision and Action", to be held at York University in June 1997.

6.4 Transitions

We offer gratis software to carry out our motion-defined letter test and our texture-defined letter test using an IBM PC. Before running the tests, the software displays an acknowledgement of AFOSR support in developing the tests and a request that this be acknowledged in any resulting publications. These tests can be used both to investigate and to aid the diagnosis of several disorders including multiple sclerosis and amblyopia[1-5], and we have supplied many hospitals and universities with the software. A possible aviation application of the motion-defined letter test is in screening pilots who are expected to undertake nap-of-the-Earth (NOE) flight in helicopters, since the ability to use motion parallax to see objects may well be important in NOE flight. I understand that the MD letter test is to be used on the Neurolab Space Mission.

Copies of the software have been sent to roughly 50 hospitals and departments Worldwide, but mostly in the USA. They include the following.

Department of Psychology
FAX: (416) 736-5814

UNIVERSITÉ YORK UNIVERSITY

FACULTY OF ARTS

4700 KEELE STREET • NORTH YORK • ONTARIO • CANADA • M3J 1P3

In the USA: Dr. B. Schwartz, Department of Neurology, Tulane University Medical Center; Dr. M. Wall, Department of Neurology, University of Iowa; Dr. J. Hotson, Department of Neurology, Stanford University; Dr. S. Wray, Department of Neurology, Harvard Medical School, Mass. General Hospital; Dr. K. Alexander, Department of Ophthalmology, University of Illinois, Chicago; Dr. A. D. Epstein, Department of Ophthalmology, University of Kentucky, Lexington.

Worldwide: Dr. T. Munte, Neurogische Klinik, Medizinische Hochschule, Hanover, Germany; Dr. Wildberger, University Eye Clinic, Zurich, Switzerland; Dr. S. Boniface, Department of Neurology, Ratcliffe Infirmary, Oxford University, U. K.; Dr. J. Fredriksen, Department of Neurology, University of Copenhagen, Denmark; Dr. R. Jacobs, Department of Optometry, University of Auckland, New Zealand; Dr. R. van der Zwan, Department of Psychology, University of Sydney, Australia.

(1). *Brain*, 1991, 114, 1129-1155. (2). *Annals of Neurology*, 1992, 31, 621-628. (3) *Investigative Ophthalmology and Visual Science*, 1992, 33, 2483-2489. (4). *Journal of Neuroscience*, 1992, 2198-2210. (5). *Neurology*, 1995, 45, 809-815. Research Period 15 December 1996 to 14 December 1997

7 STATEMENTS: INFORMATION FOR ATTENTION OF AFOSR PROGRAM MANAGER

Results and techniques that are of immediate selection and operational, or medical relevance are as follows.

7.1 Selection and operational

Our TEXTURE-DEFINED LETTER TEST (Sections 3.13 and 3.14 and Refs. 235, 241-243) assesses quantitatively intersubject differences in the ability to see and recognise texture-defined objects. This ability is presumably important in terrain avoidance and flight safety in nap-of-the-Earth

Department of Psychology

FAX: (416) 736-5814

UNIVERSITÉ
YORK
UNIVERSITY

FACULTY OF ARTS

4700 KEELE STREET • NORTH YORK • ONTARIO • CANADA • M3J 1P3

helicopter flight in either naked eye conditions or when using night-vision goggles. This is because texture contrast is an important visual cue in seeing some terrain features.

We have developed software for this test that runs on an IBM PC or true clone using an ATI VGA "Wonder Plus XL24" graphics card. On receipt of a floppy disc we will supply the test gratis to vision researchers. The software cites AFOSR sponsorship, and instructions for use are supplied. Six copies of the disc are enclosed with this report.

The test complements our MOTION-DEFINED LETTER TEST, described in the Final Report 11/01/1991 — 10/31/1993 for AFOSR 91-0080, that assesses quantitatively intersubject differences in the ability to process relative motion and in particular to recognize camouflaged objects defined by relative motion. Presumably, this ability is also important in nap-of-the-Earth helicopter flight in either naked eye conditions or when using night-vision goggles. This is because many terrain features (e.g. grassy protuberance with grassy surround) are partially camouflaged when hovering and clearly visible when moving.

Our technique for measuring discrimination thresholds for the ratio $\theta/(d\theta/dt)$ (Section 3.5 above, Refs. 220, 239) may help to predict intersubject differences in TIME TO COLLISION among pilots, and these differences may well be important in predicting an individual pilot's safety (in terrain

Department of Psychology
FAX: (416) 736-5814

UNIVERSITÉ
YORK
UNIVERSITY

FACULTY OF ARTS
4700 KEELE STREET • NORTH YORK • ONTARIO • CANADA • M3J 1P3

avoidance) in low-level flight in fixed-wing aircraft and nap-of-the-Earth flight in rotary-wing aircraft.

Our finding that judgements of time to collision with objects viewed in peripheral vision are affected by the size of an object has the following relevance for collision avoidance in aviation. It is natural that to judge time to collision a pilot should look directly at an oncoming object on a collision course. We report that that is the correct thing to do. However, it is impossible to look directly at two things at once. It is not intuitively obvious that judgements of time to contact are unreliable in peripheral vision. Our results imply that pilots should be made aware of this deficiency in the human visual system so that, when confronted by a collision hazard with two or more oncoming objects the pilot can adopt some deliberate strategy such as, for example, glancing rapidly from one to the other.

7.2 **Medical**

The texture-defined and motion-defined letter tests are also of value in medicine. They provide complementary information that can aid in the diagnosis of multiple sclerosis (specifically in detecting the effect of a subclinical lesion in the visual pathway) and in monitoring the progress of the disease (Refs. 197 and 213). The motion-defined letter test can also reveal subclinical abnormality in the "clinically-unaffected" eye of unilaterally amblyopic children (Ref. 214).